3-25-2010

Headspace Analysis of Smokeless Powders: Development of Mass Calibration Methods using Microdrop Printing for Chromatographic and Ion Mobility Spectrometric Detection

Monica Joshi-Kumar
Florida International University, mlank001@fiu.edu

DOI: 10.25148/etd.FI10041617

FLORIDA INTERNATIONAL UNIVERSITY

Miami, Florida

HEADSPACE ANALYSIS OF SMOKELESS POWDERS: DEVELOPMENT OF MASS CALIBRATION METHODS USING MICRODROP PRINTING FOR CHROMATOGRAPHIC AND ION MOBILITY SPECTROMETRIC DETECTION

A dissertation submitted in partial fulfillment of the

requirements for the degree of

DOCTOR OF PHILOSOPHY

in

CHEMISTRY

by

Monica Joshi-Kumar

2010

To: Dean Kenneth Furton
College of Arts and Sciences

This dissertation, written by Monica Joshi-Kumar, and entitled Headspace Analysis of Smokeless Powders: Development of Mass Calibration Methods using Microdrop Printing for Chromatographic and Ion Mobility Spectrometric Detection, having been approved in respect to style and intellectual content, is referred to you for judgment.

We have read this dissertation and recommend that it be approved.

_____
Kenneth Furton

_____
Bruce McCord

_____
Jeffrey Joens

_____
Krishnaswamy Jayachandran

_____
Jose R. Almirall, Major Professor

Date of Defense: March 25, 2010

The dissertation of Monica Joshi-Kumar is approved.

_____
Dean Kenneth Furton
College of Arts and Sciences

_____
Interim Dean Kevin O'Shea
University Graduate School

Florida International University, 2010

DEDICATION

This work is dedicated to my teachers' at all academic levels who have made my education a joy and specifically to my mom who was my first science teacher.

ACKNOWLEDGMENTS

I am grateful for the opportunity that was given to me to pursue my PhD at FIU. I express my sincere gratitude to Dr. Almirall for the experience that I have had at FIU and in his research group. Most importantly, I thank him for replying to my emails when nobody else would, back in 2005. My committee members, Dr.McCord, Dr. Furton, Dr. Joens and Dr. Jayachandran, I thank you for being supportive and being available to advise through the years.

I thank UGS and GSA for supporting my research, funding my travels to scientific meetings, and awarding me the DEA award. I would like to give special mention to the valuable advice I have received from Dr. Gillen, Dr. Verkouteren and Dr. Fletcher at NIST regarding microdrop printing. I thank Dr. Kelly from the FBI for being willing to share his smokeless powders database with us.

I have had wonderful colleagues during my time at FIU and I am thankful for all of them but I have to mention Waleska (for teaching me a thing or two about work ethic), Joe (for teaching me to drive), Tati (for asking me how I was, which was very important in difficult times), Erica, Emily, Sarah and Maria (for being there for me and saying what needed to be said everyday), Robert and Kia (for being so helpful), Sigalit (for her time here) and Howard and Davia (for praying for me). I thank my family for supporting me and letting me pursue my PhD in the US. I know they have prayed for me every single day since I left on Aug 22, 2005. Everything that has been said and everything that I have been able to do, is because of my husband, Anand who has been a constant support before and through all of this. I can finally go home to him now. Above all, I thank my Father in heaven because of whom all things are possible.

ABSTRACT OF THE DISSERTATION

HEADSPACE ANALYSIS OF SMOKELESS POWDERS: DEVELOPMENT OF MASS CALIBRATION METHODS USING MICRODROP PRINTING FOR CHROMATOGRAPHIC AND ION MOBILITY SPECTROMETRIC DETECTION

by

Monica Joshi-Kumar

Florida International University, 2010

Miami, Florida

Professor Jose R. Almirall, Major Professor

Smokeless powder additives are usually detected by their extraction from post-blast residues or unburned powder particles followed by analysis using chromatographic techniques. This work presents the first comprehensive study of the detection of the volatile and semi-volatile additives of smokeless powders using solid phase microextraction (SPME) as a sampling and pre-concentration technique. Seventy smokeless powders were studied using laboratory based chromatography techniques and a field deployable ion mobility spectrometer (IMS). The detection of diphenylamine, ethyl and methyl centralite, 2,4-dinitrotoluene, diethyl and dibutyl phthalate by IMS to associate the presence of these compounds to smokeless powders is also reported for the first time. A previously reported SPME-IMS analytical approach facilitates rapid sub-nanogram detection of the vapor phase components of smokeless powders. A mass calibration procedure for the analytical techniques used in this study was developed. Precise and accurate mass delivery of analytes in picoliter volumes was achieved using a drop-on-demand inkjet printing method. Absolute mass

detection limits determined using this method for the various analytes of interest ranged between 0.03 - 0.8 ng for the GC-MS and between 0.03 - 2 ng for the IMS. Mass response graphs generated for different detection techniques help in the determination of mass extracted from the headspace of each smokeless powder. The analyte mass present in the vapor phase was sufficient for a SPME fiber to extract most analytes at amounts above the detection limits of both chromatographic techniques and the ion mobility spectrometer.

Analysis of the large number of smokeless powders revealed that diphenylamine was present in the headspace of 96% of the powders. Ethyl centralite was detected in 47% of the powders and 8% of the powders had methyl centralite available for detection from the headspace sampling of the powders by SPME. Nitroglycerin was the dominant peak present in the headspace of the double-based powders. 2,4-dinitrotoluene which is another important headspace component was detected in 44% of the powders. The powders therefore have more than one headspace component and the detection of a combination of these compounds is achievable by SPME-IMS leading to an association to the presence of smokeless powders.

TABLE OF CONTENTS

LIST OF TABLES

TABLE PAGE

TABLE OF FIGURES

FIGURE PAGE

I. STATEMENT OF THE PROBLEM

The research described herein is an effort towards filling the need for accurate mass calibration of analytical instruments and the expansion of detection parameters for low explosives such as smokeless powders. The chapters that follow describe the successful implementation of drop-on-demand microdrop printing technology for calibration of several different analytical techniques and the application of solid phase microextraction (SPME) and microdrop printing towards the quantitative analysis of volatile components of a wide array of smokeless powders. The various studies discussed here demonstrate the validity and reliability of inkjet printing and establish the utility of the technique for determining mass response of detectors such as mass spectrometers (MS) and ion mobility spectrometers (IMS) and their sensitivities. The results from the smokeless powder studies illustrate the efficiency of SPME in extraction, pre-concentration and subsequent detection of various additives of smokeless powders. The SPME studies also provide evidence that ion mobility spectrometers can be used to reliably detect the constituents that make up smokeless powders by vapor sampling. Microdrop printing is used for the first time to determine mass of volatiles extracted from the vapor phase of smokeless powders and this new technique is shown to outperform other calibration methods.

1. Research motivation

Ion mobility spectrometers are the most widely used field chemical detectors of illicit substances. Currently, there are several thousands of these units deployed worldwide within the military and serve as chemical warfare agent detectors.

Domestically within the United States and internationally, a large number of these instruments are installed at various security checkpoints such as airports and other secured entry points. They are used primarily to detect traces of explosives or drugs of abuse present on various personal belongings of those passing through these checkpoints. Apart from being a rapid, field portable technique that is easy to use and interpret, ion mobility spectrometry (IMS) provides exquisite sensitivity for several analytes. The IMS instruments offer detection limits for illicit substances such as drugs and explosives in the range of a few nanograms to picograms. The instruments are programmed to produce an alarm in the presence of these compounds either in the positive or negative mode, when the particles are collected from various surfaces.

Most commercial instruments are supplied with a calibration or verification device intended to supply the user information about the status of the instrument. They indicate if the instrument is able to detect an analyte or a mixture of analytes that are part of the detection menu. However, these performance tests do not reveal if the instrument sensitivities have been affected. The calibration standards or devices available are purely qualitative and do not offer any quantitative information. They only indicate the qualitative instrument performance towards the analyte or the analyte surrogate present in the calibration device. However, IMS instruments have different detection capabilities for different analytes and each analyte could be affected differently based on the instrument conditions. Based on the current research being conducted in IMS and the trends observed in the field where IMS instruments are being used, it was concluded that there were two needs in the trace detection of drugs

and explosives by IMS. First, there was need for a method to measure instrument sensitivities and mass detection ranges accurately. Second, the particle detection menu currently available needed expansion to include volatile indicators of illicit substances. The research efforts described in this document address both these needs.

Scientists at the National Institute of Science and Technology (NIST) gained interest in the inkjet printing technique and used it as a calibration method for a vapor sensor and for printing standards of explosives on various surfaces[1,2]. Recognizing that this same technology could be used for quantitative calibration of IMS instruments, a research project was begun in collaboration with NIST to apply inkjet printing for IMS and evaluate its applicability for calibration of ion mobility spectrometers.

The purpose of this dissertation is not only to demonstrate the mass calibration method on the current detection menu of commercial instruments, but also to contribute to expanding the detection menu of these instruments. Research has shown that canines use volatiles emanating from hidden illicit substances as indicators of the presence of the substances. Following this premise, the current research aims to develop instrumental methods for the detection of organic volatiles indicative of explosives. The explosives of choice for this research are smokeless powders, which have no reliable particle detection alarm present in commercial IMS instruments. The current alarm that is indicative of smokeless powders is the peak resulting from the presence of a nitro (NO_3^-) group. This peak is non-specific to smokeless powders and could be indicative of any analyte that ionizes to produce a nitro product ion.

2. Hypothesis

Scientists at NIST in collaboration with MicroFab Technologies, Inc. (Plano,TX), demonstrated the utility of inkjet printing as a trace vapor calibrator and showed that the method was reliable for printing drops for vapor generations[3,4]. Inkjet printing as applied to this project was expected to give similar performance characteristics and enable accurate mass calibration of IMS instruments.

Based on the studies already published about smokeless powders, it is known that there are volatile chemical compounds present above the solid smokeless powder samples[5,6]. It is also known that a solid phase micro extraction device can extract and pre-concentrate these compounds. The aim of this project is to study the headspace components of smokeless powders and demonstrate that the compounds discussed in published literature and other components of smokeless powders can be extracted and detected by laboratory based chromatographic confirmation methods and field portable IMS instruments in conjunction with an SPME-IMS interface.

Experiments were designed to collect data in order to critically evaluate the following two hypotheses:

1. Drop-on-demand inkjet printing technique is a reliable mass delivery tool that could be used for the calibration of detectors such as mass spectrometers and ion mobility spectrometers and to measure the mass detected by these detectors during SPME headspace extractions of illicit substances
2. There are volatile and semi-volatile additives of smokeless powders present in the headspace of the powders that when detected by ion mobility spectrometry can be associated to the presence of smokeless powders.

II. MICRODROP PRINTING FOR MASS CALIBRATION

Trace detection techniques rely on the ability of the detector to detect analyte amounts in the nanogram to picogram range. This requires that the sensitivity of the instrument is accurately known and periodically verified. Also critical to the determination of mass of an analyte detected are the generation of instrument response graphs over a broad mass range. Current methods for determining instrument sensitivity and analyte detection are based largely on the determination of mass relative to the signal response of a standard solution. This chapter describes the application of drop-on-demand microdrop printing to determine absolute mass detected and the generation of response curves for different techniques. In addition, the development and implementation of an inkjet printing method for the determination of mass extracted by solid phase microextraction in the headspace is explained.

1. INTRODUCTION TO MICRODROP PRINTING

Microdrop printing is a method to generate fluid drops with diameters ranging from a few micrometers to several hundred micrometers. The following features of microdrop printing make it an appealing technique for several applications:

1. Generation of monodispersed microdrops
2. Ability to control the drop size and drop volume
3. Non-contact printing on various media
4. Versatility of the printing solutions

5. High production speeds

The beginnings of microdrop generation date to over a century ago when aerosols were used to study fluid mechanics and atomic theory. Lord Rayleigh gave the first description of the breakdown of liquid streams into droplets in 1878[7]. In the early 1900s, Robert Millikan performed his famous oil drop experiments with fluid microdrops using a spray atomizer and used them to determine the value of the electric charge[8]. Since then, several developments led to the use of microdrops in the inkjet printing industry where drops of fluid are jetted from an orifice onto a specified substrate position to generate images. For many years now, microdrops have dominated the commercial printing industry where reliable printing methods were developed.

Discrete microdrops can be formed by two main ways: continuously or by drop-on-demand (DOD) methods. Continuous inkjet printing was the first developed method where a continuous fluid stream is broken into nodes by applying an acoustic pressure wave. The nodes break the stream into uniform sized drops that are ejected at the orifice. The drops are electrostatically charged and deflected to their desired location. Therefore, the drops are continuously produced and are led to their printing medium by an electrostatic field. This method is still used in some commercial printing methods but has found greater popularity in applications where large volume dispensing is required since they produce drops at high frequency that are approximately twice the diameter of the nozzle. On the other hand, drop-on-demand method is the most widely used printing method in the commercial inkjet printing

industry. The DOD device ejects drops only when the jet is triggered and used for imaging on a substrate. Instead of breaking a single continuous fluid stream, each voltage pulse causes a single drop to be formed. The drop diameter can also be adjusted by changing the pulse characteristics. The 1970s and 1980s experienced a growth in the drop-on-demand printing technique and it became popular due to greater placement precision and the generation of smaller drops[7]. Several designs of DOD printers have been developed since then and some of them include thermal ink-jet, piezoelectric ink-jet, acoustic, liquid spark and electrohydrodynamic ink-jet. Of these, the thermal and piezoelectric methods are the most popular methods in current commercial printers[8]. Piezoelectric printing devices are used for the DOD printing described in this document and the following section introduces the basic principles of the technique.

1.1. Piezoelectric drop-on-demand printing

Piezoelectric printing depends upon the deformation of a piezoelectric element that surrounds the fluid. This deformation causes a volume change and generates a pressure pulse in the fluid. Different configurations of the piezoelectric material are possible; however, the most popular one patented by Epson for its printers and commercial microdrop printers is a tubular configuration[7]. In this method, the tubular piezoelectric actuator surrounds the glass capillary, which contains the fluid. Applying a voltage pulse to the piezoelectric element causes it to contract and expand thereby propagating a pressure wave along the fluid. At the nozzle orifice, the pressure wave causes the fluid to eject as a drop and the drop breaks off at the end of the wave into a

discrete drop. By tailoring the fluid ejection and retraction pulse one can generate discrete drops of desired diameter with no satellite formation[8]. Figure 1 is a typical bipolar pulse wave for a DOD printing system. A simple waveform is trapezoidal in shape with the fluid expansion, wave propagation and fluid compression segment. This segment causes the drop to form and eject[9]. Any residual oscillations in the fluid can be cancelled using the second segment and this gives more stable printing. Adjusting the pulse width (dwell time) and the rise and fall times helps in adjusting drop volume and velocity. Figure 2 depicts the generation of single drop for every voltage waveform. Since there is no post generation electrostatic deflection of the drops as in continuous mode, the drop-on-demand system is much simpler, needs minimum fluid volume and can accommodate a variety of fluid types. A tubular piezoelectric printing device with a glass capillary is easy to machine and remains relatively inert chemically. It is compatible with several different fluids as there is no interaction between the actuating material and the jetting fluid. The drops produced by this method are generally the same diameter as the diameter of the glass capillary orifice. Therefore, it is easier to determine drop size and the consequently the drop volume.

Generating monodisperse free falling drops of optimal size requires careful optimization of the printing parameters. These parameters include drive amplitude (voltage), pulse shape, pressure level of the fluid, frequency and the fluid fill level. All these parameters can affect the velocity, volume and angle of the drop. Different fluids need these parameters to be optimized through trial and error. The ability to use a wide

variety of fluids and optimizing them as desired has brought drop-on-demand printing out of the commercial document printing industry into the science and industrial development field.

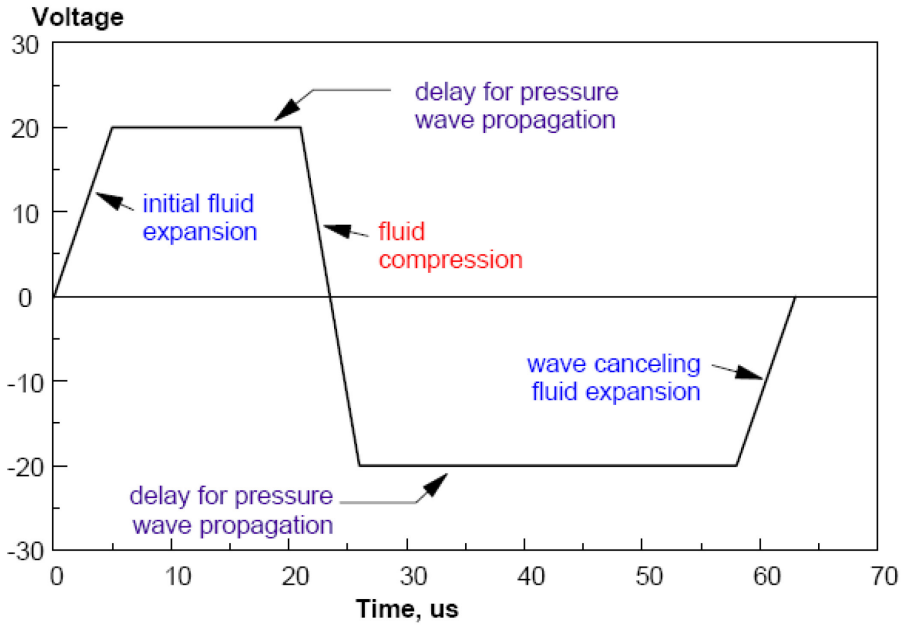

Figure 1: Typical voltage waveform used for a drop-on-demand piezoelectric actuator[9]

1.2. Development of microdrop printing for analytical applications

Several scientific and industrial applications require precise dosing of fluids and non- contact deposition of materials for manufacturing and synthesis. Though drop-on-demand based printing was introduced several years ago, only in recent years, have the scientific and industrial sectors taken interest in this technique as a sample delivery tool. Lee gives an account of all the different ways microdrop printing can be used in the pure and applied science and details the theory, practice and growing number of

applications of this technology[8]. Several papers have been published in recent times describing the use of inkjet printing for the deposition of polymers and coatings for manufacturing polymer light emitting diodes, circuits and electronics[8,10-12]. Microdrop printing has been used for a long time in biomedical applications for cell sorting and MicroFab Technologies, Inc. (Plano,TX) has recently also shown precise medicine dosing using DOD printing.

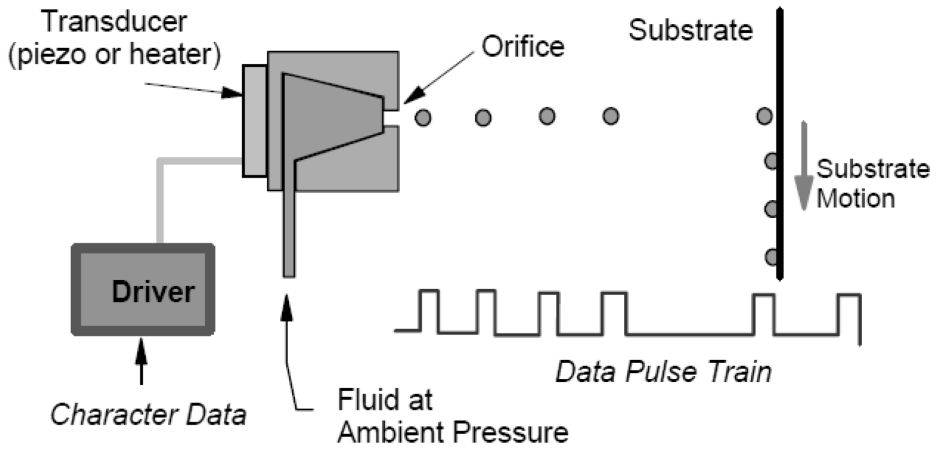

Figure 2: Schematic for a drop-on-demand system [13]

However, there is very little literature that has reported the use of microdrop printing for precise deposition of analytes for chemical analysis. As discussed earlier, scientists at NIST acknowledged the utility of the technique for generating standards for analytical applications. The portable vapor generator was developed using ink-jet microdispensing to deliver precise amounts of explosives solutions. The drops were converted to vapor by a heating element and they showed that this method could be used to calibrate the mass delivered to vapor detectors such as electronic noses [1,3,4]. The same technology was first used in the calibration of a human olfactometer[4]. The

results from these experiments furthered the use of ink-jet printing for delivering mass precisely onto fingerprint patterns to study distribution of explosives and analysis of fingerprints. Several efforts were further taken to study drop formation and drop generation capabilities. Recently printing of a polymer and printing of a explosive solution were brought together by printing emulsions using sphere jet technology to develop polymer encased explosives standards[14]. Long-term studies have yet to be conducted on these microcapsules but the method is a promising effort towards the development of reliable standards for IMS instruments. Englmann et al. reported the use of microdrop printing for use with chromatographic techniques[15] . They generated drops of standard solutions and conducted experiments to study the reliability of the drop generation and the feasibility of the technique for chromatographic purposes using ultra performance liquid chromatography (UPLC). The results from the standard addition experiments demonstrated that precise solution dispensing is applicable to chromatography and that the printing method is reliable and reproducible.

Much importance has been paid to the study of drop volume and the linearity between the overall printed mass versus drop number since the total volume printed is the product of the volume of a single drop and the number of drops printed. Factors affecting drop volume and the various methods to determine the volume during printing are discussed in great detail by Lee[8]. He describes imaging and gravimetric methods as the most popular ones. Wu et al. described an imaging system based on a computer aided simulation for measuring drop dynamics and droplet formation by a piezo electric DOD system[16]. In their studies, the drop volume was measured in relation to the nozzle diameter by taking images and translating the size into volume

by using a sphere formula. Another imaging system based on a laser and a CCD camera has been recently described for studying drop formation and deposition on substrates[17]. The results showed that a series of high-resolution images can help in determining of drop dynamics but quantitative analyses are necessary to validate such methods. Englmann et al. compared both imaging and gravimetric drop measurements to determine their reliability and found that there was insignificant difference in the measurements obtained by both methods[15]. More recently, Verkouteren et al. developed and compared gravimetric methods for measuring droplets mass generated by the microdrop printer[18]. The reproducibility, limit of quantitation and relative uncertainty of the methods were evaluated. The individual drop size measurements were obtained using high-speed videography of a burst of drops. The study also discussed and evaluated the first drop effect, which is a common phenomenon observed with microdrop printing. When several drops are jetted in a burst after a lag time in the fluid, the first few drops are of a different size compared to the rest of the drops in the burst sequence. However, the drop generation in bursts is very reliable and reproducible when the fluid lag time in the reservoir is short.

Drop measurements discussed above do not allow for the real time calculation of drop size. This can be accomplished by image processing. Thurow et al. reviewed the various drop measurement techniques currently available and proposed that image processing techniques provide the most rapid results[19]. They put forth a very detailed process of analyzing drop size based on image processing and generated an algorithm for drop measurements. Similar theories are used by commercial software in image processing such as Aphelion™ that generate drop parameter information by analyzing

images captured by the camera. This is useful for analytical applications of microdrop printing.

On surveying literature and the results discussed, it was concluded that drop-on-demand printing was an attractive option for the calibration of analytical instruments. The application of ink-jet drop-on-demand printing for the precise deposition of mass for analysis by various analytical techniques and sampling techniques will be addressed in this document. The results of experiments conducted will demonstrate and support the use of microdrop printing in multiple scientific applications.

2. INKJET PRINTING FOR IMS INSTRUMENTS

The following section describes the studies conducted with microdrop printing for ion mobility spectrometry. Drop-on-demand printing is an easily achieved task for IMS due to the simplicity of the sample introduction system of IMS instruments. The results discussed below illustrate the efficacy of microdrop printing for determining absolute mass detection limits of IMS instruments for various analytes and generation of response graphs to determine the mass detection range of two different commercial instruments.

Theory of Ion mobility spectrometry (IMS):

IMS is an analytical technique introduced as plasma chromatography in the late 1960s and early 1970s. Since then, there have been several modifications and variations to the technique. Eiceman and Karpas describe recent developments in this field in their comprehensive book[20]. The basic mechanism of the technique is that a

sample is converted into vapor phase on introduction into the instrument. The ions formed on ionization of the vapor at atmospheric conditions are introduced into a drift region where they are separated in a weak electric field. The IMS usually operates in two modes: positive mode and negative mode. Most explosive molecules are detected in the negative mode due to their high electronegativities and the formation of negative ions. Drugs of abuse generally have high proton affinities and form positive ions and therefore are detected in the positive mode[20]. The typical regions of an IMS are shown in Figure 3 below[21].

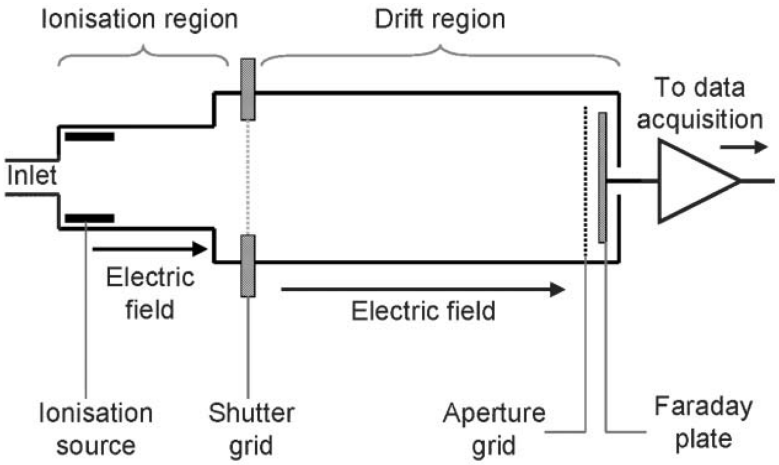

Figure 3: Diagram representing the different regions of an ion mobility spectrometer[21]

The ionization in most commercial trace detectors is by a 10 mCi ^{63}Ni radioactive source due to the several benefits it possesses over the other ionization methods. It is simple to use, produces stable reactant ions, requires low power and produces β particles spontaneously for a very long time. The ionization mechanisms involved in a ^{63}Ni ionization have been reviewed in detail in several literature sources[20-23]. Briefly,

the electrons emitted by the source form several ion electron pairs while reacting with the nitrogen in air or nitrogen gas. The ions formed react further in a cascade of reactions to form various species of positive and negative ions from the ambient air such as N_4^+, H_30^+, H_20^+ and other water adducts based on the amount of moisture present in the system. These ions are called the reactant ions and help in the chemical ionization of the sample molecules. When other reagent gases, commonly called dopants are used they create alternate reactant ions that help in adding selectivity to the instrument[22]. In instruments used for illicit substance detection, chlorocarbons such as dichloromethane and hexachloroethane have been used for improving the selectivity of explosives in the negative mode. In the positive mode, ammonia has been used to suppress the signal of all other ions that have proton affinities less than ammonia.

The gas phase mobilities or drift times of the ions are characteristic of the ions produced by the ionization. The drift times can be attributed to the ions separated based on their mass, charge and collision cross section and all these factors are dependent upon the physical characteristics of the ions, the collisional interactions between the ions and the neutrals in the drift region and the experimental conditions. The drift times in milliseconds and the length of the drift tube (usually 5-20 cm in length) can be used to calculate the drift velocity[20-22]. The drift velocity is proportional to the electric field strength and mobility (K) of the ion. This mobility is normalized to temperature and pressure to give a reduced mobility (K_o) value that is specific to a certain analyte.

Several methods of sample introduction have been used for IMS instruments for solid, liquid and gaseous samples[24]. The primary method of sample introduction in most commercial instruments is by thermal desorption of solid analytes through a desorber unit at the inlet of the instrument. The same desorption method has also been used for liquid samples by spiking known volumes of analyte solutions onto a swipe and desorbing into the desorber unit. The method of sample introduction and the matrix of the sample affect the response for an analyte[22]. This is an important factor to be taken into consideration while conducting quantitative analysis in IMS. The experimental studies described in the following sections will take into account these factors and focus on developing better quantitative methods for IMS instruments.

2.1. Inkjet printing systems used for drop on demand printing

The ink-jet printing systems used in this study were purchased from MicroFab Technologies, Inc. (Plano, TX). Two different piezoelectric printing set-ups were used for all microdrop printing studies described in this document.

In the initial experiments, a laboratory built microdrop system was used which is shown in the Figure 4 below. A PH-41 cartridge style print head from Microfab Technologies (Plano, TX) was mounted vertically with a S10120 2.5 mL capacity laboratory column purchased from Boca Scientific (Boca Raton, FL) and the MJ-AL series printing device with a 60 μm orifice. The printing device used with the different parts labeled is shown in Figure 5 below. The drop formation and visualization was facilitated by the use of pulsed LED strobe and horizontal optics system. The horizontal optics is also provided with a reticle for calibration of the screen and

determination of drop parameters. The drop images generated by the optics are shown in Figure 6 below. For the negative pressure needed for reliable jetting, a simple manometer style setting was used with the fluid reservoir placed at a slightly higher level than the level in the dispensing device. The JetDrive™ III drive electronics was used to generate drive waveforms for triggering the printing device and to control the LED strobe for drop visualization.

Drop measurements when using the Jetlab® III set-up were conducted using a micrometer. A micrometer with movable X-Y stages was mounted on a post and viewed with the camera such that the reticle and edge of the micrometer were visible. Careful stepwise increase of the micrometer was used to calibrate the distance between the markings of the reticle on the camera. The micrometer was also used to measure the approximate drop size. These drop size measurements at the optimized parameters were used to determine the volume in a drop and thereby the mass of analyte in a single drop. The camera reticle and the drops are shown in Figure 6.

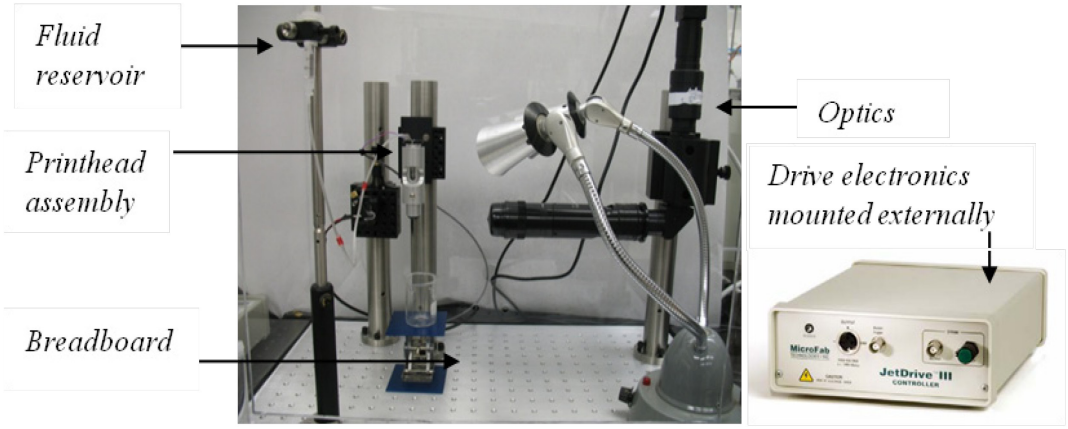

Figure 4: Jetdrive III based laboratory assembled inkjet printing system

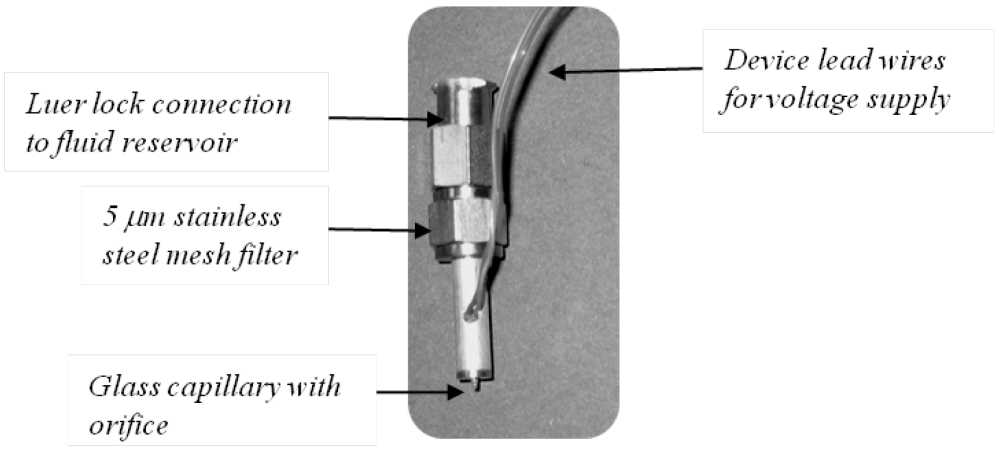

Figure 5: MJ-AL piezoelectric printing device

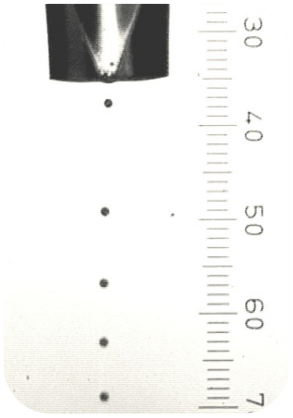

Figure 6: Continuous mode drop generation visualized with optic system

After the success with the initial system, a second complete tabletop printing platform, Jetlab® 4 was purchased. The Jetlab 4 is also based on a piezoelectric printing system with drive electronics similar to the Jetlab III. The system is equipped with an automated pressure and vaccum control, which provides long term jetting stability. This system has the added capability of visualizing the substrate with the vertical optical system and an X-Y-Z direction motion stage. This allows for printing various patterns with and visualizing of the printed patterns. The system is shown in

Figure 7 below. All the precise location printing discussed here was conducted on this system.

Figure 7: Jetlab® 4 table-top printing system

The image grabber software that comes with the Jetlab 4 provides the facility of capturing the camera images of the drop generation and the printed substrate. For all studies where the Jetlab 4 was used, the drop size was measured by taking images of the printing solutions in continuous mode using a strobe and the horizontal optics. Drop measurements were based on the imaging calculations similar to those described by Thurow et al[19]. To calibrate the drop images and the screen, a fixed object such as the edge of the printing device is used. The Z stage is moved by known millimeter values and the images saved at different Z stage heights. Each image is opened in Windows Paint and the location in pixels of the edge in x, y pixels is determined by pointing the mouse. When the mouse is moved across the image, the x and y pixel

coordinates are displayed at the bottom of the Paint program window. The difference between the larger and smaller y pixel values from the two images divided by the position difference gives the mm/pixel number that is used as the screen calibration. The images of the drops formed by the solution being printed on optimization are saved as shown in Figure 8. The images are also opened in Paint and the drop diameter is measured manually by using the computer cursor and the difference of pixels between the top edge and the bottom edge of the drop. The drop diameter is then calculated using the mm/pixel number. Since the drops are spherical the formula for the volume of a sphere is used to calculate drop volume.

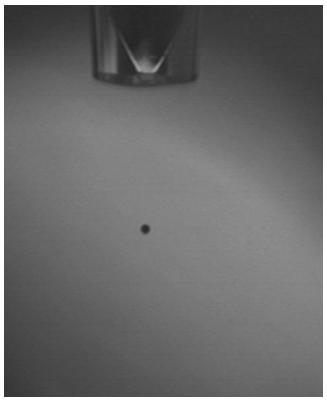

Figure 8: Drop image used for measuring drop volume

2.2. Desorption profiles of analytes

Analytical challenge:

As mentioned above, inkjet printing is compatible with any substrate that is compatible with the IMS. Ion mobility spectrometry as intended for detection of illicit substances is mainly a particle detector. Therefore, the IMS swipes provided by the

manufacturers are meant to collect particles or residues of substances when various surfaces are swiped. However, many other substrates are compatible with IMS instruments though they are not good particle collectors. Listed below are a few characteristics of an ideal IMS substrate.

1. Thermally stable (Must be able to resist the high temperature of the IMS desorber which is typically set between 200-300 ^{o}C).
2. Substrate produces no interfering peaks in the IMS plasmagram in both positive and negative modes.
3. Substrate should be relatively inert and not react with any of the target analytes.
4. Substrate should have optimal desorption characteristics, where the analyte is completely and efficiently desorbed from its surface within the IMS analysis time.

The aim of this portion of the study was to determine which of the available substrates would be best suited for the determination of absolute mass detection limits of IMS instruments. Since, the manufacturer supplied IMS swipes are intended for particle collection, a separate study needed to be conducted to determine their performance with the deposition of solutions of analytes. Current practice for determining mass response of the instrument is to deliver solutions of target analytes onto a substrate and desorbing it into the IMS to determine signal for a given concentration of solution. However, in the studies conducted with microdrop printing, the instrument response to absolute mass on substrate is determined. The desorption

profile of an analyte for a given sampling time provides information about the time it takes for the analyte to be completely sampled and if there are losses of analytes for different substrates. This study is important in that, the results obtained for an instrument are dependent upon the type of substrate used and thus affect the determination of sensitivity of the instrument.

Experimental method:

Substrates and swipes suitable for two IMS instruments were studied for desorption characteristics. A General Electric Ion Track Itemiser II IMS (Wilmington, MA) and a Smiths Detection Ionscan 400B IMS (Mississauga, ON, Canada) were used for all IMS studies. The desorbers for the two instruments are different in design with the Itemiser II having an open desorber system whereas the IonScan instrument with a smaller desorption area and slightly more enclosed sampling mechanism. The two instruments are shown in Figures 9A and 9B respectively.

A B

Figure 9: IMS instruments available in the lab A) General Electric Ion Track Itemiser II B) Smiths Detection Ion Scan 400B

Substrates tested for the Itemiser II include Whatman ashless filter paper No. 42 (Piscataway, NJ), GE multiuse swipe (Wilmington, MA) and 0.015 inches thick Polytetrafluoroethylene (PTFE, Teflon) circles. For the Ionscan 400B IMS, the swipes and substrates tested include the manufacturer supplied filters for narcotics testing and explosives testing, manufacturer supplied Teflon film rings, PTFE circles similar to those used for the Iontrack IMS and polydimethylsiloxane (PDMS) coated glass slides. Figure 11 below shows the shows the different swipes and substrates tested.

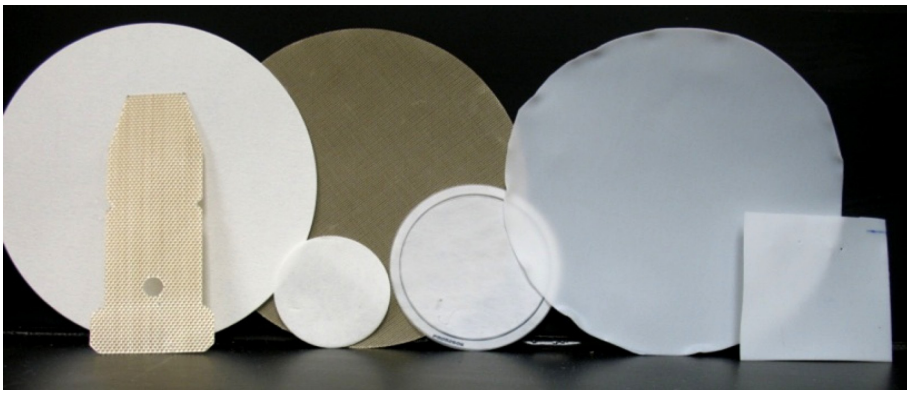

Figure 10: Substrates studied for desorption profiles in IMS instruments

2,4,6-Trinitrotoluene (2,4,6-TNT) was chosen as the analyte for this study because of its high volatility which could affect its retention on the substrate, high sensitivity of the IMS instruments to this analyte and availability of literature for the IMS behavior of 2,4,6-TNT. A 10 ng/µL solution was prepared with 2-butanol as the solvent. Solvents such as 2-butanol, isopropanol and ethanol are best suited for printing analytes of interest for this research study and literature suggests that these solvents provide reliable and stable jetting. A total mass of 0.43 ng of 2,4,6-TNT was

printed on different substrates and desorbed into the instrument and analyzed in the negative mode.

The voltage pulse used for printing is a bipolar waveform with +10 V/-10 V voltage pulse with a rise and fall time of 3 μs and the dwell and echo time were maintained at 25 μs. At these parameters and the adjustment of the backpressure manually, stable jetting with no satellites was observed in the continuous mode. 500 drops of the analyte solution were printed by placing the substrate of choice centered under the print head and triggering jetting.

All the substrates of interest for a particular IMS were studied under the same sampling time and desorption conditions. The Instrument Manager 5.052 software for the Smiths Detection instrument automatically generates desorption profiles for every analyte. However, Microsoft excel was used to plot the sample times versus the analyte signal from the raw data of the Itemiser II instrument to generate desorption profiles. To maintain consistency between the Ionscan 400B instrument and Iontrack Itemiser II instrument, cumulative amplitudes were plotted against mass to generate mass response curves to determine linearity of drop generation, linearity of response for a given substrate and its response as compared to other substrates. The cumulative amplitude is the sum of the signal response for the analyte at every scan.

Results:

The graphs shown in Figures 11-16 depict the results obtained for the substrates studied for the Itemiser II IMS. The default sampling time in this instrument is 7

seconds. The five replicates are shown in one graph to illustrate the reproducibility of a substrate.

1. Whatman No. 42 filter paper: The substrate inherently produces several peaks that interfere with the IMS analysis. However, heating the substrate for a few seconds in the desorber before depositing the analyte mass removes many of these interfering peaks. The diameter of the filter paper is the same as the surface area of the desorber. However, the inlet for the desorbed analyte into the ionization region is in the middle of the desorber. Therefore, if the analyte particle or analyte solution spike is not located at the center of the filter paper, all of the analyte is not introduced into the ionization region of the IMS. The IMS analysis of the filter paper was conducted immediately upon printing. There was no time given for evaporation since the filter paper tends to absorb the printed solution. From the desorption profiles it is observed, that desorption of the analyte is instantaneous and complete. The peak maximum however, is different between the different replicates and leads to large standard deviation when plotting replicates. In addition, losses are observed with the initial desorption of the analyte where the beginning of the profile seems to be cut off. This can lead to errors when plotting cumulative amplitudes because of the lack of data for the first few segments where the analyte is lost from the desorber. However, the mass response graph was linear over the range studied.

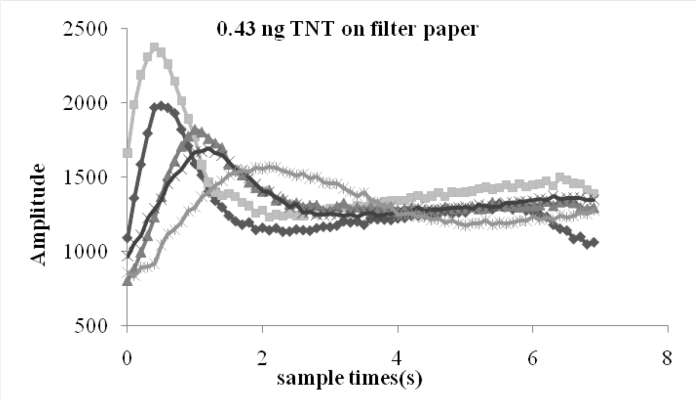

Figure 11: Desorption profile replicates for TNT on filter paper in Itemiser II

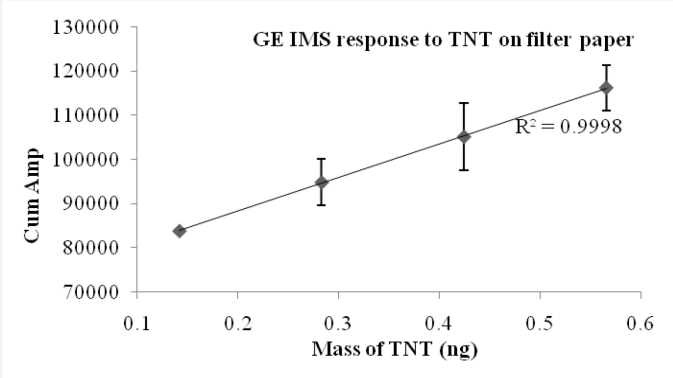

Figure 12: Response curve of TNT on filter paper generated by inkjet printing onto filter paper and analyzing by Itemiser II IMS

2. Teflon circles (0.015 inches thick): The substrate was made by cutting out circles of the same size as the filter paper from a 0.015 inches thick Teflon sheet. The thick Teflon was chosen as part of the study because of its beading property, heat resistance and the inertness of the Teflon surfaces. For equivalent comparison between substrates, no time is given for the solvent evaporation of the printed drops. Similar printed spot restrictions

as seen with the filter paper are applicable to this substrate as well. However, since there is no reinforcement to the edges of the Teflon, the circle deformed at the high temperatures of the desorber and added desorption errors. The Teflon also proved to be very thick and did not allow for rapid heating of the substrate and even heat distribution. All these effects are noticed in the desorption profiles depicted in Figure 13.

It is observed from the desorption profiles that desorption is not reproducible between replicates and is not sharp. Desorption is slow, uneven and incomplete. A response for the analyte was observed in a second desorption following the first. From the response curves, it is evident that the signal is less than that observed for the filter paper and that line is not as linear. The error associated with each data point is also higher. Therefore, this substrate would not be very effective in determining instrument sensitivity and response over a broad mass range.

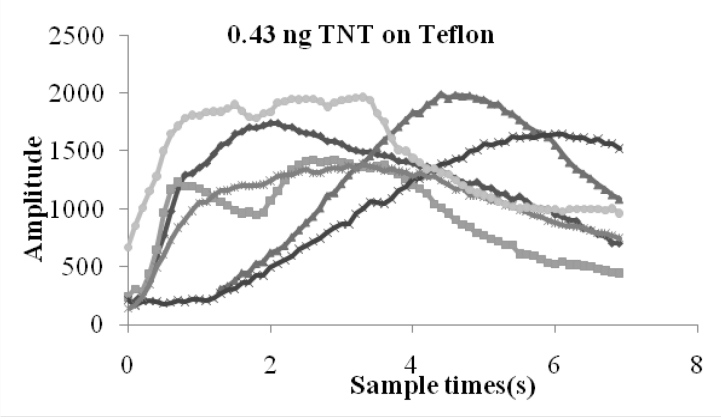

Figure 13: Desorption profile replicates of TNT on Teflon circles in Itemiser II

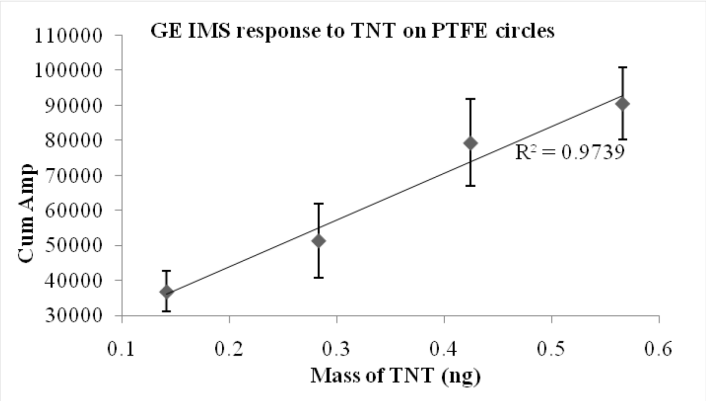

Figure 14: Response curve of TNT on Teflon circles generated by inkjet printing onto filter paper and analyzing by Itemiser II

3. GE Multiuse swipes: These swipes supplied by the manufacturer are synthetic polymer and mesh like in nature intended to trap particles when swiping surfaces. The swipe however has not been tested for solution-based analyses. The swipe was chosen for this study due to its availability, assumed trapping of analytes, heat resistance and thin film like nature. However, the swipe produces interfering peaks and needs to be pre heated to remove surface contaminants before deposition of the analyte. The swipe is also as the same size as the filter paper and gives irreproducible results based on where the analyte is deposited.

   The desorption profiles are sharp and give higher amplitudes than those observed for filter paper or for the multiuse swipes. Since the polymer material takes longer to heat than the filter paper, desorption is not as rapid as that of the filter paper. This is a preferred feature since, there are no significant initial loses in the desorber and yet desorption is complete

within the given analysis time. The mass response graph is much linear than that of the Teflon but gives higher cumulative amplitudes for the same mass when compared to the other substrates tested. The cumulative amplitudes are higher because of the higher amplitudes for each analysis segment. Though the desorption profiles are promising and has features of interest, this substrate was not included in further studies because of the multiple interfering peaks for other analytes not only in the negative mode but also in the positive mode IMS analysis.

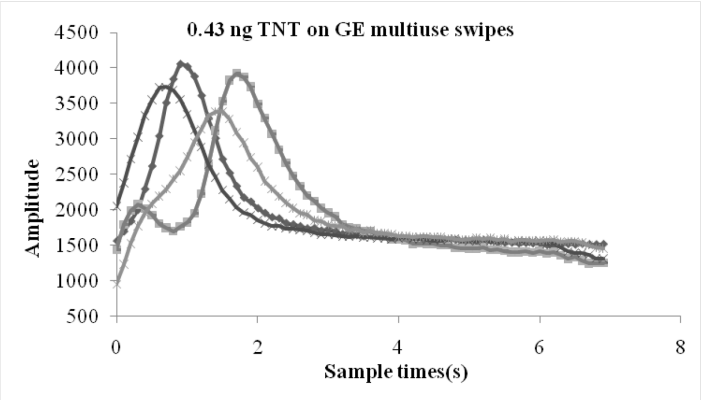

Figure 15: Desorption profile replicates of TNT on GE multiuse swipes in Itemiser II

The results described in the following paragraphs are for the Ionscan 400B instrument. Desorption profiles shown below are shown as obtained from the instrument software and therefore do not show several replicates in one graph. Therefore, the most representative profile for each substrate is shown. The default desorption time is 10 s in the Ionscan 400B which is longer than the default conditions

for the Itemiser II instrument. This increased sampling time accommodates analytes which have slow desorption times and substrates that take longer to heat.

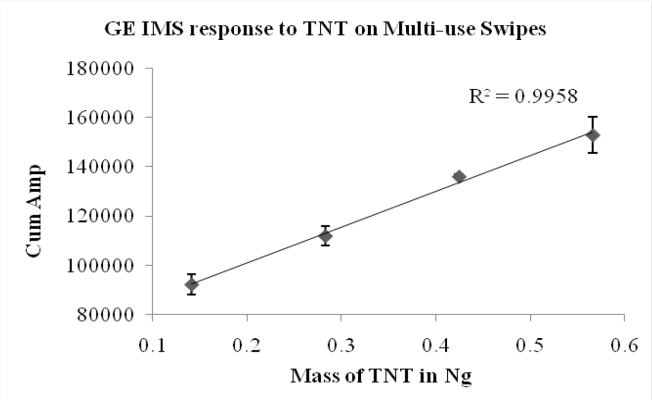

Figure 16: Response curve of TNT on Swipes generated by inkjet printing onto filter paper and analyzing by Itemiser II

1. Smiths Detection filters for narcotics: This filter is a cellulose based filter for collection of particles of drugs of abuse from surfaces. The other filters available for particle collection in the negative mode are polymer based. They were found not suitable for solution deposition and hence were not included in the study. The narcotic filter absorbed the printed drops and for the printed volume of less than 1nL, no evaporation time was given for the solvent.

   The desorption profile shown below reveals sharp, complete desorption of the analyte. The rise and decline of the analyte from the substrate indicates that there is sufficient time for both highly volatile and less volatile analytes to be completely desorbed from the surface without facing losses.

The peak maximum is representative of the entire desorption profile and can be used for accurate correlation of mass. The mass response graph is linear with about 5% RSD observed on an average.

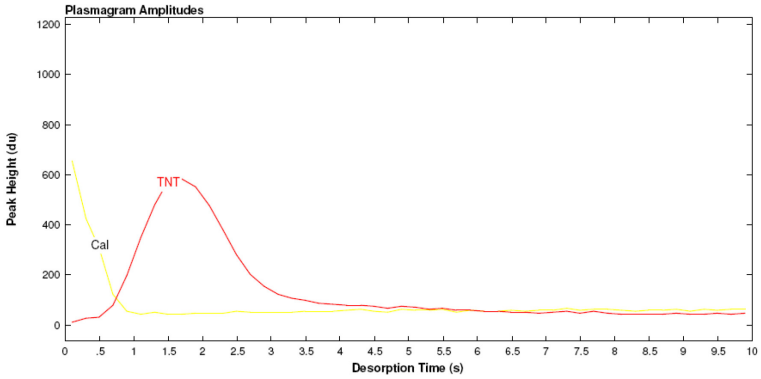

Figure 17: Desorption profile for TNT on Smiths narcotics filter

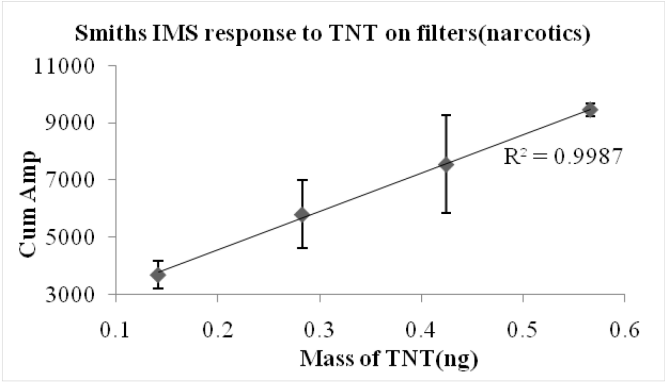

Figure 18: Response curve of TNT generated by inkjet printing onto Smiths filters and analyzing by Ionscan 400B

2. Smiths Detection Teflon film rings: The manufacturer supplies these Teflon films primarily for use in the pharmaceutical sector for solution spike analysis. The thin Teflon film is reinforced with a plastic ring to help the Teflon retain its shape on heating. This substrate could not be included

in the substrates studied in the Itemiser II instrument because of the melting of the plastic ring in that heated inlet design. In the Ionscan 400B instrument, the film tends to be damaged by the heated anvil during analysis and cannot be reused several times.

Overall, the Teflon surfaces are best suited for solution analysis and gives sharp, rapid and reproducible desorption profiles. Different solvents behave differently on the Teflon film affecting desorption and this has to be taken into consideration before choosing the solvent for the analyte. The peak maximum is higher than that obtained by the filter but the cumulative amplitude is much smaller since desorption is completed in less than five segments. Therefore, it is misleading to compare mass response between the filters and the Teflon films. Higher evaporation of the sample than absorption was observed with the Teflon substrates whereas greater absorption than evaporation occurred with the filters discussed earlier.

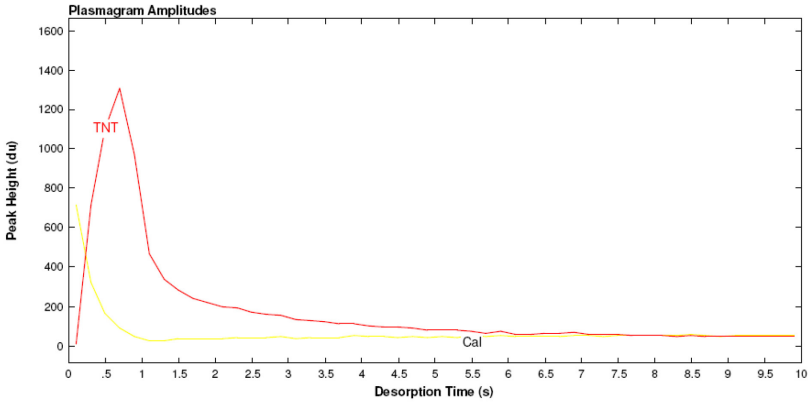

Figure 19: Desorption profile for TNT on Smiths Teflon film

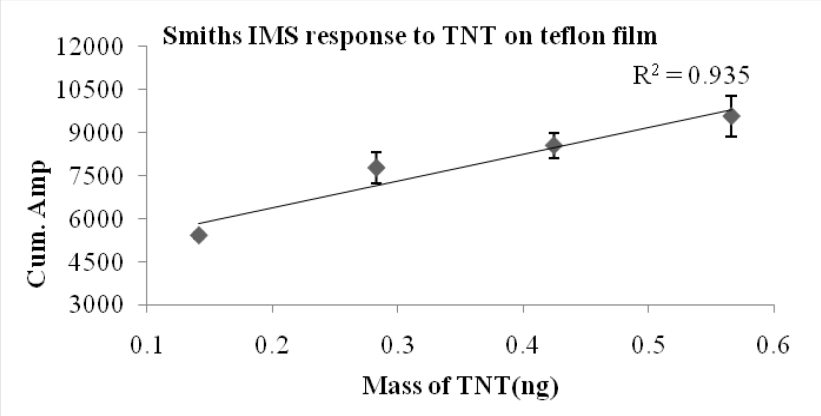

Figure 20: Response curve of TNT generated by inkjet printing onto Smiths Teflon film and analyzing by Ionscan 400B

3. Sample traps from GE Itemiser II: These sample traps are supplied by the manufacturer of the Itemiser II instrument and are intended to be used with a swipe handle for swiping surfaces. They are similar to the GE swipes discussed earlier but are stiffer and smaller. They were chosen for the Ionscan study because they were sized appropriately for the anvil of the desorber.

   The desorption was observed to be erratic for these substrates. Non-reproducible desorption characteristics were observed within the replicates. The mass response graph was also not linear for the range studied. The polymer based trap took longer to heat and gave slow but complete desorption of the analyte.

4. Teflon squares (0.015 inches thick): The same Teflon sheet that was used for the Itemiser II studies was used as a substrate for this study by cutting

it into the appropriate size for the desorber. The results were same as those observed for the Itemiser II. Several interference peaks with deformation of the substrate were the two main negative features of the Teflon surfaces.

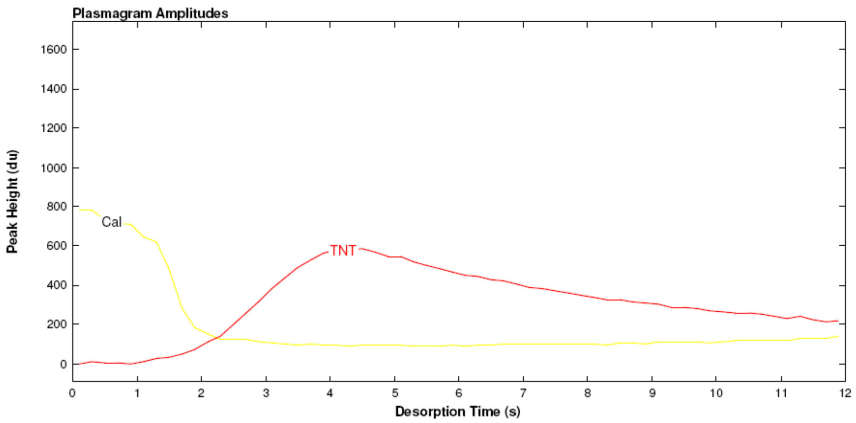

Figure 21: Desorption profile for TNT on GE Sample traps

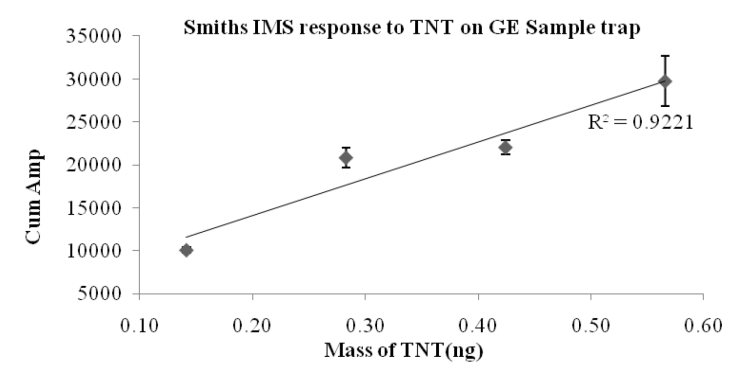

Figure 22: Response curve of TNT generated by inkjet printing on GE sample trap and analyzing by Ionscan 400B

As can be seen from the desorption profiles, the longer analysis time of the Ionscan enables complete desorption. Since desorption is slow and a

response for the analyte is seen in all the segments, the cumulative amplitude values are very high whereas the peak maxima are lower than other substrates.

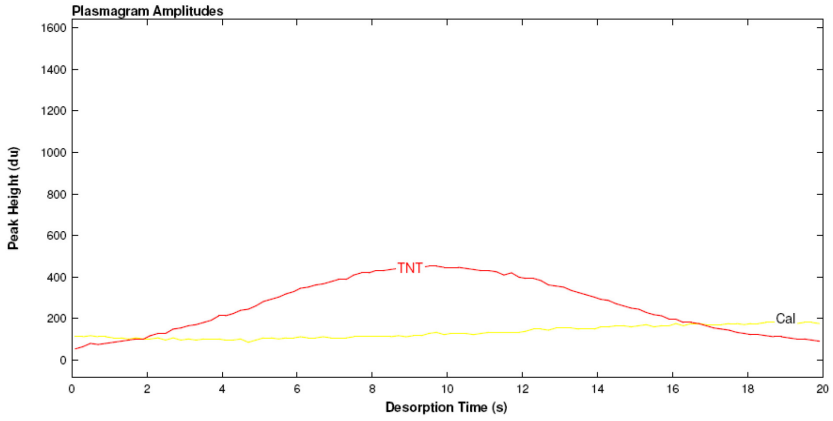

Figure 23: Desorption profile for TNT on Teflon squares

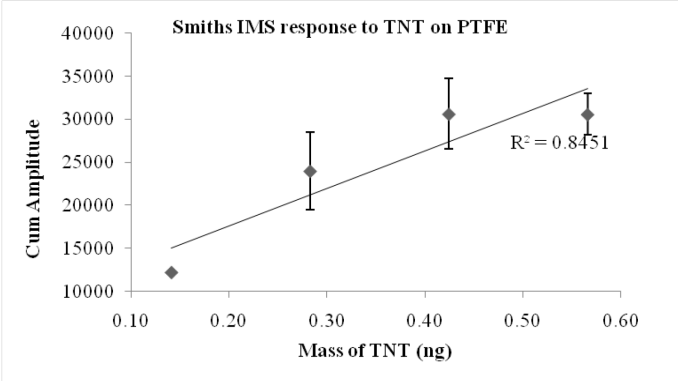

Figure 24: Response curve of TNT generated by inkjet printing on Teflon and analyzing by Ionscan 400B

5. PDMS coated glass slides: The polydimethylsiloxane (PDMS) coated glass slides were developed by Guerra et al., at FIU as an alternate SPME geometry[25]. They have been shown to have effective extractions of

organic volatiles from the headspace of target matrices. The substrate was chosen for this study due to its analyte absorption and retention properties. The analyte is expected to be released only on thermal desorption while the environmental losses are at a minimum.

From the desorption profiles, it was observed that when an analyte is spiked in solvent on the surface, desorption is delayed. A response for the analyte is seen towards the end of the sampling time. Increasing the sampling time and giving time for the solvent to evaporate helps improve the profile but does not improve the overall quantitation. Therefore, quantitation was not possible by such a printing method and no response curve is shown below that is comparable to the other substrates. It is also evident that the peak maximum is very small whereas the cumulative amplitude would be very high. Reducing the printed volume to a few picoliters (less than 1000) helps desorption a lot and enables quantitation. It is important to note that the response observed by these slides cannot be correlated using any other substrate. In order to determine mass extracted by these coatings from the headspace, a response curve of absolute mass present on the coatings is necessary since the peak maxima and the peak cumulative amplitudes do not correlate with the other substrates.

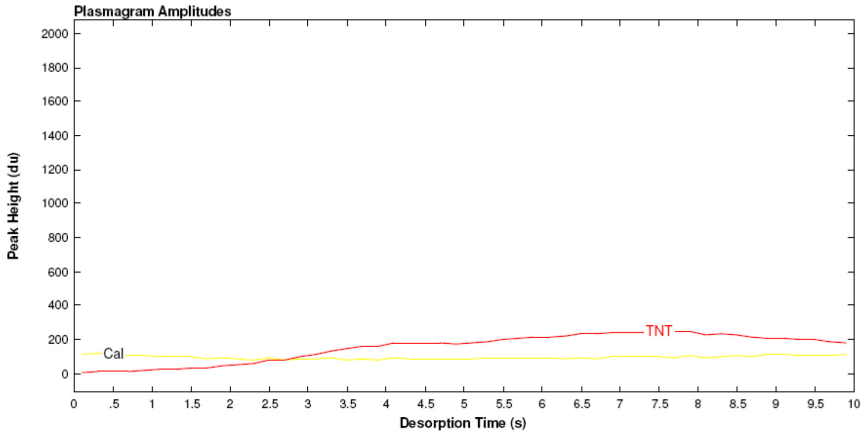

Figure 25: Desorption profile for TNT on PDMS coated slides

Conclusions:

Based on results observed for all the substrates in both IMS instruments, the following conclusions were drawn:

1. Not all substrates give similar mass response curves and determination of instrument sensitivity is based on the type of substrate used.
2. Comparison between the peak maxima or the peak cumulative amplitude of two different substrates leads to inaccurate mass correlations due to differences in substrate desorption profiles.
3. Of the substrates studied for printing low mass loadings, the ideal substrates are the Whatman filter paper and the Smiths narcotics filter, because of the complete desorption of analytes. The substrates are suitable for highly volatile fast desorbing analytes as well as low volatility slow desorbing analytes. Among the two, the Smiths narcotics filter is preferred because it has a cleaner blank profile and the size is suitable for both

instruments. The smaller size compared to the filter paper reduces the losses observed with the GE Itemiser II when using a larger surface area substrate.

2.3. Determination of limits of detection

The following section details the determination of absolute mass detection limits of the IMS instruments for a variety of illicit substances and related compounds. Microdrop printing is employed as a precise mass deposition tool for the delivery of mass onto substrates chosen from the study above. Inkjet printing allows for the introduction of known mass into the IMS instead of a solution of known concentration. The limit of detection (LOD) reported here is therefore the lowest mass present on a substrate that reliably produces a produces a peak that is significantly different from the blank signal.

Analytical challenge:

The primary feature of ion mobility spectrometry that continues to attract interest from security and law enforcement agencies are the low detection limits to known illicit substances. Apart from the nature of the compound being analyzed, response in an ion mobility spectrometer is determined by various factors such as moisture content in the drift tube, analysis temperatures, sample introduction methods, sample matrix, stability of the analyte product ions in the drift tube and the abundance of the reactant ions. The sensitivity of an instrument to the compound therefore depends on its ionization characteristics and varies with changes to analysis conditions. Compounds

with favorable proton affinities and electronegativities have lower IMS detection limits with reported values being in the parts per billion ranges[20,22].

Detection limits are described by various terms in different literature sources. In most analytical procedures, the mass level at which the analytical procedure reliably leads to detection is chosen as detection limits. Usually this is determined by drawing linear regression line of the response obtained by analyzing standards of known concentration. In IMS analysis, the formation of product ions is associated with a decrease in reactant ions. As such, formation of product ions occurs until all reactant ions are depleted. Thus, there is a narrow mass range within which the response is linear, beyond that the response is independent of the mass introduced. As discussed above, IMS response is affected by sample matrix and sample introduction methods and the response is based on the abundance and stability of the product ions formed from the analyte. The alarm level in an IMS instrument is a user-defined value and is the signal level, at which the instrument is programmed to give an alarm for the presence or absence of the substance. The alarm level does not always mean the detection limit. The following study establishes the absolute mass detection limits of IMS instruments while highlighting the differences in response between instruments and does not consider the programmed alarm levels.

Experimental method:

The analytes of interest for this portion of the study include drugs of abuse such as cocaine, 3, 4 methylenedioxymethamphetamine (MDMA), explosives such as 2,4,6-Trinitrotoluene (TNT), Hexahydro-1, 3, 5-trinitro-1,3,5-triazine (RDX) and

target odor signatures such as diphenylamine (DPA) and ethyl centralite (EC). The explosives and drugs were purchased as analytical standard solutions from Cerilliant (Round Rock, TX). DPA and EC standards were purchased from Fisher Chemical (Fairlawn, NJ). A 5 ng/ μL solution of each analyte in isobutanol was prepared and the mass delivered onto a substrate was varied by varying the number of drops printed. Each solution was optimized for optimal drop generation and printed onto the chosen substrates. The substrate used for the Itemiser II was the Whatman filter paper and for the Ionscan 400B, the narcotics filter was used.

Table 1: Operating parameters of IMS instruments

GE IONTRACK ITEMISER II	SMITHS DETECTION IONSCAN 400B
1. Heated desorber with large surface area for inserting sample. 2. Positive mode (+ve): Cocaine, MDMA, DPA, EC 3. Negative mode (-ve): 2,4,6-TNT, RDX 4. Drift tube temperature: 180 ^{o}C 5. Desorber temperature: 220 ^{o}C 6. Sample flow: 1000 mL/min 7. Drift flow: 200 mL/min	1. Enclosed heated desorber unit with smaller surface area. 2. Positive mode (+ve): Cocaine, MDMA, DPA, EC 3. Negative mode (-ve): 2,4,6-TNT, RDX 4. + ve mode parameters: Drift tube: 235 ^{o}C; Desorber: 285 ^{o}C; Drift flow: 300 cc/min; Sample flow: 200 cc/min

8. +ve mode dopant: Ammonia 9. –ve mode dopant: Methylene Chloride	5. -ve mode parameters: Drift tube: 115 ^{o}C; Desorber: 245 ^{o}C; Drift flow: 351 cc/min; Sample flow: 300 cc/min 6. +ve mode dopant: Nicotinamide 7. -ve mode dopant: Hexachloro ethane

Table 1 above lists the operating parameters for both the IMS instruments used for the detection of the printed analytes. Since the aim of this study is demonstrate the lower mass detection limits and the sensitivity of the instruments, a narrow mass range of less than one order of magnitude was chosen. The mass response graph for each analyte is used to depict the behavior of the analytes for each of the instruments. In cases where there is an inherent instrument signal or blank signal at the drift time of interest, the detection limit for the analyte was chosen as the mass response that was three times the standard deviation from the blank signal and blank subtraction was used to plot signal values. In cases where the blank has no signal at the analyte drift time, the lowest mass deposited on a substrate that gave a peak reliably for the analyte was chosen as the limit of detection.

Results and discussion:

The mass response curves for each analyte are shown in Figures 26-31below. Not all compounds of interest could be analyzed in both instruments. Isobutanol generates

peaks in the positive mode of the Itemiser II with ammonia as the dopant. These peaks interfered with the analyte peak as the number of drops printed increased. This led to the improper quantitation and therefore the response curves for many of the analytes for positive mode in Itemiser II are not presented below. The K_0 values of each compound, their drift times in both instruments and the absolute detection limits are listed in Table 2.

1. 2,4,6-TNT: The IMS behavior of TNT has been well studied and reported[23]. It is used as a model compound for IMS due to its known sensitivity. The formation of the proton abstracted product ion $(M-H)^-$ is considered to be favorable and hence leading to lower limits of detection and good sensitivities. Literature and manufacturer reported values lie between 200 pg- 500 pg. Its high vapor pressure and therefore short lifetime of residues on surfaces make the study of detection limits and instrument sensitivity important.

   In the response curves shown below it is evident that the response of the instrument is linear over a short mass range. Percent relative standard deviations (% RSD) of less than 20% were observed for both instruments. The significant change in instrument response to a small change in mass indicates that both instruments have high sensitivity to the analyte. Limits of detection for the Ionscan 400B (30 pg) were lower than the Itemiser II (60 pg). This is attributed to the differences in the desorber design, substrate used and analysis temperatures.

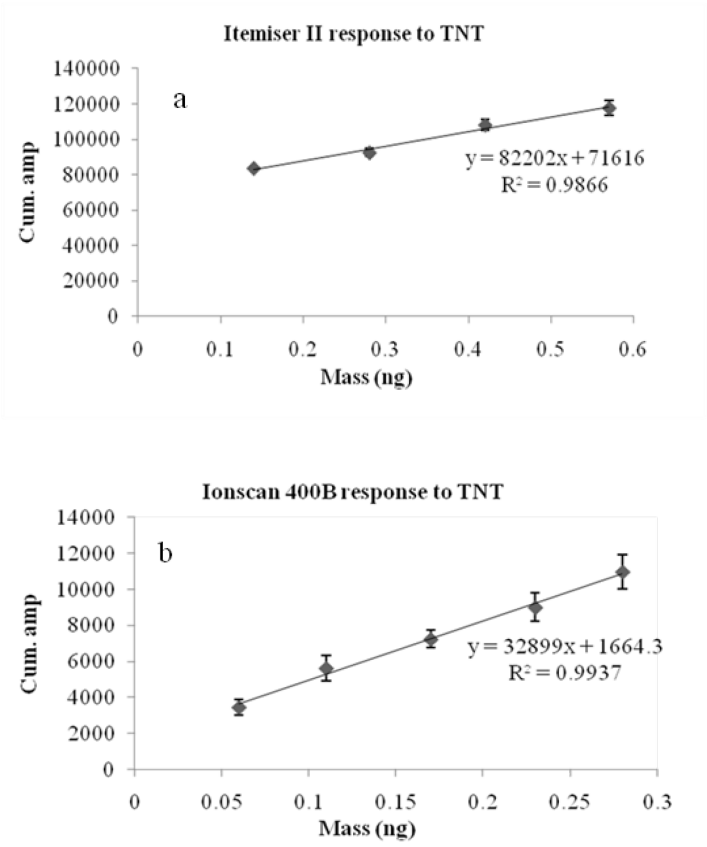

Figure 26: Mass response graphs for 2,4,6-TNT generated by microdrop printing onto filters chosen for a) Itemiser II b) Ionscan 400B and analyzed in the negative mode

2. RDX: This is a military grade high explosive used in the making of Composition 4 explosive. As such, this explosive is rarely detected as a pure analyte in the field. RDX has low volatility and by nature tends to stick to surfaces, and therefore residues and particles transferred onto surfaces tend to remain for a long period. This makes this analyte an important target analyte for IMS instruments installed in high security areas.

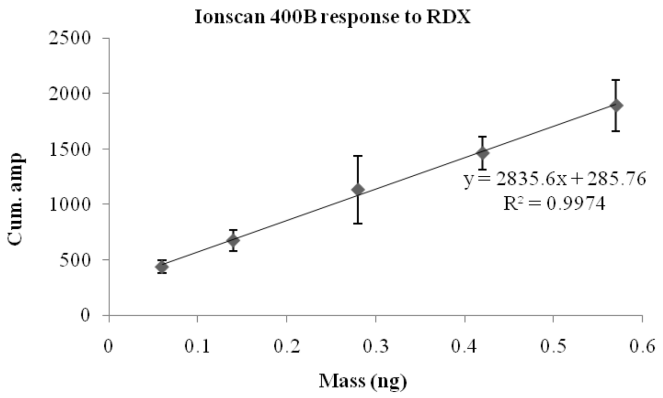

Figure 27: Mass response graph for RDX generated by microdrop printing onto the filter chosen for Ionscan 400B and analyzed in the negative mode

The thermal instability of RDX leads to its fragmentation in the ionization and drift region leading to the formation of various product ions. In the Ionscan 400B ionization and temperature method, three peaks are observed for RDX- RDX1, RDX2 and RDX3. Based on literature, the most stable adduct formed in a chlorine environment is a $M.Cl^-$ ion[23]. The fragmentation makes quantitation difficult. Shown above is the graph of RDX1 (chloride adduct peak) response on the Ionscan 400B. The graph depicts that the response of the product is linear over the mass range studied but the analysis is associated with errors. As the mass of RDX introduced into the IMS increases, the standard deviation of the replicate signals increases. This is due to the formation of other product ions giving rise to RDX2 and RDX3 peaks. Similar graph could not be conducted on the Itemiser II due to the lack of reproducibility in response.

3. Cocaine: Cocaine is a drug of abuse, found very commonly as a white powdery residue. It has been studied well in the IMS for positive mode detection. It forms product ions by protonation. The $(M+H)^+$ ion is formed in abundance and low detection limits have been reported by instrument manufacturers and other literature sources.

   From the response graph shown below for the Ionscan 400B, it is evident that the response of the instrument is linear over the mass range tested and the error associated with each point on the graph is minimal. The mass limits of detection are as low as 30 pg.

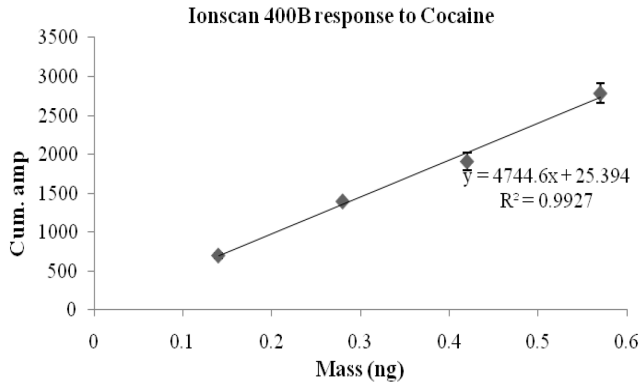

Figure 28: Mass response graph for cocaine generated by microdrop printing onto the filter chosen for Ionscan 400B and analyzed in the positive mode

4. MDMA: 3,4-Methylenedioymethamphetamine is a drug of abuse commonly available as the ecstasy tablets. The ionization and formation of product ions occurs through the proton transfer from the nicotinamide atmosphere in the Ionscan. The response graph below depicts the

sensitivity of the instrument to the analyte with the large change in response for a small change in mass. The analyte response is linear within the analyzed mass range with low detection limits.

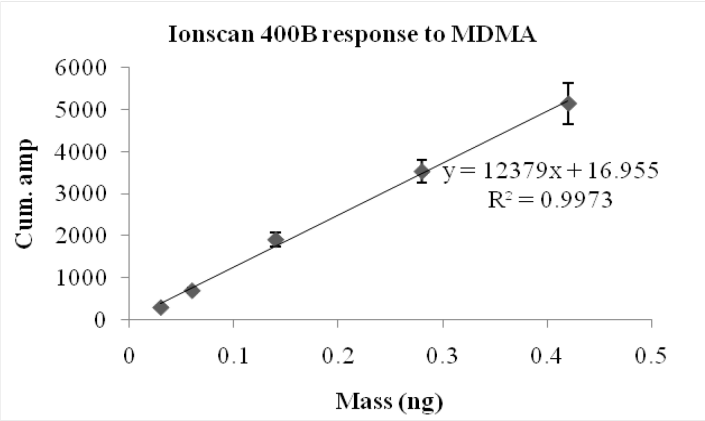

Figure 29: Mass response graph for MDMA generated by microdrop printing onto the filter chosen for Ionscan 400B and analyzed in the positive mode

5. Diphenylamine: This compound is not present in the IMS manufacturer detection menu. Diphenylamine and ethyl centralite are compounds of interest to this because of their use in smokeless powders manufacturing. Later sections of this dissertation will discuss their uses and their detection by IMS. They are both detected in the positive mode by proton transfer and formation of a protonated species.

   Figure 30 below shows the response of the two IMS instruments to diphenylamine. In both instruments, the response is linear but associated with greater than 25% RSD. The mass range studied for the Ionscan 400B is between 0.05ng- 0.8 ng whereas for the Itemiser II a larger range from

0.1-2.5 ng was studied. The sensitivity to of the Itemiser II to the diphenylamine is observed to be lower than that that of the Ionscan 400B due to the smaller changes in response associated with same change in mass. The diphenylamine also loses linearity beyond a certain mass and establishes a second linear range where the slope is much smaller.

6. Ethyl centralite: Literature suggests that the product ion formed by protonation of ethyl centralite is highly stable and thus leads to its lower detection limits[26]. This is evident in the graph shown below. As the mass reaches the limit of detection, the response is non-linear. In addition, it can be observed from the graph, that the higher end of the mass limit before the response plateaus is also being reached. A response graph for the Itemiser II could not be generated in this solvent and current method, due to the non-linearity of the response and the very high detection limits. The analyte response graph for Itemiser II is discussed in the following sections with a different solvent. A response to the analyte in this printing method and substrate was observed at 12 ng, which is very high compared to the 15pg observed for the Ionscan 400B.

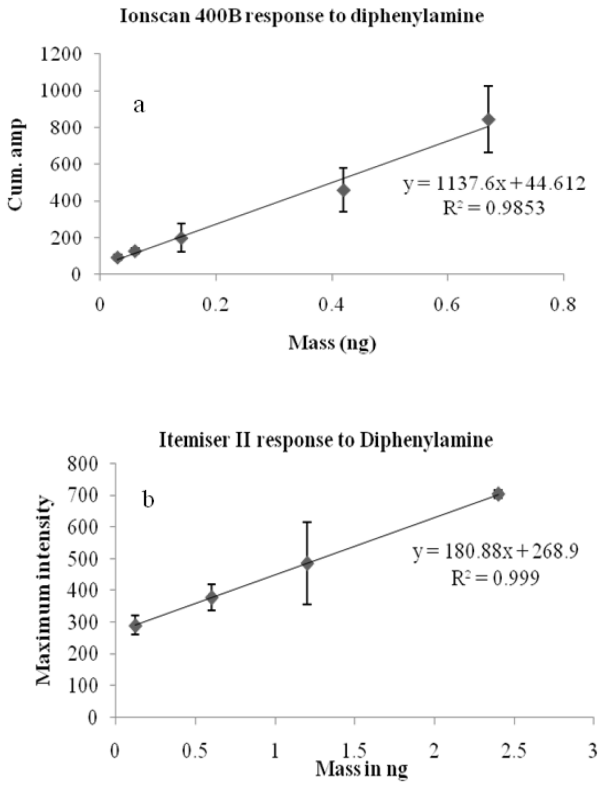

Figure 30: Mass response graph for diphenylamine generated by microdrop printing onto IMS filters for a)Ionscan 400B b) Itemiser II and analyzed in the positive mode

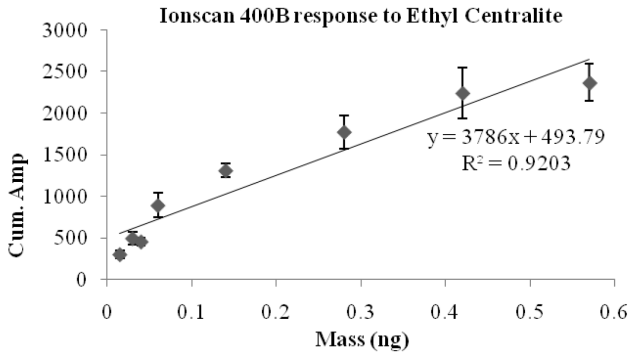

Figure 31: Mass response graph for ethyl centralite generated by microdrop printing onto an IMS filter and analyzed in the positive mode

Table 2: Analyte detection parameters for both IMS parameters and their LOD values

Analyte	K_0	Drift times (ms)		Limits of detection (ng)	
		Ionscan 400B	Itemiser II	Ionscan 400B	Itemiser II
2,4,6 -TNT	1.45	12.804	6.32	0.030	0.060
RDX	1.38	13.367	6.61	0.040	0.060
Cocaine	1.16	15.456	8.52	0.030	NA
MDMA	1.47	12.086	6.61	0.030	NA
Diphenylamine	1.61	11.185	6.20	0.030	0.120
Ethyl centralite	1.24	14.416	7.66	0.015	12.0

Study of stability of printing and instrument response:

In order to evaluate, the printing method and the response of the Jetlab 4 printing station, a four-week study was conducted. 2,4,6-TNT was chosen as the analyte for the study and a standard solution of 10 ng/μL was prepared in 2-butanol. The printing parameters were optimized as before for this solution. A mass range of 0.1 to 2 ng was delivered to the substrates by varying the number of drops printed. The printing was conducted once every week using the same optimized parameters and analyzed using

the Ionscan 400B IMS. The volume of a single drop as measured for the four weeks varied between 181 pL to 209 pL with an average of 190 pL.

The graph with the curves for each of the four weeks is shown below in Figure 32. The graph demonstrates that the printing parameters were optimized well and that the printing was stable at these parameters within a single day and between weeks. The smallest drop volume was measured on week 1 leading to a graph with lower instrumental response. Within a single day the %RSD's on an average varied between 3 and 20 while the overall % RSD's over the four weeks was about 15.

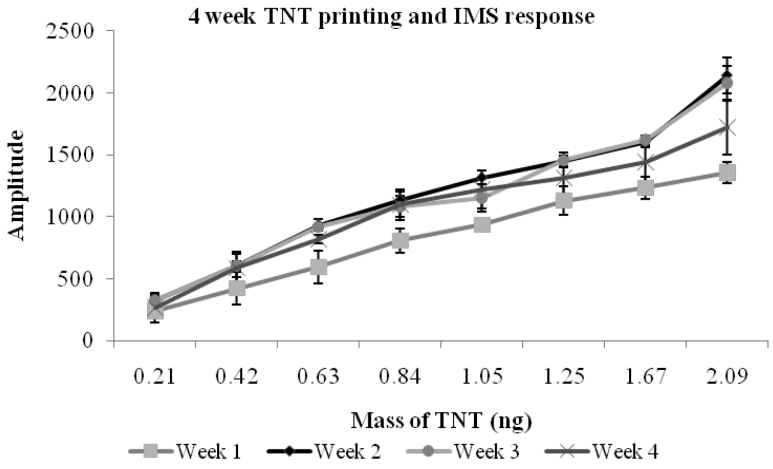

Figure 32: Response curve for 2,4,6-TNT showing instrument stability and printing method stability over four weeks for the negative mode of the IMS

Conclusions:

From the above results, it is reasonable to conclude that microdrop printing is a precise mass delivery method that can be used to determine absolute mass detection limits. It is also evident that the limits of detection reported in literature are generally

close to one order of magnitude higher than those reported here. This will be further examined in the subsequent sections of this dissertation. Inkjet drop-on-demand printing is a very effective tool for depositing mass on surfaces that are then subjected to chemical analysis. In analytes where more than one product ion is formed or in cases where dimer formation is observed, inkjet printing can be useful to determine the mass of the analyte introduced into the IMS that result in the formation of dimers or secondary product ions. The stability of the printing and IMS response graphs provide substantial evidence that the availability of such graphs can be indicative of radical changes in instrument sensitivity or response to an analyte.

3. INKJET PRINTING AS MASS DELIVERY METHOD FOR LIBS

Successful implementation of microdrop printing for IMS led to its application to other surface analysis techniques such as Laser ablation- Inductively Coupled Plasma Mass Spectrometry (LA-ICPMS), Infrared spectrometry, Raman spectroscopy and Laser Induced Breakdown Spectroscopy (LIBS). The section that follows describes the utilization of drop on demand printing as a mass delivery method for analysis by LIBS.

Introduction to LIBS:

Laser Induced Breakdown Spectroscopy (LIBS) is an atomic emission technique that provides qualitative and quantitative analysis of elemental composition of gaseous, liquid and solid samples[27,28]. A laser pulse of sufficient energy is focused by a lens into or onto a sample causing the sample to breakdown and generating a plasma.

The plasma contains neutral atoms, excited atomic and ionic species of sample. The sample preparation and ionization therefore occurs in a single step. The light emitted by the excited species during the plasma decay is collected and dispersed into different wavelengths using a spectrometer. These wavelengths are specific to the different elements present in the sample each of which produce an exclusive element spectrum. Therefore examining the spectral information of the plasma gives elemental characterization of the sample[27,28]. A schematic of a functional LIBS set-up is shown below in Figure 33.

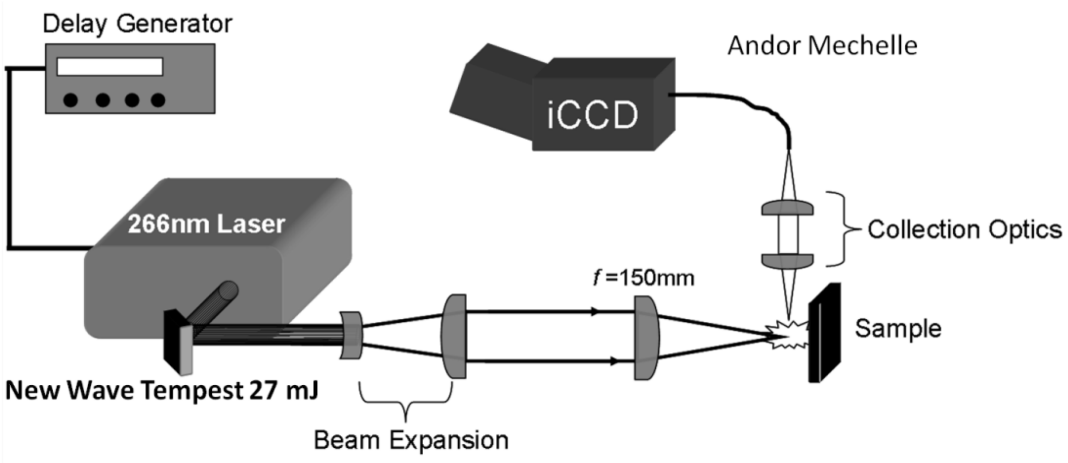

Figure 33: Schematic of LIBS experimental setup[29]

Typically, no sample preparation is necessary and any material that interacts with a laser can be analyzed. Qualitative elemental information is obtained immediately and careful calibration gives quantitative information. However, the processes involved in the ionization and low sample laser interaction spot make the overall sensitivity of the technique poorer compared to LA-ICPMS[27]. Different elements have different LIBS behaviors with reported limits of detections varying between parts per

million to parts per billion range[30]. In LIBS analysis, several factors such as sample matrix, analysis methods, laser parameters and detector parameters affect the precision, accuracy and sensitivity of the method. Several calibration methods such as calibration standards, matrix matched standards have been used to provide optimum quantitative information[27,31]. The research discussed here furnishes evidence for the utility of calibration strategies for LIBS instrumentation that are based on the delivery of sub-nanogram quantities of elements onto surfaces. The possibilities of such microdrop analyses were first mentioned by Godwal et. al. as applications of the lab on chip method applications of LIBS[32]. The following section exemplifies the various ways in which microdrop printing methods can be applied for LIBS techniques.

3.1. Method for printing aqueous metal solutions

Objective:

Laser induced breakdown spectroscopy can provide useful quantitative information for the determination of elemental composition of a variety of matrices. In practice, the LIBS emission intensity is relative to the absolute mass or relative concentration of the metal present in the matrix. However, calibration methods are necessary to calibrate the instrument response for a specific matrix. For solid samples, matrix matched standards are made by preparing standards in the same method as the samples but with known elemental concentration. Some calibration standards available from NIST may be used for spectral and intensity verification. However, all these methods are based on determination of the concentration of the element or elements in the standard. Absolute mass calibration is quite hard to achieve with LIBS due to the

effects of the laser and matrix interaction and homogeneity of the prepared standards. Within this section is described an inkjet printing method to deposit known mass of analytes onto a solid surface and performing LIBS analysis on the surface. This helps to determine instrument response to ablation of known mass in a precise location on the sample. My role in this collaborative project was to conduct all the sample preparation and the sample delivery by microdrop printing, while the LIBS teams conducted the analysis.

Experimental method:

Metals such as strontium (Sr), Barium (Ba) and Titanium (Ti) were chosen for this study due to their known sensitive LIBS behavior. A 250 ppm aqueous solution of each analyte was prepared in 5% HNO_3. The substrate chosen for the analyte deposition was a standard aluminum scanning electron microscopy (SEM) pin stub mount purchased from Ted Pella, Inc. (Redding, CA). The analytical data for the stub was obtained from the manufacturer to ensure that there were no inherent traces of Sr, Ba or Ti in the stubs. In order to make the stub amenable for the printing process and the LIBS sampling, the pin of the stub was mechanically removed so that a flat surface was obtained on both surfaces.

Vital to the accuracy and precision of this technique are pre-determined locations of analyte deposition that assist in the accurate focusing of the laser during analysis. The sample wells were made using a laser ablation process using the Cetac LSX 500 (Omaha, NB) equipped with a Nd:YAG laser at 266 nm. A spot size of 200 μm and 100 shots were used to create a crater with a depth of 15 μm. Several craters were

made on the stub such that each column of craters corresponds to a printing replicate. These craters were used as sample cells into which the analyte drops were printed.

Optimal printing of the aqueous elemental solutions was obtained with a bipolar waveform at a voltage of +18.0/-18.0 V, dwell at 11.0 μs and echo at 35.0 μs. The rise and fall times were maintained at 3.0 μs. Drop generation frequencies between 300-600 Hz were used. Printing varying mass was achieved by varying the number of drops printed in each crater. Based on the volume and depth of the crater it was determined that no more than 14 drops could be printed in a single crater. The stub was placed on the stage of the printing station and the printing device aligned with the crater using the cross hairs of the vertical optics and the visualization of the horizontal optics. Instead of a burst method, a single drop trigger method was used to print the drops, so that each drop was placed in the crater individually and no spillage occurred. Images of the craters before and after LIBS analysis are shown below in Figure 34. The scanning electron microscopy (SEM) images were taken on a Philips XL30 SEM (FEI, Oregon), while the 3D images of the craters were generated using a Keyence (Atlanta, GA) VHX-500F series digital microscope.

Results and discussion:

LIBS analysis was conducted by the LIBS collaboration team to generate absolute mass response graphs for LIBS and to determine the limits of detection for the elements of interest. On aligning the LIBS laser and focusing it onto the crater, the analysis is conducted such that the number of laser shots used completely ablates the printed analyte. An accumulation of the signal over the various shots provides the

cumulative signal for the mass of the analyte present in the crater. The graphs shown below in Figures 35 and 36 for Ba and Sr demonstrate the reproducibility of the printing and the feasibility of the printing method for LIBS analysis on surfaces. The relative standard deviations (% RSD) of the printing for the calibration graphs were within acceptable range and varied between 6- 14% for Sr and 15-22 % for Ba. The results from the multi-elemental standards indicate that this method can be used effectively as a LIBS standard preparation method and will be further studied to develop robust calibration schemes. Unlike pressed pellet standards, these standards provide homogenous mass distribution within the laser focus and enable absolute mass quantitation for a given LIBS analysis method. The same printing method can be applied for the standard addition method for calibration of LIBS analysis.

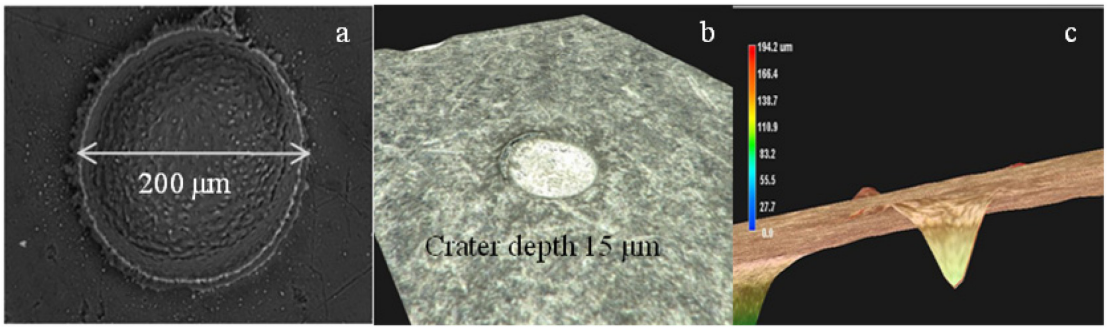

Figure 34: a) SEM image of crater to measure width; b) topographical images of the crater c) 3D image of a drop after ablation showing the conical crater

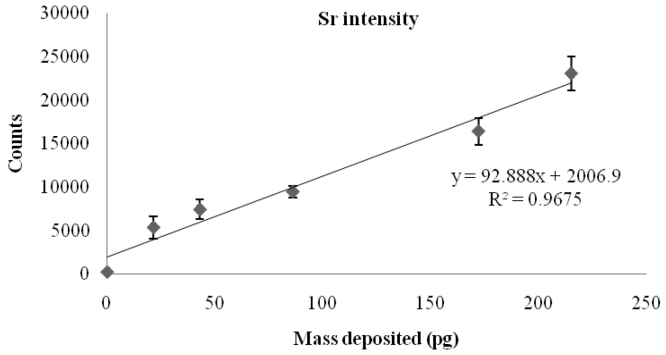

Figure 35: Drop-on-demand printing generated LIBS calibration graph for Strontium

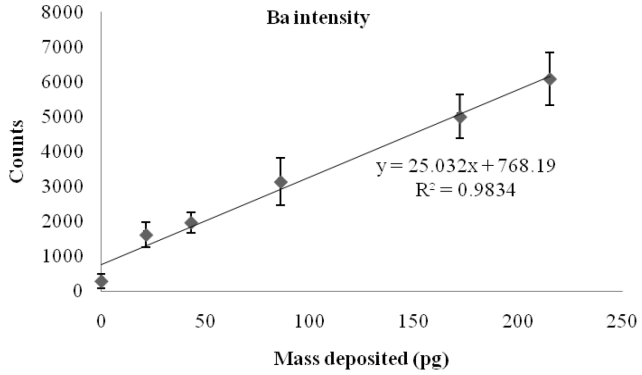

Figure 36: Drop-on-demand printing generated LIBS calibration graph for Barium

3.2. Printing patterns on surfaces for mapping

Objective:

LIBS as discussed above provides rapid elemental characterization of surfaces. With the flexibility available for changing spot size and laser energy, several surfaces can be characterized with minimal sample preparation to study surface compositional

changes within a small area[30,32,33]. An application of LIBS that has recently been studied is the development of LIBS as a surface mapping technique. In the research study described below, inkjet printing is employed as a tool to deposit known mass over a surface followed by LIBS analysis. The precise mass deposition provided by inkjet printing is used to demonstrate the resolution of the laser and the ability to differentiate elemental changes on the surface.

Experimental method:

The Jetlab 4® station with the Jetlab™ software features 3D motion stages that can be programmed to move precisely and print a specific number of drops at a certain location. Thus with the help of a script for the stages and the jet trigger, the software and the stages can be controlled to print a pattern of an analyte on any given substrate. This feature is utilized to generate a script for the university logo. The script is shown below in Figure 37. The script is programmed such that the stages move by a step size of 0.25 mm between drops. The drops printed per spot can be determined before printing. The substrate on which the pattern is printed is the same aluminum stub used for the study discussed above.

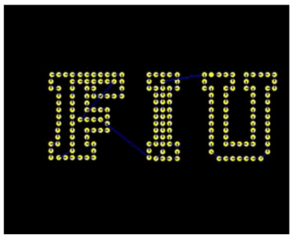

Figure 37: FIU logo printing pattern resulting from the script written to program the Jetlab 4 stages

The size of the pattern was determined such that it would cover substantial area of the stub. The number of drops per trigger was chosen such that the drops would not flow into each other and that there would sufficient resolution for the laser to differentiate between the drops. On printing the pattern, the stub was scanned using a 266 nm laser with a 215 μm spot size. Figure 38 below shows the stub before and after laser analysis.

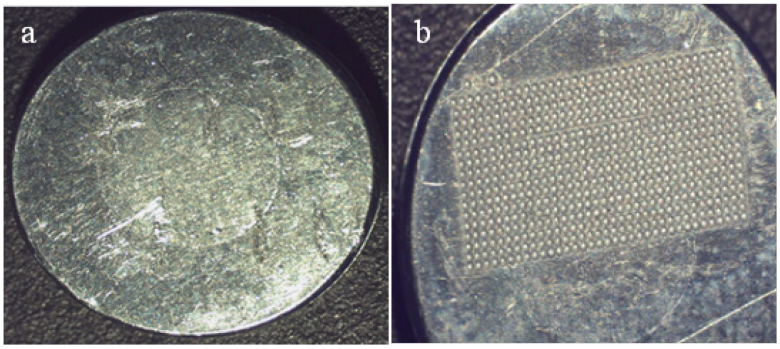

Figure 38: a) Stub with FIU pattern printed on it; b) Printed stub scanned by laser for mapping Sr on surface using an optimized LIBS method

Results:

The results of the laser ablation are shown in the Figures below. The data is processed such that the signal for the analyte, Sr in this case is seen as lighter compared to the background. The data was processed using Wolfram Mathematica® software. The 2D images show a clear pattern Sr in the FIU logo. The 3D images with the color legend show the highest concentration as the lightest color. It is evident that the mass was printed evenly across the surface and the inkjet printer can be used to generate patterns of analyte onto a substrate reliably. Printing of aqueous solutions

poses some issues with the wetting of the printing device and satellite production. Careful optimization of the printing solutions and printing parameters can resolve the few satellite drops evident in Figure 39. The 2D and 3D mapping of the surfaces is a very important application of LIBS and will be further studied.

The drop-on-demand printing method can be successfully used as pattern generator of analytes with varying concentrations. Multi-elemental patterns can be printed for LIBS analysis to validate the LIBS mapping method and to demonstrate the mapping in applications such as gunshot residue analysis where the different elemental components are distributed over a surface. Mapping can also be applied in heterogeneous matrices and pellets to establish the distribution of the elements on the surface.

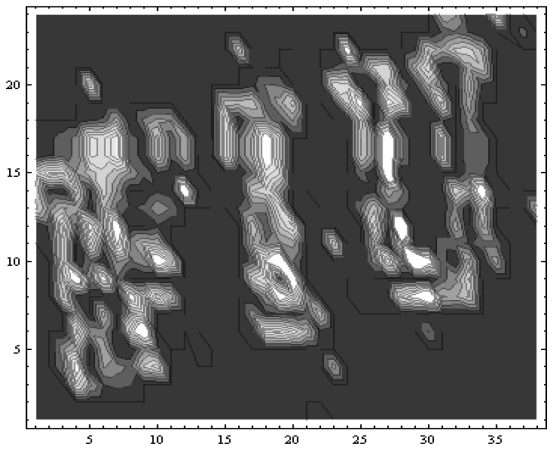

Figure 39: 2D surface mapping by LIBS of the printed analyte pattern

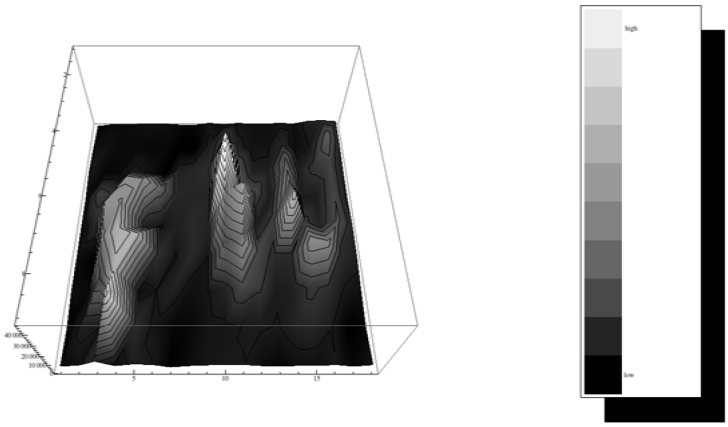

Figure 40: 3D surface mapping result by LIBS of the printed pattern of FIU on an aluminum surface

3.3. Other drop-on-demand applications for LIBS

Shadowgraphy for studying drop generation:

The drop-on-demand print station utilizes a strobe light to generate images of the drops as they are produced. Adjusting the strobe delay allows one to visualize the drops at their various stages of generation and deposition. A laser can also be used as a strobe for studying the same phenomenon by generating time-resolved images of the drops. It was expected that the study of the drops and their generation characteristics would be useful for further LIBS applications. Shadowgraphy with lasers has been used in several applications to study plasma generation characteristics and other dynamic phenomena. The technique of shadowgraphy was employed to develop these images where the drop image is generated as a dark object in the path of the laser light.

In this study, a 532 nm continuum laser with a pulse width of 5 ns was used as the strobe for the drops. The JetDrive™ III electronics were triggered externally with the laser trigger and the delay of the laser Q-switch was used to generate time-resolved images of the drops being formed. A series of filters were used to reduce the intensity of the laser light such that only the shadow could be observed. A movie of the drops being generated was sequenced by the images and developed by Dr. Cleon Barnett. The images are shown below with the time scale of the drop generation.

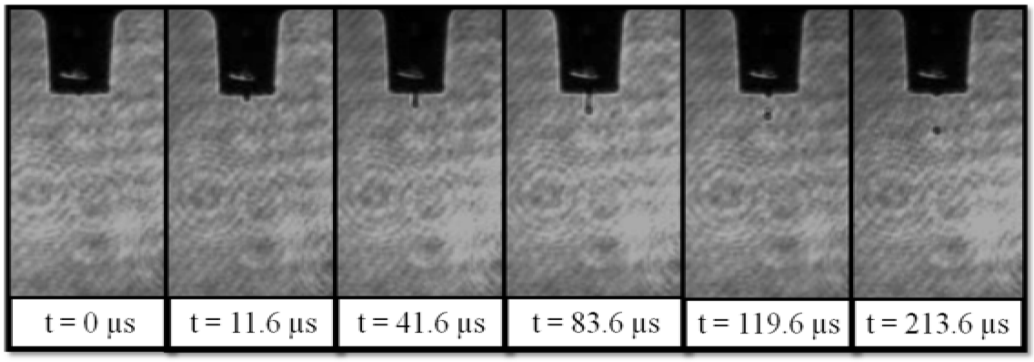

Figure 41: Time-resolved images of microdrops created by LIBS shadowgraphy technique

The study was later to be extended to study microdrop-produced plasmas in air from the laser ablating the microdrop before it hit the substrate. However, there needs to be further optimizing of the repetition rate of the laser and the drop such that the laser is able to ablate the drop mid-air. Such studies can give further information about the signal observed for absolute mass of an analyte in the laser focus.

Printing explosives for LIBS

LIBS has been used for the generation of rapid real-time elemental information in the laboratory based setting which make it as an attractive technique for field analysis. Several recent research efforts of LIBS have been directed towards making the technique robust for the field. LIBS applications require optics that focus the laser onto a sample to ablate and generate the plasma and optics to collect the emission. These optical systems can be configured for long-distance operations such that the laser is accurately focused onto a target that is several meters away. This led to the testing of LIBS for the standoff detection of hazardous substances such as explosives.

The Army Research Lab (Adelphi, MD) was testing a sensor developed by A3 Technologies (Aberdeen, MD) for the standoff detection applicability of LIBS. The remote sensing capabilities and the sensitivity of the sensor were two important characteristics to be tested. A3 approached FIU to generate standards that they could use for the LIBS sensor testing. Drop-on-demand microdrop printing method was chosen to generate standards within the detection mass range of the instrument.

A mass range of 0.001- 5 mg/cm^2 was required within a small area for the laser to focus upon. Therefore, similar approach as was taken for the mass response curves for LIBS was used with the formation of craters on an aluminum stub to be used as sample cells. Shown below is a Philips XL30 SEM backscatter image of a sample crater on the edge of an Al stub to reveal the depth of the crater. Each crater created had an average area of 3.8 x 10^{-4} cm^2 area with walls created by the aluminum ejecta that prevent overflow of the analyte from the crater.

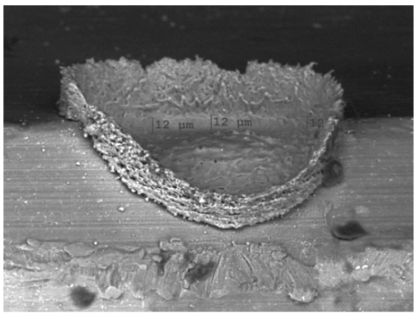

Figure 42: Crater on Al surface for microdrop deposition of explosives- Slanted edge measurements taken using a scanning electron microscope

The explosive chosen for this project was composition 4 M112 explosive with an RDX mix. Because of the low volatility of RDX which accounts for its longer lifetime on surfaces, it was anticipated that the explosive would be retained in the craters until analysis was conducted. The explosive was dissolved in cyclohexanone and different concentration solutions were made such that five different concentration ranges- 0.001mg/cm^2, 0.01 mg/cm^2, 0.14 mg/cm^2, 1.4 mg/cm^2 and 42 mg/cm^2 could be printed. Average drop volume for cyclohexanone at optimized printing conditions was 113 pL ± 20 pL and five drops were required to evenly coat the crater floor. Based on this five drops of each standard solution were printed such that every concentration had three stubs with five craters each thus having 15 replicates per mass value. The final absolute mass amounts printed in a 3.8 x 10-4 cm^2 area were: 0.526 ng, 5.26 ng, 52.6 ng, 526 ng and 16 µg.

Analysis results from the above LIBS testing could not be obtained due to the classified nature of the research. However, the contribution of drop-on-demand printing for standoff techniques is very important. It helps generate information about

the reliability of the standoff technique for detection analytes within a precise area accurately. Further testing of these standards will be conducted in-house to study differences between a laboratory based technique and standoff techniques.

4. SPME CALIBRATION USING INKJET PRINTING

The above sections have described the successful use of drop-on-demand printing for instrument calibration. In the study described below, drop-on-demand printing is applied to the calibration of a sampling technique. The results from the calibration graphs generated for IMS established that the mass deposition on filters is accurate and the absolute mass response obtained by the microdrop method is significantly different from the calibration graphs observed by standard solution analyses. This premise was used to determine instrument response to the absolute mass extracted by the SPME fiber.

4.1. Solid Phase Microextraction (SPME)

Introduction to solid phase micro extraction (SPME):

The various steps in an analytical procedure include sample collection, preparation, sample concentration, analysis, quantification and data processing. The sampling steps are crucial to obtaining sound analytical results and usually are time consuming and require careful optimization. Solid phase micro extraction (SPME) was developed to simplify the process by combining sampling and pre-concentration into one single step. Pawliszyn et al. introduced the technique in 1990 and since then it has rapidly become one of the most widely used sampling technique[34]. The method relies

on the extraction of analytes by fused silica capillaries coated with a few microns thick film of cross-linked polymers that act as the extraction phase. SPME is a micro extraction technique since the extraction phase volume is much smaller than the sample volume[35,36]. On exposing the extraction phase to the sample matrix, the analytes are preferentially transferred to the extraction phase by either absorption or adsorption depending on the phase chemistry. SPME has gained popularity because of the ability to extract analytes from target matrices rapidly, in the field without the use of solvents and with minimal sample preparation. It can be applied to a variety of matrices based on the mode that it is used in.

Currently two SPME analyses configurations are most common: direct immersion (DI-SPME) mode used for extraction of analytes from aqueous matrices and headspace (HS-SPME) mode[35]. While the DI mode is not dependent on the analytes volatility, the latter is mostly applied for the analysis of volatile and semi-volatile compounds suspended in air or present in the headspace volume above liquid or solid matrices. The figure below by Pawliszyn demonstrates the difference between the both[35].

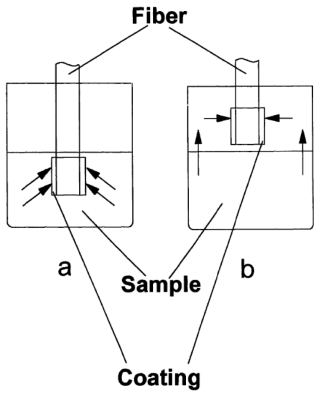

Figure 43: SPME extraction modes: a) Direct immersion b) Headspace extraction[35]

In both modes, since the extraction phase volume is small, exhaustive extraction of analytes does not occur. SPME is generally considered a non-exhaustive extraction, though methods for exhaustive extraction can be developed when the partition coefficient is large[36,37]. Extraction occurs until equilibrium is established in the multiphase system. The research described here is limited to headspace extraction of analytes using SPME and the factors affecting such extractions will be addressed.

In headspace extractions, the concentration equilibriums are established between the analyte and the matrix, analyte and the headspace above it (volatile and semi-volatiles) and the analyte and the extraction phase. The amount of analyte extracted however is dependent on the partition coefficient of the analyte between the matrix and the extraction phase. The partition coefficient is expressed as a ratio between the concentration of the analyte in the extraction phase and the concentration in the sample (K_{fs}). In headspace extractions, the equilibria are described by two distribution constants: K_{fh} (fiber/headspace) and K_{hs} (headspace/sample). In fiber chemistries

where the analyte is absorbed, the mass extracted by the fiber in equilibrium conditions is given by the following equation[36,38]:

$$n = \frac{K_{fs} V_f C_0 V_s}{K_{fs} V_f + V_s} \quad (1)$$

Where V_f is the volume of the fiber extraction phase, V_s the volume of the sample and C_0 the analyte concentration in the sample. Since the volume of the sample is so much more greater than the volume of the fiber, the equation can be simplified to Equation 2 below[36,38]:

$$n = K_{fs} V_f C_0 \quad (2)$$

In equilibrium conditions, knowing the partition coefficients, volume of the fiber and the initial concentration therefore can result in the determination of the mass extracted by the fiber.[36]. In theory, the absolute mass present on the fiber is proportional to the concentration of the analyte in the headspace with which it is in equilibrium with. This principle has been used for the determination of SPME calibration factors which allow for quantitation by the instrument peak areas[39]. However, the equations above are mostly valid only for fibers that trap analytes by absorption.

In field applications where the analyte has very long equilibrium times, pre-equilibrium extractions are preferable. Careful calibration of the SPME process is necessary for the determination of the mass extracted of each compounds since sensitivity for each analyte varies and these calibration factors are necessary for every

target compound[39]. Since most field applications involve non-exhaustive pre-equilibrium extractions, calibration is crucial for quantitative results.

Calibration methods for SPME:

Quantitative analysis by SPME involves the consideration of several factors that affect the precision and accuracy of the method. The equilibrium time, the extraction time, the extraction temperature and the technique of extraction all affect the quantitative information obtained by SPME. Specifically in pre-equilibrium conditions, if the extraction time is not kept constant the mass extracted can be influenced significantly. Therefore, calibration of the technique for the target analytes is applied. Several methods of calibration have been employed for the determination of mass extracted by SPME devices during analyses. Most of these calibration methods are based on the multiphase equilibrium and mass transfer principles. Various literature sources have reviewed and discussed current calibration methods in detail[36,40,41]. Chen and Pawliszyn summarized most popular calibration methods as shown in Figure 44[40,42]. As can be seen from the figure, all the calibration strategies are based on the distribution constants except for the exhaustive extraction methods. Exhaustive extractions do not require calibration because the mass extracted is the total mass present in the sample. However, it is not practical in many applications and equilibrium extractions with associated mass calibration are used. Briefly, the methods currently in use are divided into 4 categories[41]: (a) traditional methods i.e. external standard, internal standard and standard addition (b) equilibrium extraction (c) pre-equilibrium extraction and (d) diffusion-based calibration methods developed

from Fick's first law of diffusion, interface model, cross-flow model and the kinetic process of absorption/adsorption and desorption.

$$\text{Calibration in SPME}\begin{cases}\text{Equilibrium extraction}: n=\dfrac{K_{fs}V_fV_S}{K_{fs}V_f+V_s}C_0\\ \text{Exhaustive extraction}: n=V_sC_0\\ \text{Pre - equilibrium extraction}: n=\left[1-\exp(-at)\right]\dfrac{K_{fs}V_fV_S}{K_{fs}V_f+V_s}C_0\\ \text{First - order reaction rate constant}: v=K^*C_0\\ \text{Diffusion}:\begin{cases}\text{Grab sampling}: \text{various empirical mass transfer correlations}\\ \text{Time}-\text{weighed average sampling}: \text{Fick's First Law of Diffusion}\end{cases}\end{cases}$$

Figure 44: Calibration methods in SPME[40,42]

Traditional methods involve the preparation of standard solutions in sample matrices and either external standard, internal standard or standard addition methods are used to generate instrument response curves. These methods do not require the absolute mass information of the analyte. Absolute mass information is required for all other calibration methods and therefore these methods are more tedious[41]. The most common mode of obtaining absolute mass information is by injecting liquid standard solutions into the instrument. Here the presumption is that there is similar mass transfer into the instrument by both the liquid standard injection and the solventless SPME injection. This method of determining SPME response remains the most popular method used in most analytical labs. Ouyang et al. investigated several factors that affect the transfer of analytes in GC coupled to MS, TOF-MS and FID detectors

while comparing liquid injection to SPME injection[43]. Although each injection method was affected by different critical parameters, it was observed that for both methods, the highest sample transfer efficiencies were achieved with a direct injection (DI) liner and a program temperature vaporizing (PTV) injector.

Recently a new calibration method, called the in-fiber standardization or kinetic calibration method was introduced by Chen[40,44]. The method involves the pre-loading of standards onto the extraction phase and introducing this pre-loaded fiber into the agitated sample matrix. This is an alternative to the traditional internal standard addition, since the internal standard here is loaded prior to the extraction on the fiber. On introducing the fiber to the matrix, desorption of the standards and absorption of the analytes occurs simultaneously. Desorption of the standard can be used as a means of calibrating the mass extracted by the fiber. Both Chen and Zhou have discussed this method extensively in publications relating to liquid extraction phases and solid extraction phases[40,44,45]. The kinetics involving desorption of the standards from the different phases are explained by theoretical models. Zhao et al studied the various methods of loading standards on the fiber and discussed the variation involved in each method and their applicability to different analytes[46]. One of the methods of pre-loading standards onto a fiber was the direct transfer of 1 μL of analyte solution onto the fiber using a syringe. The solvent is allowed to evaporate at ambient conditions and the fiber subjected to GC analysis. The results indicate that such a technique was useful only for the low volatility analytes such as pyrene and decachlorobiphenyl with very low % RSD[46]. The sample transfer efficiencies were observed to be about 95%

when compared to the direct injection of 1 μL of the solution. Mass losses greater than 90% were observed for high volatility compounds. This limits the method application for field analysis.

All the methods mentioned above have been demonstrated for various extraction procedures. There is an abundance of literature on the extraction of analytes using SPME from aqueous matrices in environmental applications[36,38,47,48]. The quantitative principles of direct immersion methods are not always feasible for the use with headspace analysis and very rarely for field sampling of suspect solid materials of forensic interest. There is still a dearth of information on the calibration of field and laboratory based instrumental methods that are used for sampling of materials of forensic interest.

4.2. Printing on fiber for instrument response curves

The section that follows describes an alternative approach for the calibration of SPME extractions and determining the amount extracted from the matrix. The method proposed here is suitable for applications where traditional methods, exhaustive extractions, equilibrium extractions and other in fiber standardization methods cannot be used. The study discussed below aims to answer the following questions:

1. Is there a difference between the instrument response observed when the same mass is introduced into the GC-MS by liquid injection and by printing onto a SPME fiber?

2. Is the loading of absolute mass onto a fiber by microdrop printing a viable method for determining mass extracted by SPME fibers from headspace of target matrices?
3. Is the IMS response obtained by desorbing analytes printed on IMS substrate comparable to the response obtained by desorbing a SPME fiber with the analyte printed on it?

Analytical challenge:

In environmental sampling, the sample matrix is collected, sampled and in many cases processed for the appropriate calibration method. However, in forensic applications, most field sampling of illicit substances do not allow for any manipulation of the sample. Traditional calibration methods can be applied when the sample matrix is known and collected. Rapid pre-equilibrium headspace extractions of complex matrices of unknown nature are the norm for field sampling of volatiles of forensic interest. In such cases, tedious and complex calibration methods are impractical. The most common method for determining mass extracted in a SPME process is the use of the regression line equation obtained from the calibration graphs generated by analysis of liquid standard solutions. This method however, is plagued by the disadvantages of differences between the solvent based liquid injections and the solventless SPME injections. There are significant differences in sample transfer efficiencies from the GC injectors to the column between the two injection methods as discussed by Ouyang et al[43].

In IMS analysis, the common method of generating calibration graphs is by spiking microliter volumes of standard solutions onto a substrate and desorbing it into the IMS. However, as the previous sections have already demonstrated, the absolute mass response of the IMS for printed analytes is significantly different from the liquid spiking of analytes. The microdrop printing method was proposed as the method of choice for determining absolute mass response of the instrument. When conducting SPME analyses by IMS, the general practice is to generate a calibration graph by the traditional method and determining mass extracted by the fiber. In the light of the information gathered by the microdrop printing, it is understood that there may be error associated with determining the mass extracted by using traditional methods. A calibration graph generated by microdrop printing may give accurate mass determinations.

Of the methods discussed in literature, the in-fiber standardization by loading standards onto a fiber was most intriguing. The in-fiber calibration is based on desorption of the standard and absorption of the analyte simultaneously and requires knowledge of the mass transfer principles of the analytes[40]. The approach to the loading of standards onto the fiber proposed here is a combination of the traditional external calibration curve method and the in-fiber calibration method. The calibration graph depicting the instrument response for the different mass introduced is generated by loading standards onto a fiber. Therefore, this unique method does not have the disadvantages of the methods that depend on mass transfer principles. It has the advantage that the known mass on the fiber and the headspace extractions of unknown

mass are all performed with the exact same analysis conditions and are affected by the same instrumental parameters.

The syringe-fiber method of loading standards as described by Zhao, involved the loading of 1 μL of a standard solution onto a fiber. As discussed in the previous sections of this document, microdrop printing allows for the precise and accurate delivery of mass onto a substrate for analysis by an analytical instrument. This method was demonstrated as a valid tool for calibration of detectors. The same premise is demonstrated in the following section where microdrop printing is used for the calibration of a sampling technique. Solvent volumes deposited by microdrop printing are in the range of a few picoliters and are therefore negligible compared to the 1 μL loadings described by Zhao. These small volumes reduce any possible changes to the absorption polymer due to loading of the solvent. The standard loaded onto the fiber by printing therefore is the delivery of absolute mass of analyte onto the fiber. This mass is directly desorbed into the GC inlet and analyzed with the same method that the headspace samples will later be analyzed. Similar analyses are conducted in the IMS where the SPME fiber is desorbed into the SPME-IMS interface with the same conditions as the headspace extractions. The calibration graph generated by the microdrop standard loading onto the fiber will be used to determine mass of analytes extracted by headspace analysis. This will be the first reporting of the use of microdrop printing for loading standards onto a fiber for calibration of headspace SPME sampling for both IMS and GC-MS analyses.

Experimental methods:

The analytes chosen for this study were diphenylamine (DPA), 3 diethyl-1, 3 diphenylurea (Ethyl centralite, EC) and 2, 4-dinitrotoluene (2,4-DNT). These are three common headspace components of smokeless powders of interest and will be discussed further in the second chapter of this document. Each of these compounds has a vapor pressure that is significantly different from the other. This property can also be used to evaluate if the results of the standard loading onto a fiber are significantly different for compounds with varying volatilities.

Printing parameters were optimized for 2-butanol, which is the solvent used for dissolving the analytes. The microdrops generated by these parameters were evaluated using the manual drop size measurements described earlier. The volume of a single drop was calculated to be 133 ± 20 pL. Based on these measurements, the concentrations of the solutions to be printed were calculated. The dimensions of the fiber restrict the total number of drops printed on the fiber. A series of drops can be printed along the length of the polymer coating on the fiber, but to maintain the integrity of the extraction phase and to keep the volume printed as negligible as possible a single burst of drops was chosen. By conducting a series of printing experiments it was determined that a burst of 5 drops was optimal with no overflow and were centered accurately on the rounded surface of the fiber. The 5 drops were printed at approximately the midpoint of the length of the extraction phase.

The printing solutions were prepared such that 665 pL (total volume of 5 drops) contained the target printing mass. Standards of each of these compounds were purchased from Sigma-Aldrich (St. Louis, MO) and solutions were made in 2-butanol

such the mass range of 0.032 ng – 10 ng was obtained when printing 5 drops of analyte standard solution. Stock solutions for printing on SPME fibers were prepared by dissolving individually approximately 30 mg of each analyte in 2 mL of 2-butanol to make the concentration of the solution approximately 15,037 ng/μL. This solution was further diluted in 2-butanol to make concentrations ranging from 6015 ng/μL – 48 ng/μL. These solutions are used for printing analytes onto the SPME fiber for analyses by both GC-MS and IMS and for printing analytes onto the substrate for IMS analyses. The upper mass level printed is limited by the concentration of the solution. Use of highly concentrated solutions can lead to the incorporation of errors due to saturation and precipitation of solutions in the fluid reservoirs of the printing device.

Calibration graphs were also generated for both analytical techniques by the traditional methods. Standard solutions for the analysis of a 1 μL sample volume by liquid injection into GC-MS or by liquid spiking into an IMS substrate were prepared by diluting the printing solutions for each mass in methanol such that a concentration range of 0.032 ng/μL – 10 ng/μL was achieved. For the IMS analyses, to demonstrate that the signal differences observed were due to the solvent volume and not due to the mass delivery method, the same volume of standard solution was deposited on an IMS substrate by both the printing and syringe spiking method. A standard solution of known concentration was taken and a 1 μL spike was deposited onto an IMS filter and analyzed. The same solution was loaded into the reservoir of the inkjet printer and several drops were jetted onto an IMS substrate such that the total volume of the drops printed was 1 μL.

GC-MS analysis method:

A Varian (Palo Alto, CA) CP 3800 gas chromatograph coupled to a Saturn 2000 ion trap mass spectrometer (GC-MS) was used for this study. An analysis method previously optimized for a mixture of compounds including DPA, EC and 2,4-DNT was used for all GC-MS analyses. A 50 m DB-5 column 0.25 mm ID 1 μm film thickness with a column flow of 2 mL min^{-1} was temperature programmed starting by holding for 1 min at 40 ^{o}C, ramped to 200 ^{o}C at 15 ^{o}C min^{-1} and held for 1 min. It was then ramped to 240 ^{o}C at 15 ^{o}C min^{-1} and held at 240 ^{o}C for 6.50 min, the temperature was then increased to 270 ^{o}C at 25 ^{o}C min^{-1}. The final temperature of 280 ^{o}C was reaching by ramping it by 5 ^{o}C min^{-1} and held there for 4 min. The GC injection port was set at 280 ^{o}C in split mode (split ratio 5:1) and fitted with a 2 mm straight liner. The split injection mode was chosen as it enabled better sensitivities by reducing background level for the liquid injection analyses when compared to the splitless mode. The retention times obtained were 13.42, 14.33, 16.84 minutes for 2,4-DNT, DPA and EC respectively. The same analysis method was used for both liquid injections and SPME fiber desorptions, generating two instrument response curves for each analyte. Injections of 1 μL standard solutions were used to generate response curves of liquid injections. Response curves for microdrop printed fibers were generated by direct introduction of the fiber into the GC injection port for complete thermal desorption.

IMS analysis method:

A GE Ion Track Itemiser II IMS (Wilmington, MA) was used in this study for both SPME and solution based analyses. The IMS parameters are listed in Table 4. Instrument response graphs for traditional methods were obtained by spiking 1 μL of standard solution by a syringe. The microdrop printed response graphs were obtained by printing 5 drops of the prepared printing solution. For both analyses, the substrate used was a narcotics filter substrate supplied by Smiths Detection (Mississauga, ON, Canada) that was thermally desorbed into the IMS on deposition of the analyte.

The loading of analyte onto the fiber was achieved by microdrop printing 5 drops of the standard printing solution on the extraction phase of the fiber. The SPME fibers were analyzed by introducing the printed fibers through an SPME-IMS interface (patent-pending) that was built here at FIU by Perr et al for the efficient desorption of analytes from a SPME fiber into the IMS[49]. The interface was set to the same temperature as the GC injection port to maintain similar conditions. Therefore, three response curves were generated by IMS for each analyte. The analytes DPA and EC were analyzed in the positive mode whereas 2,4-DNT was analyzed in the negative mode.

Table 3: Itemiser II IMS operating parameters

Operating conditions	Negative/ Positive
Desorber temperature (^{o}C)	250
Drift tube temperature (^{o}C)	180
Sample flow (mL min^{-1})	1000
Detector flow(mL min^{-1})	200
Reagent gas in negative mode	Methylene chloride
Reagent gas in positive mode	Ammonia
Interface temperature (^{o}C)	260
SPME-IMS interface temperature (^{o}C)	280
Compounds drift time	
2,4-DNT	DPA	EC
5.83 ms	6.20 ms	7.66 ms

For printing known mass of an analyte, the target printing solution was loaded into the fluid reservoir and connected to the microdrop device. Using the optimized drive waveform, the solution was jetted in the continuous mode to determine stability in drop generation. Known mass of an analyte was delivered to the SPME fiber or

onto the IMS substrate by triggering the deposition of five drops in the burst mode from each standard solution concentration. In preparation for printing, the jet was triggered to print five drops on a secondary surface and the jetting observed with the horizontal camera. When the jetting on the surface was found satisfactory with no satellites and with no angled deposition, a SPME fiber or an IMS substrate was placed on the stage and aligned with the glass capillary of the printing device. When printing on a SPME fiber, the fiber was exposed just before jetting was triggered. The placement of the fiber under the printing device is shown in Figure 46.

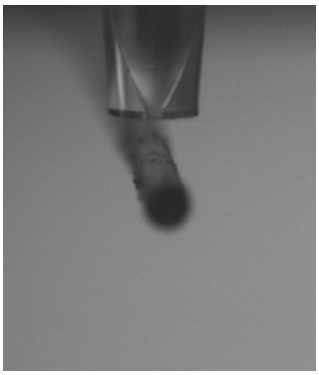

Figure 45: Printing of analytes onto fiber- Image showing print head positioned over the exposed SPME fiber

Results and discussion:

The effect of solvent on IMS signal response was demonstrated by delivering the same volume (1 μL) of a 10 ng/ μL standard solution, either by spiking or by microdrop printing onto an IMS substrate. It was presumed that there should be no difference between the two sample delivery methods as long as the volume delivered was the same. The results obtained support this presumption. As can be seen in the

graph shown in Figure 47, for all three analytes of interest, the signal variation between both the methods of sample delivery was less than 5%. These results confirm that when known mass is delivered in equal volumes onto a substrate whether by printing, similar IMS responses are observed. The results also provide evidence for the drop number and drop volume calculation, since based on calculations, it was determined that 7519 drops would be required to deliver 1 μL onto a substrate.

The results further discussed below will support the argument therefore that the signal increase observed is due to the negligible solvent volumes delivered by the microdrop printing method.

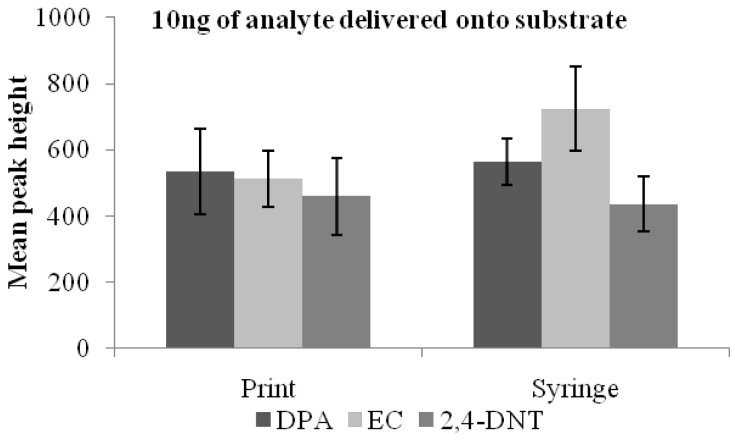

Figure 46: Delivering same mass in the same volume by two methods: Printing 10ng onto a filter and spiking 10ng of analyte onto a filter

Response curves

Instrument response graphs for each instrument were generated by two methods: traditional microliter solution analyses and microdrop printing analyses. Each point on

the graph was the result of three replicate analyses and every response curves was evaluated in terms of dynamic range, limit of detection (LOD), precision and accuracy. A mass range covered by all sample delivery and analyses methods was kept consistent such that there was an overlap between the response graphs. This overlap can further be used to determine if there a correlation factor present between the traditional and printing sample delivery methods.

GC-MS: The GC-MS analysis resulted in two response graphs for each analyte- one by injection of 1 μL of standard solutions in the range of 0.032 -20 ng/μL and the other by microdrop printing of absolute mass of 0.032- 10 ng onto a fiber in 665 pL. The graphs were fitted with the best fit trend line to get a regression equation that was used later for calculation of mass extracted during headspace analyses. The dynamic range obtained for liquid injections of DPA and EC was 0.16 to 20 ng mass with 0.16 ng being the LOD. The LOD for 2,4-DNT was found to be 0.8 ng. Although a broader dynamic range could be obtained for this compound, an upper mass limit of 20 ng was studied for all three analytes. The response graphs obtained by microdrop printing onto a fiber exhibited a higher dynamic range of 0.032 - 10 ng for all analytes. The overall instrument response to the analyses of absolute mass on fiber was 10 times greater than the traditional injection of 1 μL of standard solution. This implies that the instrument is capable of higher sensitivities and lower LOD's all for analytes. Important to note however, is that the GC-MS analysis method was optimized for liquid samples and set to a split mode injection to reduce background level caused by the solvent. The solventless SPME analysis was also analyzed with the same split

method for consistency and for fair comparison between the methods. However, SPME has the advantage of splitless mode injection which could be used to obtain greater sensitivities. The slip ration used and the injector conditions can affect the signal obtained significantly. As part of a comparative study, three different split levels, 5:1, 10:1, 20:1 and three liners 2 mm straight, 4 mm packed with gooseneck and 4 mm unpacked single gooseneck liners were also studied briefly to examine if similar GC-MS print on fiber and liquid injection results were obtained. In all cases similar results were observed. The GC-MS results clearly demonstrate the affect of injection volume on the instrument response, sensitivities, LOD's and linear dynamic ranges. The mass transfer efficiencies with the high volume liquid injections and the SPME injections are not equivalent, and therefore the graphs obtained for liquid injections cannot be used to compare signals obtained by SPME injections. The solvent fraction introduced into the column also gives rise to a higher background level which results in lower sensitivity of the least retained analyte such as 2,4-DNT.

IMS: The IMS analysis resulted in three response curves: The traditional microliter liquid spike generated mass response graph, microdrop printing of analyte mass onto IMS substrate and loading of analyte onto fiber by microdrop printing. Diphenylamine and ethyl centralite were analyzed in the positive mode whereas 2, 4-dinitrotoluene was studied in the negative mode. The dynamic range obtained for all three compounds was one order of magnitude smaller than measured by GC-MS. This is in agreement with previous reports, that IMS analysis has smaller dynamic range than GC-MS. All compounds gave a consistent dynamic mass range of 0.8 – 10 ng

with the drop-on-demand microdrop printing method. However, when using the microliter liquid spike of standard solutions the dynamic range observed for each compound varied. Overall signals and sensitivity were greater by 5% for the microdrop printing method. When a large solvent volume is used as in the liquid spike method, the vapor concentration of the analyte in the reaction chamber is smaller compared to the solvent concentration. The ion package pulsed into the drift region through the ion gate therefore contains lower analyte ions. Since IMS is not intended to separate analytes in their mixture during the ionization, a simultaneous competing for protonation occurs with the solvent, which would influence both sensitivity and dynamic range of the method. This could explain the smaller analyte signals observed when using liquid spikes in the IMS as compared to the microdrop printing method

All the results are compiled together in the graphs shown in Figure 47 A- C. Each analyte are graphs are plotted in a single chart to give an overall picture of the differences between the methods. Since two instrument responses are being plotted in a single chart log scale of the X and Y axes are used. Each chart therefore has five graphs: 1) liquid GC-MS analyses 2) Mass loading by print on fiber analyses 3) liquid spike IMS analyses 4) printing on substrate analyses 5) Mass loading on fiber IMS analyses. Each response graph is plotted individually to determine the best-fit trendline and a regression equation is generated for each graph to be used for headspace extraction mass determinations. These will be discussed in the next section. Figure 48 A-E illustrates the graphs obtained for diphenylamine for each technique.

Figure 47 provides crucial information on several aspects of the study. The graph clearly shows that the response obtained for the loading of standards onto the fiber in negligible solvent volume (665 pL) is significantly higher than the liquid spike response. It is also evident from the graphs that the linear dynamic range and sensitivity of the GC-MS is greater than the IMS. The results support the calculated amounts printed from the drop volumes. These are consistent across a single graph and across the three compounds analyzed. Another significant conclusion that can be drawn from these graphs is that the SPME-IMS interface gives similar desorption characteristics as the filter and the instrument response to whether the analyte is printed on a fiber or a filter is the same. The same trend is observed for all compounds. Also important is that the instrument response to the mass printed analytes is much higher than the analyses of the microliter spikes on the substrate. It once again supports the conclusion that the volume of the sample solution affects instrument response.

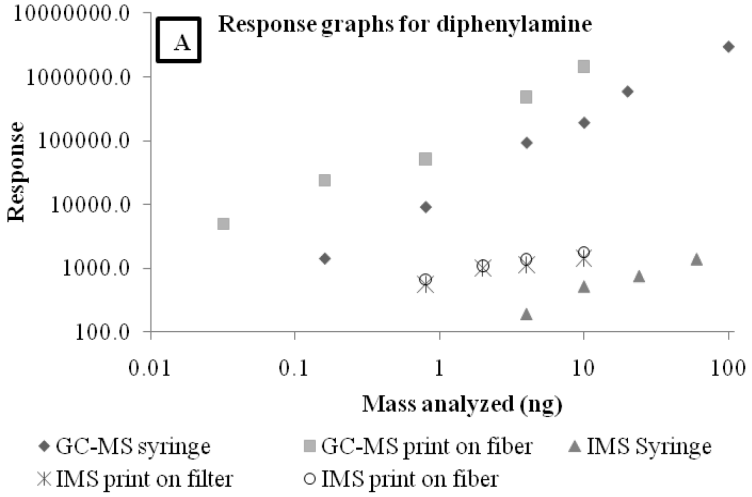

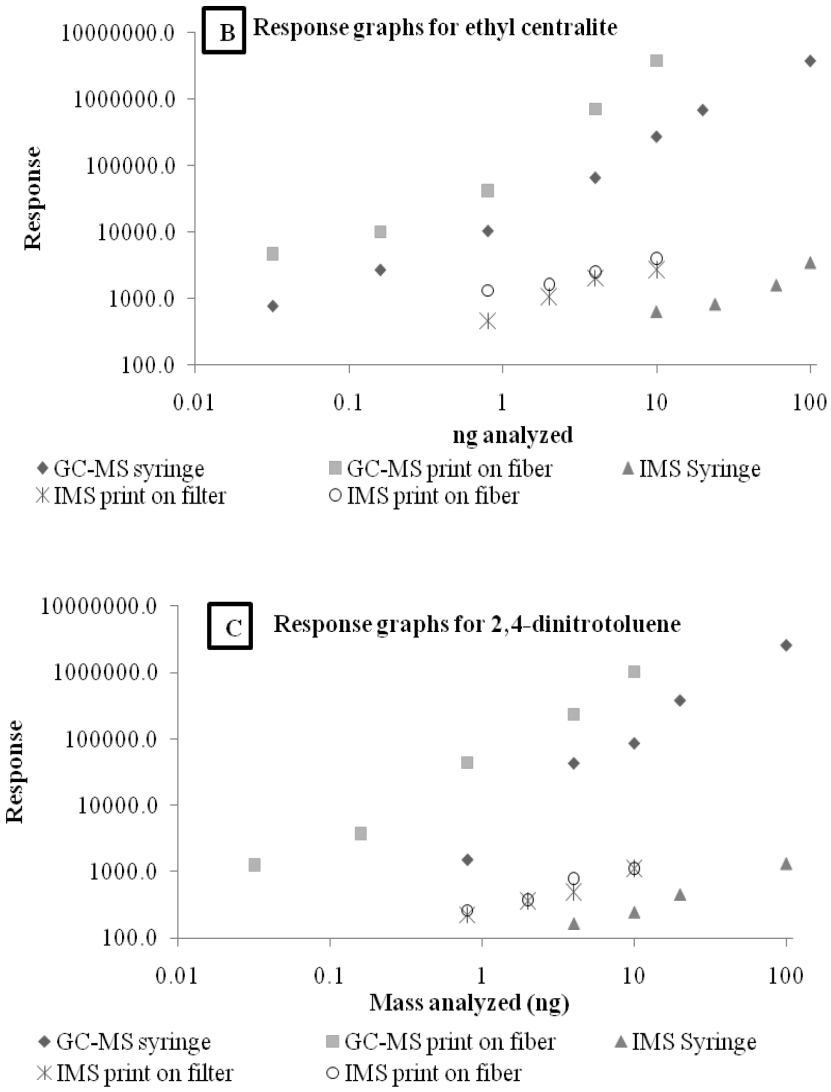

Figure 47: Mass response graphs obtained for IMS and GC-MS by traditional and microdrop printing methods for A) Diphenylamine B) Ethyl centralite C) 2, 4- dinitrotoluene

Figure 48 below is the representation of all the graphs drawn for DPA. Such graphs were drawn even for EC and 2,4-DNT. Each graph was evaluated for its accuracy and precision using the regression line equation. The GC-MS graphs had a linear trendline where a linear regression line equation was used to evaluate the bias

and precision associated with each value. The IMS response graphs had polynomial trend line and a 2nd order polynomial regression line was used to study the graphs. On an average for all compounds, better repeatability was observed with the graphs generated by printing. An average uncertainty of less than 20% was determined for the quantification of analytes using the liquid injection in the GC-MS at mass range level of 0.16 – 20 ng for DPA and EC and 0.8 – 20 ng for 2,4-DNT. At levels closer to the minimum detection limits, as attained by the print on fiber response curve, higher uncertainties were measured. For the IMS analysis, high repeatability with less than 13% average deviation and high accuracy with less than 17% average bias was measured for most analytes response curves along their dynamic range. Higher average bias of 22% and 29% were measured for DPA liquid injection and print on IMS substrate response curves, respectively.

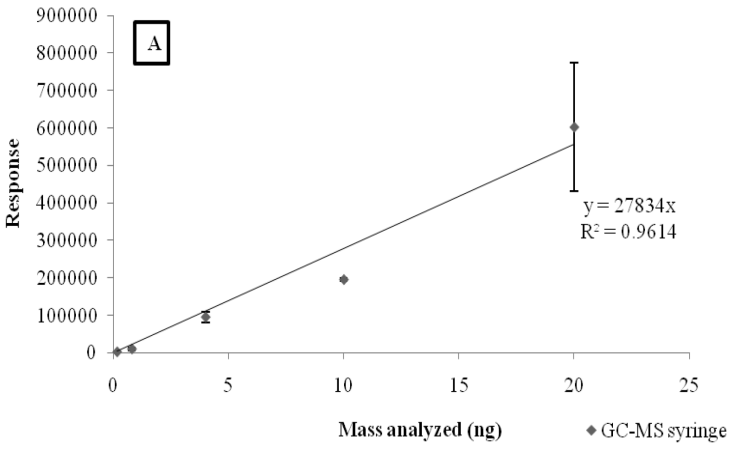

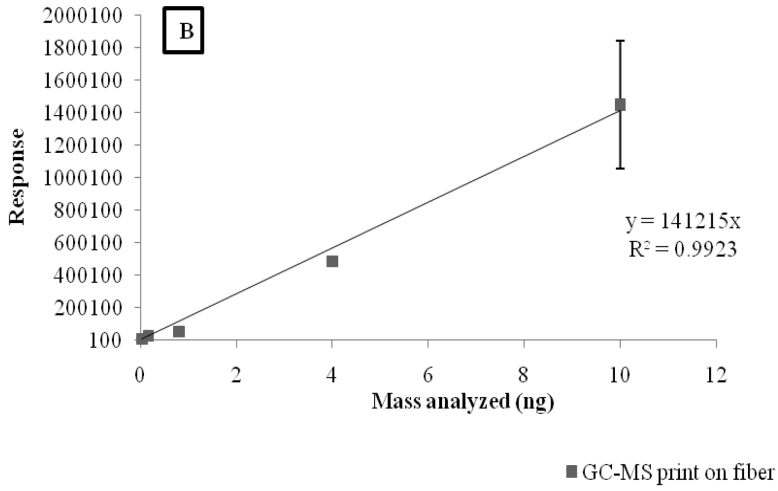
B
Response
2000100
1800100
1600100
1400100
1200100
1000100
800100
600100
400100
200100
100
0
2
4
6
8
10
12
Mass analyzed (ng)
y = 141215x
R² = 0.9923
GC-MS print on fiber

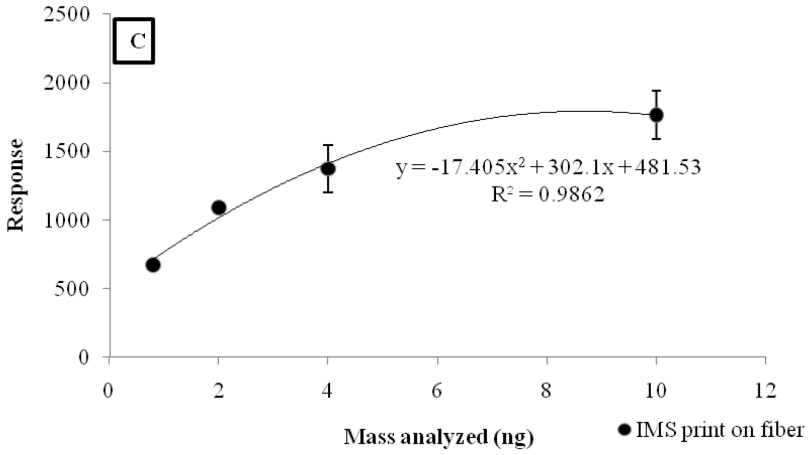
C
Response
2500
2000
1500
1000
500
0
0
2
4
6
8
10
12
Mass analyzed (ng)
y = -17.405x² + 302.1x + 481.53
R² = 0.9862
IMS print on fiber

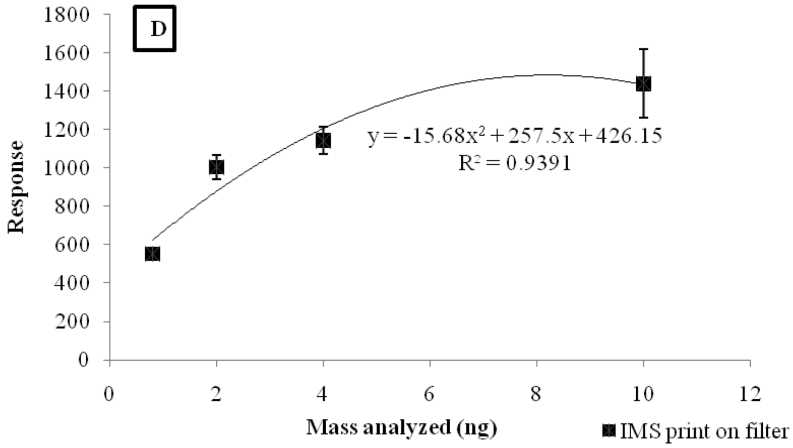
D
Response
1800
1600
1400
1200
1000
800
600
400
200
0
0
2
4
6
8
10
12
Mass analyzed (ng)
y = -15.68x² + 257.5x + 426.15
R² = 0.9391
IMS print on filter

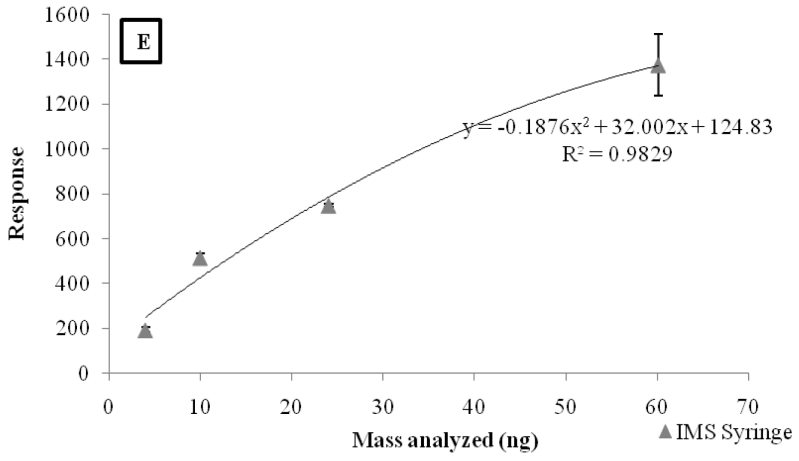

Figure 48: Response graphs for diphenylamine A) GC-MS liquid 1 µL injection B) GC-MS print on fiber C) IMS print on fiber D) IMS print on filter E) IMS liquid 1 µL spike

4.3. SPME mass calibration for headspace extractions

The main application of this study as stated before is to demonstrate the utility of microdrop loading of standards onto a SPME fiber for calibration purposes. In order to evaluate the graphs shown above, headspace extractions of the target compounds were carried out. It would have been better and more useful to conduct this study with real samples but to conduct an interference free study standards were used to generate the results discussed below. This study required the comparison between the IMS and GC-MS response to headspace extractions. However, as mentioned before, when complex mixtures are analyzed by IMS, preferential ionization occurs though all analytes are introduced into the IMS. This complicates quantitative analysis. The response observed for an analyte in a complex mixture may not be close to the true value of the mass on the fiber when there is competition between two analytes.

In this portion of the study, the aim was to assess the absolute mass of an analyte extracted onto the fiber by the different response graphs.

Experimental:

Approximately 10 mg (weighed by microbalance with error of ± 0.1 mg) each of solid standards of DPA, EC and 2,4-DNT were placed individually in 50 mL vials purchased from Fisher Scientific (Pittsburgh, PA), sealed and allowed to equilibrate overnight. The headspace inside each vial was sampled by 100 μm PDMS SPME fibers at two different extraction times in three replicates. DPA was extracted for 1 and 3 min, EC for 10 and 20 min and 2,4-DNT for 1 and 5 min. The times for each analyte were chosen such that the response observed fell within the range of the standard response curves obtained for both analysis techniques and the signal would be approximately at the centroid of all the response graphs where the accuracy is highest. The final mass extracted on the SPME fiber was calculated by using the equations of the best-fit line obtained for each of the five response curves generated using standards of each compound.

Results:

The assertion for the validity of the SPME calibration method investigated here was that the absolute mass extracted by the fiber should be the same whether determined by the IMS or GC-MS calibration graph. The strength of the calibration method also lies in its accuracy and precision for the determination of unknown mass. These figures of merit have been discussed above.

The instrument responses to the different headspace extraction times were evaluated with each of the five response graphs obtained for an analyte. Figures 49 A-D below, illustrate the differences within an analytical technique using the traditional and microdrop printed graphs. For the GC-MS, the graphs 49 A and 49 B clearly show the difference in the mass estimations using the response graphs generated with the liquid injection and the response graphs generated by the absolute mass loading onto the fiber by microdrop printing. There is a significantly higher mass estimation using the traditional microliter injection method at both the shorter and longer extraction times.

The IMS graphs shown below as 49 C and 49 D also follow the same trend as the GC-MS graphs. However, it is interesting to note that the mass determination by the two microdrop generated graphs is similar for all analytes. These results support the claim that microdrop printed graphs are best suited for absolute mass determinations. The standard loading on fiber is not necessary for IMS when a response graph generated by microdrop printing on an IMS substrate is available.

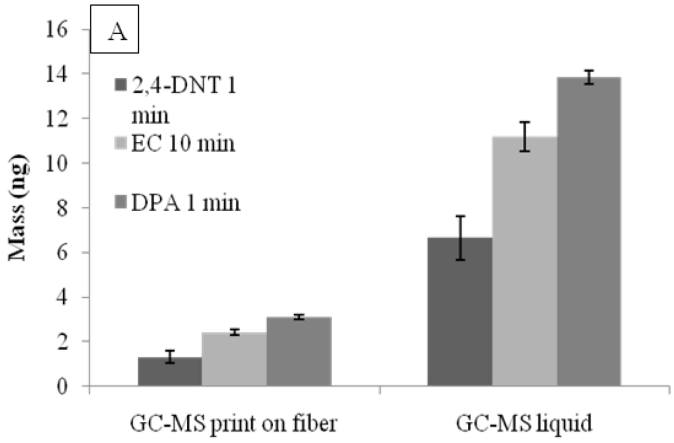

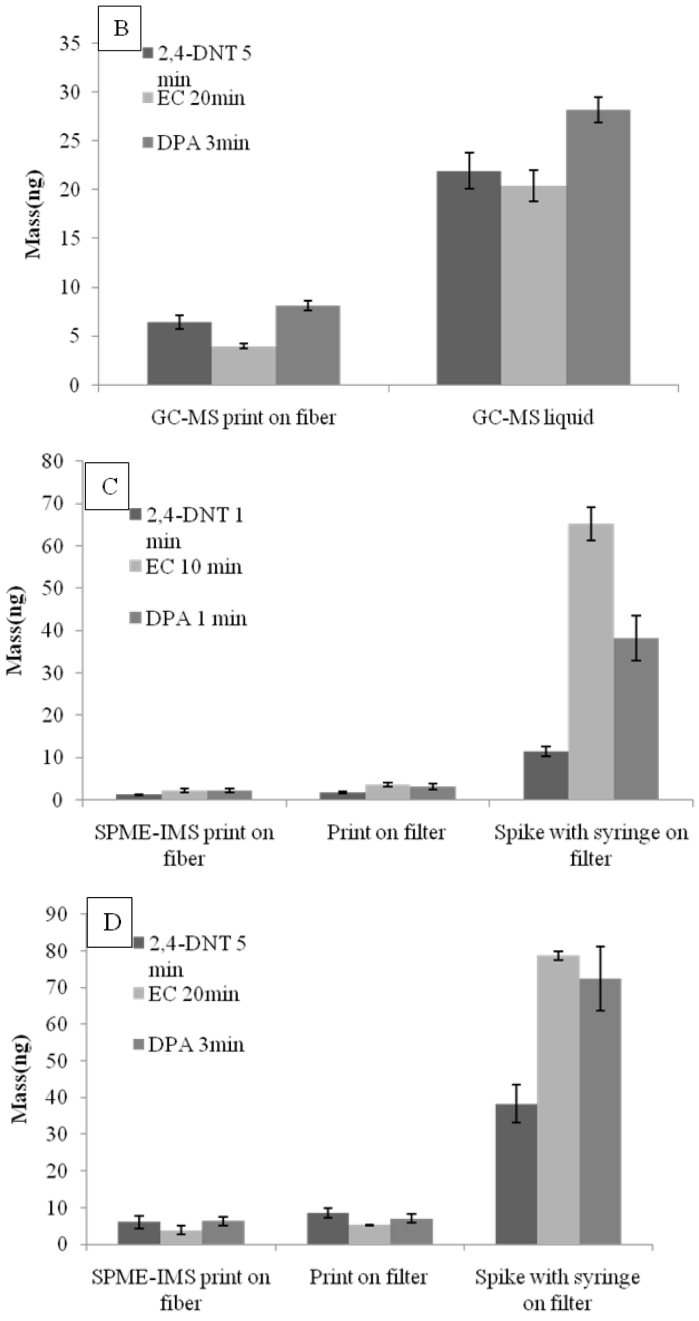

Figure 49: Absolute mass extracted calculation: A& B - GC-MS comparison between liquid injection and microdrop printed response curves for lower and higher time extractions, B & D- IMS comparison of the mass extracted at different times for the three analytes using different response graphs

The table below lists the mass estimations between the different methods and the two analytical techniques. As indicated before, the main assertion of this study is that the mass absolute mass extracted by the fibers as determined by IMS and GC-MS should be the same. The table provides evidence in support of this assertion. The mass of each compound extracted at the different times is consistently calculated to be higher using the traditional methods used for both GC-MS and IMS. The GC-MS results indicate that the overall mass calculations for all three compounds at all extraction times are on an average 4.4 times higher for the liquid injection method. This factor varies between 3.41- 5.14 for all analytes but gives valuable information that there could be a correlation factor between the liquid injection and SPME mass loading method. The factor may be affected by injector conditions. In the research described here, two different GC liners and different injector temperatures were studied for the same analytes and similar factor of increase in signal between the liquid injections and the microdrop printed SPME was observed. Such a correlation of signals is harder to express for IMS analyses, since several factors affect the IMS sensitivity to each analyte. On an average, the mass calculated by the liquid spike method for IMS was 11.4 times higher than the microdrop printing on a substrate. However, the factor varied widely for the three analytes with 2,4-DNT showing the smallest factor of about 5 times, whereas EC had the highest difference of about 17 times. These numbers are very high and indicate that the IMS may require individual response graphs for every analyte and a generalized correlation factor as determined for GC-MS cannot be given for IMS.

It is also important to note that both the traditional methods do not result in comparable mass determinations. The mass extracted by the fiber as given by the liquid spike method of IMS was consistently higher than the GC-MS liquid injection method. The mass calculations were higher by an average of 33.68 ng with the range being between 4.83 – 58.27 ng. However, the mass determinations by the microdrop printed methods are comparable. When a headspace extraction and detection is performed by either GC-MS or SPME-IMS, the mass calculation for the amount extracted by the fiber is similar when determined by the microdrop printed graphs. The results obtained by the GC-MS graphs are slightly higher than the IMS fiber response graphs, however the average difference in mass is only 0.56 ng with a range of 1.7- 0.05 ng. The results from the two IMS printed graphs are similar but the mass determined by the printing on substrate graph was slightly higher on all counts. Certain small differences are to be expected since the printed graphs are generated by printing on two different substrates: IMS filter and fiber. Also of note is that both surfaces are desorbed into the IMS by two different desorption units. Inspite of this, the differences are within an acceptable range. The average mass difference is 1.17 ng with the lowest difference being 0.45 ng and the highest seen for 2,4-DNT at 2.45 ng.

Table 4: Absolute mass extracted by SPME fibers as determined by different response graphs

Compound analyzed	Extraction time (mins)	Average mass determined by GC-MS (ng)		Average mass determined by IMS (ng)		
		Liquid injection (1 μL)	Microdrop printing on fiber (665 pL)	Liquid spike (1 μL)	Microdrop printing on substrate (665 pL)	Microdrop printing on fiber (665 pL)
DPA	1	13.84	3.09	38.15	3.09	2.24
	3	28.16	8.07	72.41	7.03	6.37
EC	10	11.17	2.42	65.24	3.35	2.23
	20	20.38	3.96	78.65	5.25	3.79
2,4-DNT	1	6.65	1.30	11.48	1.70	1.25
	5	21.93	6.43	38.28	8.50	6.05

These numbers therefore prove that there is a significant mass overestimation of mass extracted from the headspace of target analytes when using traditional methods. It also shows that using just the liquid spike method of IMS or the liquid injection

method for GC-MS to estimate mass gives erroneous results and leads to incorrect conclusions. This is specific to those applications where an analyte is analyzed by both GC-MS and IMS techniques. Within the same context, it is sufficient to have a substrate printed absolute mass response graph for IMS to arrive at accurate conclusions for both IMS and GC-MS. However, when GC-MS analyses alone is used, it is necessary to have an absolute mass response curve.

Discussion and conclusions for the calibration method:

This study was initiated to determine the response of an analytical instrument when a known absolute mass was present on a SPME fiber. The results presented above successfully answer all the questions raised at the beginning of this study. There is a distinct difference between the instrument response observed for the same mass when is introduced by different injection methods. The GC-MS liquid injection method clearly gives lower sensitivities and the sample introduction volume affects the signal. The instrument response to the analyte loaded in negligible solvent volume of 665 pL establishes that the absolute mass response is greater. The accuracy and precision associated with each graph and the mass calculated from them validate the printing method. Therefore, it can be stated with confidence that the microdrop printing method is viable method for loading standards onto a SPME fiber. This method as mentioned earlier is designed to avoid consideration of the mass transfer principles and partition coefficients associated with SPME sampling. However, there are desorption factors associated with the desorption of mass from the fiber and transfer of mass into the GC injector. Also of importance is that this study was

demonstrated using an absorption type extraction phase- PDMS. The liquid extraction phase of PDMS was preferred for its larger extraction phase volume and its utility for all the applications described in this document. The same fiber is also used in the several studies cited here that discuss calibration methods. It is expected that an adsorption extraction phase would have different desorption characteristics in the GC injector. The loading of mass by microdrop printing is expected to be applicable to all kinds of extraction phases and extraction phase geometries.

Also addressed here is the use of the response graphs for the determination of absolute mass extracted by the SPME fibers during headspace extractions. Based on the evidence presented above it is accepted that microdrop printing is a desirable method for generating graphs that help in calibrating SPME headspace extractions. It is known however that drop-on-demand microdrop printers are not accessible to everyone. This technique therefore is proposed as a guideline for SPME users such that when reporting mass values they are aware that there is a significant overestimation of mass when using traditional methods. There exists a correlation factor between the traditional and SPME injections for GC-MS. Under the experimental conditions used here, the correlation factor was determined to be approximately five. This could differ depending on the liner volume used, desorption temperature, the type of SPME extraction phase and the analyte. With users who have access to microdrop printing, it is suggested that absolute mass response graphs for each analyte of interest are available. The microdrop printing method is also not extended as a routine calibration method. It is proposed as a measure of instrument

sensitivity to introduction of absolute mass. Once these graphs are available at the initiation of a study, they would serve to determine absolute mass extracted by the fibers irrespective of the extraction conditions. However, as stated above, analyzing complex matrices can complicate quantitation by IMS. In such a case, these graphs would still give better mass estimates than the liquid spike method.

Of importance among the IMS results are the results that compare the printing of analytes onto a substrate and the fiber. The results show that there is insignificant difference between the two substrates. The experiments also inadvertently also provide evidence that the SPME-IMS interface is efficient and provides absolute mass introductions to the detector that are similar to the desorption characteristics of the GC injector.

Simply stated, the overall conclusion of this study is that traditional high volume sample injections lead to the overestimation of mass extracted in SPME experiments and this can be avoided by use of an absolute mass response graph.

5. CONCLUSIONS AND SIGNIFICANCE

This chapter introduced microdrop printing as a sample delivery method for analytical applications unlike those that have been reported before. Drop-on-demand microdrop printing is presented here as a mass delivery tool to various applications for a wide variety of chromatographic, spectrometric and spectroscopic techniques.

Scientists at NIST as discussed above have applied microdrop printing to IMS before, but the experimental methods and results presented in this document give a

unique perspective of the different applications of microdrop printing to ion mobility spectrometry. The results presented here address questions related to the absolute mass sensitivities of the different IMS instruments and the sample introduction factors affecting them. The absolute mass detection limits of IMS instruments are reported here for the first time.

The application of inkjet microdrop printing to LIBS is also a novel method of calibration of LIBS that had not been previously reported. It is anticipated that this research will further progress towards the development of validated calibration methods and standard generation methods for LIBS. Preliminary results with FT-IR, Raman and LA-ICPMS that have not been detailed here suggest that there is potential for use of microdrop printing in these avenues and will be further studied.

The extension of the instrument calibration methods using microdrop printing towards the calibration of a sampling technique was a natural progression of the project. The results of the SPME calibration method have several implications to the projects currently underway here at FIU. The next chapter will demonstrate the applicability of the microdrop printed response graphs to real samples.

The availability of the drop-on-demand system on presents a unique advantage for the application of this work to all future SPME-IMS and SPME-GC-MS projects. The results discussed above suggest that irrespective of the SPME geometry or substrate used for IMS quantitation, the absolute mass extracted by the extraction phase is not determined accurately by a traditional calibration method. The instrument response of

the solventless SPME technique should be equivalently compared to the solventless (negligible in microdrop printing) calibration graphs.

Despite the many advantages of microdrop printing, the technique is currently not widely available to analytical chemists. As researchers outside of the medical and cell technology field discover its potential, it is anticipated that this technique will be used for several applications in analytical chemistry. Though there are certain fluid parameters that restrict some fluids from producing monodisperse drops, several designs of printing devices are currently available that increase the range of solutions that can be printed.

III. SMOKELESS POWDERS HEADSPACE ANALYSIS

Explosives detection methods can be broadly classified into two categories: Bulk detection and trace detection[50]. Bulk detectors such as X-Ray and other imaging techniques are aimed at detecting the signatures of an explosive device such as shape of an assembled explosive or the parts necessary to build a functional explosive. Trace detectors are generally focused on the chemical detection of explosive particles present as residues on various surfaces due to cross contamination or the vapors released from a hidden explosive devices. The project described in this document is geared towards the pre-blast detection of explosives through a vapor phase sampling technique. The following pages detail the accomplishments in the headspace analysis of smokeless powders. The volatile organic chemical components released from the smokeless powders serve as vapor phase or odor signatures to the smokeless powders. Mass of these odor signatures available for detection and the amount detected by laboratory based and field portable techniques is valuable information for the development and improvement of current trace chemical detectors. This chapter describes the generation of this information and future applications of this information.

1. INTRODUCTION TO SMOKELESS POWDERS DETECTION

1.1. Smokeless powders

Approximately 10 million pounds of smokeless powders are produced every year in the United States, much of which is sold commercially[51,52]. The powder is mostly

used in the manufacture of ammunition domestically or exported to international companies that manufacture ammunition and foreign military use[51]. A large portion of the manufactured powder is sold in containers as reloading powders. This source of powder has become widely used by criminal elements for the making of improvised explosive devices (IED's) and as discussed earlier, smokeless powders account for a large fraction of the incidents caused by IED's. Smokeless powders are low explosives that deflagrate (burn and release heat and gas with subsonic waves of pressure) as opposed to high explosives, which detonate with supersonic shock waves. The particle-to-particle linear propagation of pressure as occurs in deflagration of low explosives gives them unique properties that can eject or propel a projectile on complete combustion. Therefore, smokeless powders are also called propellants and are used in ammunition. Though the pressure wave is subsonic and the rate of burning is slow, these powders on containment can produce build up of high pressures and cause the container to explode[51]. This is the property used in making of IED's where the powder is packed into a container with other shrapnel. On explosion of the container, the shrapnel and container pieces cause extensive damage.

Paul Vieille developed the first nitrocellulose based smokeless powder in 1886. Called "Poudre B", it was the first version the single based powders. Two years later, Alfred Nobel manufactured "Ballistite" by mixing nitroglycerine and nitrocellulose together and this became known as the first double based powder available[53,54]. Several years later, addition of nitroguanidine to the mix led to the development of triple based powders, which has been used mainly in higher ammunition. Several

improvements have been made to the manufacturing process of the powders but the base propellants have remained the same over the years. Smokeless powder, as the name suggests, is smokeless in comparison to black powder, which was its predecessor in gunpowder.

As described above, powders are classified as single, double or triple based powders depending on the number of energetic materials in the powder. Apart from the energetic materials, the manufacturers add several other additives to control the burn rate and flash characteristics. The different classes of additives include stabilizers, plasticizers, energetic materials, opacifiers, deterrents, flash suppressants and dyes[52,55,56]. Several additives serve multiple purposes and therefore are added in combinations specific to the properties of the marketed powder. The energetic materials have not changed over the years and most powders use nitrocellulose, nitroglycerine and nitroguanidine which aid in explosive properties of the powders. Compounds such as diphenylamine and the centralites (ethyl and methyl) are added to increase the shelf life of the product by preventing the buildup of nitrous and nitric oxides formed by the decomposition of nitrocellulose and nitroglycerine. Plasticizers help in making the nitrocellulose pliable and improve the gelatinizing properties and hygroscopic properties. Ethyl centralite, phthalates and 2,4-dinitrotoluene (2,4-DNT) are the most commonly used plasticizers. Dibutyl phthalate that is one of the several phthalates used in the manufacturing process also is added as a flash suppressant along with other salts to reduce secondary flash created in the muzzle of the gun. The flash suppressants maybe coated on the surface of the powder granules/particles. Other

surface coatings include deterrents and dyes. The processes involved in the manufacture of three different classes of smokeless powders play a significant role in the morphology of the powder.

Different manufacturers add different additives in varying concentrations and forms based on the properties of the powder they wish to control. This makes the additive composition unique to manufacturers and to the product marketed. The combination of the additives with the energetic materials leads to characteristic degradation products of the different additives[57]. The reaction products formed also depend on the storage conditions of the bulk powders before packaging and the powders packaged in containers for sale. Moisture content and temperature have been discussed as two main parameters affecting the change of the propellant additive composition in time[58-61]. As described above, stabilizers are added to the powders to scavenge the nitrous and nitric oxides formed as part of the degradation of nitrocellulose. The most common stabilizer added is diphenylamine. Several papers have been published over the years describing the reactions involved in the aging process and the methods to study the aging products[59-64]. The characteristic brown fumes of nitrogen dioxide released during the degradation of the nitrate esters react with the diphenylamine to form several nitration and nitrosation species. The amount of each of these products observed in the analysis of the powders can serve as an indication of the extent of degradation of the powder[61]. As the diphenylamine is consumed one of the first products formed are the nitrosation products with N-Nitrosodiphenylamine (N-NODPA) being the most prominent. Apart from the N-

nitroso derivatives, the C-Nitro derivatives such as 2-Nitrodiphenylamine (2-NDPA) and 4-Nitrodiphenylamine (4-NDPA) are also formed[59]. Most of these products also serve as stabilizers and can be further nitrated to form the di, tri and tetra nitrated species. These later species are usually an indication of the fast degradation of the nitrocellulose and depletion of the main stabilizer, diphenylamine[61]. A study has also reported 2-nitro-N-nitroso-N-ethylaniline (2N-NO-EA) to be a degradation product of N,N'-diethyl-N,N'-diphenylurea (Ethyl Centralite, EC)[63]. Detecting these degradation products adds strength to the detection result since the stabilizer, diphenylamine by itself is used in other industrial applications. Table 5 below lists the main propellant additives, degradation products with their structure, function and vapor pressures.

Table 5: **Smokeless powder components**

NAME OF COMPOUND	FUNCTION	STRUCTURE	VAPOR PRESSURE TORR @ 25°C
Nitrocellulose	Energetic	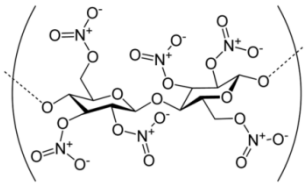	NA
Nitroglycerin (NG)	Energetic	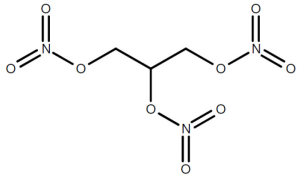	2.63×10^{-3}
Diphenylamine (DPA)	Stabilizer	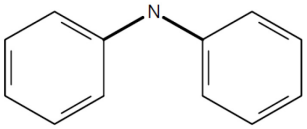	1.02×10^{-3}

N,N’-diethyl-N,N’-diphenylurea (Ethyl centralite, EC)	Stabilizer, plasticizer, deterrent	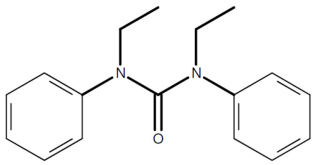	6.04×10^{-6}
N,N'-Dimethyl-N,N'-diphenylurea (Methyl Centralite, MC)	Stabilizer, deterrent	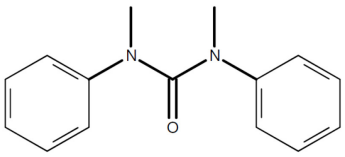	4.53×10^{-5}
2,4- Dinitrotoluene (2,4-DNT)	Energetic, Plasticizer, deterrent	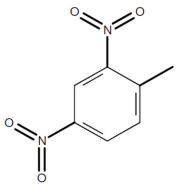	2.07×10^{-3}
Diethyl phthalate	Plasticizer, deterrent	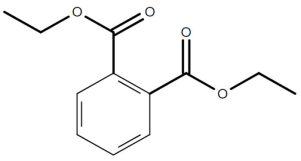	1.67×10^{-3}
Dibutyl phthalate	Plasticizer, deterrent	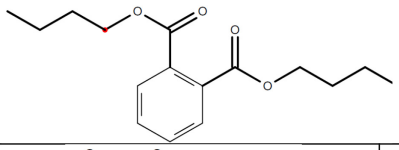	1.08×10^{-4}
2-Nitrodiphenylamine (2-NDPA)	Stabilizer, degradation product of DPA	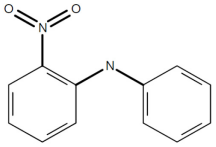	3.51×10^{-5}
4-Nitrodiphenylamine (4-NDPA)	Stabilizer, degradation product of DPA	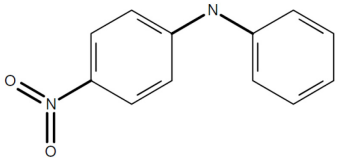	4.68×10^{-6}
N-Nitrosodiphenylamine (N-NO-DPA)	Degradation product of DPA	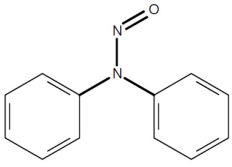	5.72×10^{-5}
N-Ethylaniline	Unknown. Possible degradation product of DPA. Observed in one powder	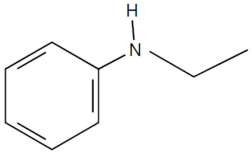	0.304

	where no DPA was detected		

1.2. Current analysis methods

The widespread availability of smokeless powders and the myriad number of commercial products currently available make the analysis and detection of smokeless powders a formidable task. Several approaches have been taken by researchers worldwide for the detection of smokeless powders in pre-blast and post-blast scenarios. This section is a compilation of some of the major contributions that have been made to the analysis of smokeless powders.

The research in smokeless powders for forensic purposes has been oriented towards two main goals: a) Identification of an explosive residue as a smokeless powder b) Identification of the manufacturer and brand origin of a smokeless powder. Thus far, the primary research conducted in identifying an unknown explosive material as a type of smokeless powder has been based on the analysis of explosive residue. In some cases where there is questioned powder evidence present that has not yet been consumed, chemical and physical tests may be used to determine the identity of the particle. Identity of the brand of a powder is mostly useful to homeland security and other federal agencies as they attempt to keep track of all the powders currently on the market. Identifying the powder to the manufacturer usually is a difficult proposition due to the changing nature of products and the high probability of smokeless powder mixtures in an IED. Moreover, manufacturers of smokeless powders several times recycle the powders and mix different batches and

compositions until the desired product is obtained. However, both these research areas together provide a valuable resource to investigators.

The morphologies of smokeless powders are of great significance and studies have been reported where the morphology is used as a powder identification method. The shape and morphology of the powder granules are attributes that add specific burn rates and flash qualities to the powders. The manufacturer chooses these features based on the characteristics needed for the final product. Smokeless powder granules have several shapes but of these ball, tubular and discs are the most common ones. The shape of the powder particles can be indicative of the nature of the powder (double or single-based). Most but not all single-based powders are tubular whereas double-based powders are usually ball or disc shaped. The morphology of the powder can also serve as an indicator of the additives present in the smokeless powder, since the additives can be added at different manufacturing stages such as blending, extrusion, drying, screening and blending. Other features of the smokeless powder granules such as texture, color, diameter, thickness and distortions are also characteristic of the powders. Moorehead has reported an in depth study of the morphology and micrometry of the powders. The following pictures taken by Moorehead illustrate the differences in morphology for different brands of powders.

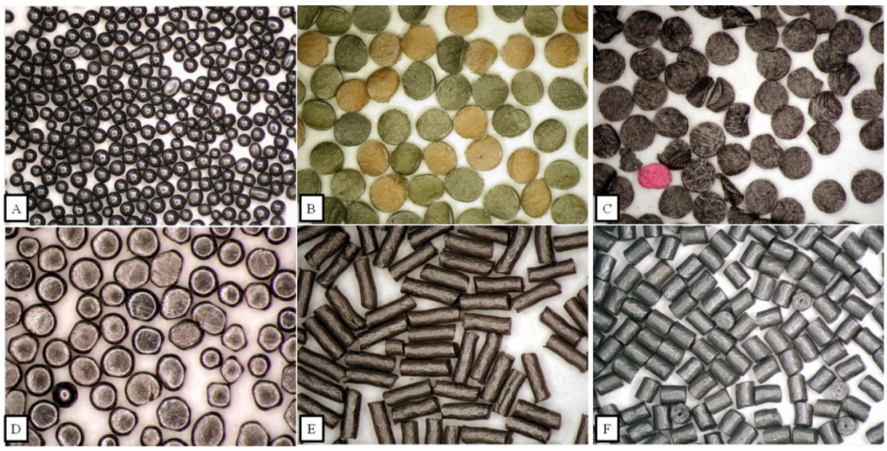

Figure 50: Smokeless powder morphologies: A) Ball powders - H380 B) Thick discs - H International Clays C) Thin discs- Alliant Red dot D) Flattened balls- H BL-C(2) E) Long tubes- IMR 4198 F) Short tubes- IMR 4320[65]

However, morphologies are only useful when the unburned flakes are available and in substantial amount for accurate identification. They can help in identification and in the discrimination of mixtures of powders along with other chemical tools. These studies are also useful mainly in discrimination of canister powders. The gun powder used in ammunition is usually a mixture and morphological studies make only a minor contribution to the identity the brand identity of the gunshot residue.

The various unique organic additives of smokeless provide adequate identification and discriminating characteristics to the powder. Since the introduction of smokeless powders, researchers have been studying the organic components of smokeless powders using various analytical techniques. Much of the chemical analysis of the post-blast or burned powder residues has been conducted with chromatographic techniques. A few studies have also been reported using infra red spectrometry and

other spectroscopic techniques[66,67]. Unlike microscopic techniques, most chemical techniques currently in use are destructive techniques and require extensive sample preparation.

The organic additives are present in the powder particles and need to be extracted to generate analytically adequate qualitative and quantitative information. Several extraction procedures have been discussed in reported literature to successfully extract these analytes. Most processes involve the dissolution of the residue or the particles in methylene chloride and extracting over long periods of time[68]. Extracting the organic additives from a powder sample or a residue gives information about the bulk organic composition of the powder which can serve to a useful discriminating tool. Most of the studies described below employ a solvent extraction method as a sample preparation step.

In an early paper, Schroeder et al published a study on the chromatographic analysis of the additive diphenylamine which tends to degrade with aging of the powder[60]. This study and similar studies[62,69-71] laid the foundation for the analysis of organic components as possible distinguishing characteristics of smokeless powders. Electrophoresis has been investigated for the separation and analysis of smokeless powders components successfully. Northop et al. using micellar electrokinetic capillary electrophoresis (MECE) identified organic additives in residues of a hundred smokeless powders and ammunition[72]. The study showed that MECE is a suitable technique for the identification of organic residues of smokeless powders collected from hands and clothing. Other studies with MECE and zone electrophoresis have

been successfully developed for the detection of organic residues and ion profiles of these additives[73,74].

Of the chromatographic techniques, gas chromatography and liquid chromatography are the most widely used analytical separation techniques. Gas chromatography (GC) coupled to detectors like mass spectrometry, electron capture detector (ECD) and thermal energy analyzer (TEA) has been used widely for the detection of explosives. However, several explosive compounds and smokeless powder additives are thermally labile making them highly unstable in the GC-MS. Some compounds do not survive the injector temperature of the GC-MS. In the analysis of smokeless powders, components such as nitroglycerin, nitroso derivatives of diphenylamine have low thermal stabilities making their detection by GC-MS challenging. Nitroglycerin however, has been studied successfully with ECD demonstrating excellent sensitivity of the detector for the analyte[75].

Liquid chromatography methods are preferred for thermally stable compounds. HPLC methods have been investigated for their applicability to smokeless powder organic additives. However, the range of compounds detected by HPLC coupled methods is small due to the wide range of polarity of the analytes to be analyzed. Methods have now been developed for the identification of various additives of smokeless powders using gradient reversed phase HPLC[76-78]. Wissenger and McCord developed a reversed phase gradient HPLC method that proved to very efficient for the separation of several organic additives[79]. The peak profiles of the smokeless

powders were used to compare the variations between different lots of the smokeless powders.

MacCrehan et al. have conducted several studies on gunshot residues and smokeless powders using capillary electrophoresis and HPLC methods[80-82]. The qualitative and quantitative measurements conducted on smokeless powders involving several different laboratories have led to the development of a smokeless powder reference material[83]. The NIST RM 8107 contains principal additives of smokeless powders such as nitroglycerin, ethyl centralite and diphenylamine with its primary degradation product N- nitroso diphenylamine. This reference material is supplied by NIST as standard measure of organic additives in smokeless powders.

Apart from these important contributions to smokeless powder analysis, mass spectrometry methods such as nano electrospray ionization[84], time of flight mass spectrometry[85] and tandem mass spectrometry[64] methods have also been discussed. However, it is important to note that all the analysis methods mentioned thus far are laboratory-based techniques. These techniques do not allow for identification of questioned powders as smokeless powders or provide information that a post blast residue is that of smokeless powders in the field. However, they are excellent tools for the characterization of smokeless powders and provide valuable information that can be used for field portable techniques.

Ion mobility spectrometry is a field portable analytical technique that has popularly been used for the detection of explosives. However, many of the explosives currently detected by the IMS are high explosives. The IMS instruments currently

available do not have built-in methods for the detection of low explosives such as smokeless powders. Smokeless powders have been detected by their nitro component in IMS instruments on the recovery of particles from surfaces[86,87]. The particles of the smokeless powders or liquid spikes of their extracts on substrates are desorbed into the IMS. Neves et al. demonstrated that solutions of some powders also produced ions of ethyl centralite in the positive ionization mode[88]. Apart from ethyl centralite, other additives such as DPA were also reported to be present in solutions of post-explosion residues by West et al.[26]. The additives shown in Table 5 that are amine derivatives tend to have high proton affinities and can be detected in the positive mode due to the formation of stable positive ions. The additive 2,4-DNT forms a negative ion by proton abstraction and is detected in the negative mode. Detection of 2,4- DNT in the IMS has been well studied, since it is almost always present as an impurity in 2,4,6-TNT.

1.3. Research gaps

It is clear from the above discussion that there are currently no adequate analytical methods for the detection of smokeless powders in the field. The characterization methods based on morphological features and chemical composition are useful only in a post blast situation and require laboratory and analytical skills for sample preparation and collection. The pre-blast detection of smokeless powder devices is currently only by imaging techniques and the use of canines as biological detectors of odors. Rapid field portable analytical techniques that are capable of unambiguous

detection of low explosives are currently lacking from the arsenal available for detection of explosives.

Canine trials have shown that canines use the volatile chemicals emanating from the illicit substances as scent compounds to track and detect them. Harper et al combined SPME-GC-MS and canine trials to authenticate this claim and generated a list of chemicals that are of canine scent interest[6]. The premise of canine trials is that there are wide arrays of chemicals that are present in smokeless powders and some of them are sufficiently volatile to be present in the headspace above the powders. They form a unique scent that canines use to determine the presence of an illicit substance. These scent compounds may not always be the actual explosive molecule itself but other additives and excipients from the manufacturing process. The study by Harper et al list 2,4-DNT as a potential odor chemical for smokeless powders but also mentions that other additives such as diphenylamine were not of canine interest[6]. Other studies have indicated that canines use a mixture of chemicals as scent profiles. Solvents such as acetone and toluene have been reported as some of these scent compounds[89]. Instrumental methods for the detection of these odor compounds such that they complement canine detection in the field are lacking.

Research approach to fill the need:

As has already been mentioned, IMS is one of the most widely used field portable analytical technique. However, all the commercial variations of the technique are designed for the collection and detection of particles. Perr et al developed a SPME-IMS interface at FIU as a special application of IMS[49]. This interface adds the SPME

sample introduction capabilities to the IMS. The SPME device is used to pre-concentrate analytes of interest from the headspace of target matrices and then introduced into the interface for thermal desorption of the analytes from the fiber into the reaction region of the IMS. The SPME-IMS interface is designed to be identical to a GC injector and therefore allows for equal comparison of both analyses.

The project described in this chapter offers an analytical solution for the pre-blast detection of smokeless powder improvised explosive devices based on the detection of their volatile chemicals. Two analysis stages are employed in this project to develop sound detection techniques. In the first stage, confirmatory chromatographic techniques are used to determine the range of compounds that are extracted by the fibers from the headspace of the powders in closed static system. The second stage involves the study of these compounds in the IMS to determine their detection parameters. Once the peaks of interest have been defined, the same SPME extractions are conducted with the smokeless powders for the IMS. By this research approach, a comprehensive profile of smokeless powders is developed which can be used for expanding the detection methods currently available for smokeless powders. The research scheme is shown below as a visual representation of the research method development and the applications for field use.

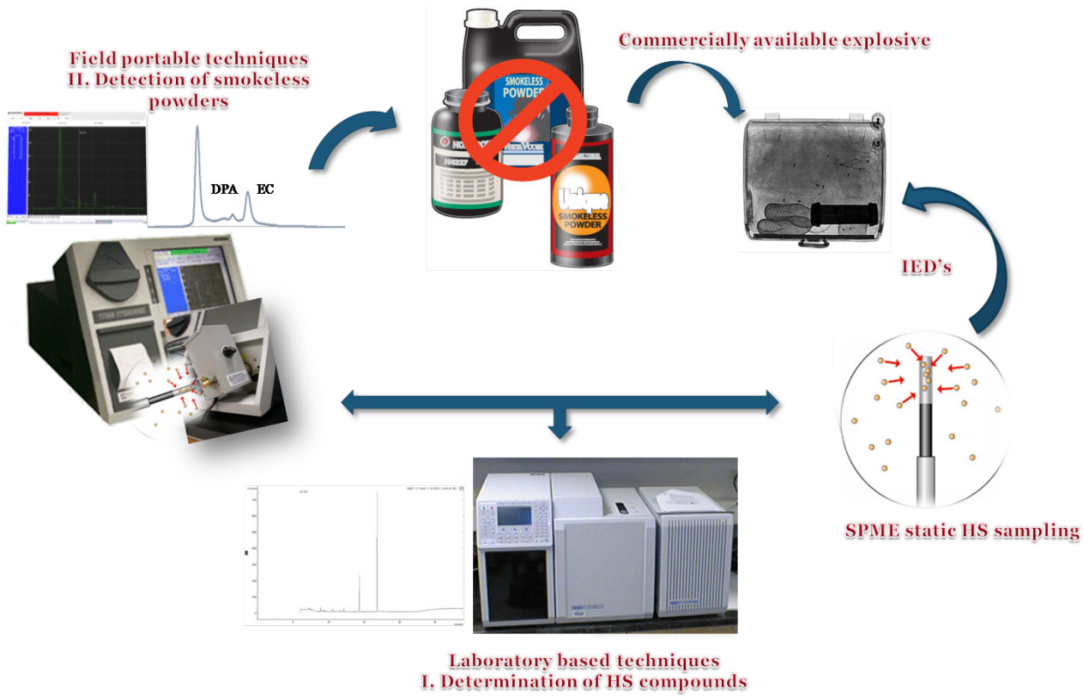

Figure 51: Research approach for smokeless powder detection by headspace sampling using SPME[90,91]

2. SMOKELESS POWDER SAMPLES

As stated before, smokeless powders are available commercially in canisters in several hunting and hobby stores. The purchase of these powders is not regulated and the public can buy these powders and store them in households for use in hunting season. To test the powders available locally, five powders were chosen randomly from the shelf of a local outdoor supplies store. These powders were used to test the hypothesis that the organic components of smokeless powders maybe detected by IMS in the headspace of smokeless powders.

On success with the five powders, the study was extended to a much larger set. In collaboration with Dr. Ronald Kelly from the Federal Bureau of Investigation (FBI) research team, a sample set of 63 powders were obtained. The FBI chose these powders such that they were representative of all the powders available in both the domestic and international markets.

This chapter therefore will be laid out into two sections. The first section will detail the results from the preliminary study that led to their publication in Forensic Science International journal. The second section will detail the large-scale study and various experiments that were carried out to characterize the powders. The second study will also provide mass information based on the calibration method discussed in Chapter II of this document.

3. SPME MICROEXTRACTION AND DETECTION TECHNIQUES

The theory and principles of solid phase microextraction have been discussed in the previous chapter. SPME not only allows for sampling of the volatiles of interest but also pre-concentrates the analytes within the same step. The portability of the SPME devices and their ability to retain analytes until they are thermally desorbed are their most appealing features. The geometry of the SPME fiber is such that it can be injected into a GC injector without any change in configuration. The same fiber geometry can now be used with the SPME-IMS interface.

The chromatographic techniques used for this project were GC-MS and GC-ECD. Mass spectrometry is an excellent detector for several analytes of interest in smokeless

powders and combined with GC it provides superior separations and detections of thermally stable volatile compounds. However, some of the compounds of interest to this project are not compatible GC injector and the mass spectrometer transferline temperatures. Nitroglycerine is one such compound and can be detected in the GC-MS only under drastically different conditions than used for most other analytes. The electron capture detector is a highly selective detector for electronegative compounds and has been used widely for various environmental samples for detection of pesticides. Literature reports exceptional sensitivity and limits of detection of this detector for nitroglycerin[75]. Therefore, an ECD was used in this study for nitroglycerine and 2,4-DNT. All other analytes including 2,4 –DNT were detected on the mass spectrometer.

Figure 52: SPME-IMS interface for Ion Track Itemiser II

The interface for SPME introduction into the IMS has been successfully adopted for the detection of volatiles from the headspace of drugs and explosives. The interface has been reported as an efficient desorber of a wide array of compounds such

as methyl benzoate from the headspace of cocaine, piperonal from the headspace of MDMA, limonene and pinene from the headspace of marijuana and headspace components of high explosives such as SEMTEX and Composition 4[92-94]. Figure 52 is an image of the interface as is applied to the GE Ion Track Itemiser II IMS. The same interface was used in this study for SPME-IMS studies to determine the profiles of smokeless powders in the IMS.

4. STUDY OF FIVE LOCALLY AVAILABLE POWDERS

The interest in smokeless powder detection began when a research group at FIU was conducting canine trials of the powders. At the same time, literature review revealed successful detection of a few additives from the bulk sample of smokeless powders[26]. Therefore a small-scale study was initiated to determine the feasibility of the detection of these additives in the vapor phase using SPME-IMS. Five different types of powders, Alliant Unique, Alliant Red dot, Hodgdon 322, Hodgdon BL C-2 and IMR 4198 were randomly chosen to represent the variety of powders available in the market.

4.1. SPME-GC-MS analysis

Instrumentation and methods:

A Varian (Palo Alto, CA) CP 3800 gas chromatograph coupled to a Saturn 2000 ion trap mass spectrometer was used to determine the compounds present in the headspace of the smokeless powders. Smokeless powders samples were weighed and about 100 mg of each powder was placed individually in 50 mL glass vials

manufactured by Fisher Scientific (Pittsburgh, PA). The vials were then sealed and left undisturbed to equilibrate overnight. A 100 μm polydimethylsiloxane (PDMS) fiber purchased from Supelco (Bellefonte, PA) was used as the sampling and pre-concentration device for the headspace components. The portable SPME holders used in all SPME studies described in this dissertation were purchased from Field Forensics (St. Petersburg, FL). A GC-MS method suitable for the entire range of target compounds was developed. A Varian WCOT 50m x 0.25 mm ID CP Sil- 8 GC column was used for the analysis. The GC injector temperature was kept at 280 ^{o}C ensuring complete desorption of all analytes from the SPME fiber. Splitless injection mode was used and the method run time was 18.33 minutes with the column oven temperatures beginning at 45 ^{o}C and going up to 300 ^{o}C. The temperature ramp was set at 20 ^{o}C/min at the lower temperatures, 15 ^{o}C/min at 200 ^{o}C, 10 ^{o}C/min at 250^{o}C and was increased to 50 ^{o}C/min at 300 ^{o}C where the temperature was held for 1.5 minutes. The ion trap analyzer was maintained at 180 ^{o}C while the transfer line was at 280 ^{o}C/min. Electron impact (EI) ionization was used with a mass scanning range from 40 m/z to 400m/z.

Response curves for the samples were obtained by sampling the headspace for different extraction times with the SPME fibers described above and then desorbing the fibers into the GC inlet. Studies were not conducted to determine the headspace equilibrium time. Pre-equilibrium extractions were chosen to simulate practical operational conditions for trace explosives detection at checkpoints. The peaks of interest were identified using the NIST mass spectral library. The specific additives of

the powders found to be in significant amounts in the headspace for the smokeless powders and those previously studied in canine trials were determined to be the volatile chemicals markers.

Results and discussion:

It was observed from the GC-MS results that diphenylamine (DPA) was the common volatile additive among all the powders tested. 2,4-dinitrotoluene (2,4-DNT) was detected in both the single based powders tested (IMR 4198 and Hodgdon 322) and because of its high vapor pressure, is extracted in large amounts from the headspace. Ethyl centralite (EC), an additive that serves the same purpose as DPA was found in both the Alliant double-based powders tested (Alliant Unique and Alliant Red dot). In the Red dot powder, it was present in quantities that were measurable in the headspace. However, in the Alliant Unique powder, the EC was detected amounts close to the detection limits at the longest extraction times.

Apart from these main additives, other compounds were also extracted from the headspace of the smokeless powders tested. The nitro derivatives of DPA were detected in small amounts in some of the powders, but were not considered as analytes of interest at this point of the study. They are well known degradation products of diphenylamine and their amounts could not be quantified accurately with the GC-MS method used for this study. The Alliant powders were observed to have a lot of residual solvent with toluene and guanidine being detected in high amounts. Another compound of possible interest, 2- Ethyl 1-hexanol was found in the double-based Hodgdon BL C-(2) powder. This compound has been reported to be one of the volatile

markers for plastic bonded explosives through canine trials[6]. It is known that nitroglycerin (NG) is present in large amounts up to 40% of the total mass in double-based powders. It is also expected that there would be significant amounts present in the headspace of the powders due to it high volatility. However, in the current GC-MS method, NG was not detected in the headspace of any of the powders. Therefore, this compound was not included as an analyte in the current study and its detection will be discussed further later in this chapter.

Based on the GC-MS results, DPA, EC, 2,4 – DNT and 2-Ethyl 1-hexanol were chosen as four analytes of interest for this study. Standard solutions of each analyte in the concentration range of 2.5 ng/μL - 25 ng/μL were prepared and 1 μL of each solution was injected into the GC-MS to develop calibration graphs for each analyte. The liquid injection method was used for this study, as the microdrop printing SPME calibration method discussed in the previous chapter was developed after the results of this project were obtained. Extraction time profiles were generated for each powder to determine the mass extracted at the different extraction times. The time vs. response graphs obtained for each powder were plotted as the peak area observed at different extraction times. These graphs were converted to mass vs time graphs on interpolating the response of the extraction time graphs to the calibration graphs using the regression equations obtained.

The figures below are representative of the type of graphs obtained for each of the powders. In Figure 53 A, the profile of Alliant Unique powder is depicted where diphenylamine is the major compound of interest and in 53 B the DPA mass extracted

at the different times for the same powder is shown. Figure 53 C is a representation of the Red dot powder extraction profile with two compounds of interest, DPA and EC. Figure 53 D is shown to illustrate the high mass extraction of 2,4-DNT in a single based powder Hodgdon 322 and 53 E is the representation of the same powder as a mass vs. time graph. As can be seen from the graphs, the mass extracted from the powders increases over time and even at the highest extraction time, the graph shows that the extraction has not yet reached the plateau region of equilibrium. Also of importance is that at the lowest extraction time of 5 minutes, there is sufficient mass extracted by the fiber from headspace. In powders where there was more than one compound present in the headspace, both were extracted in sufficient amounts at the lowest extraction time. When 2,4 –DNT was present as is seen in Figure 53 D, it dominates the extraction profile and is the major compound detected.

The mass of the DPA extracted from headspace of 100mg of the five powders tested in this study ranged from 0.15 - 6 ng. The mass range of 2,4-DNT for the IMR 4198 and H322 powders ranged from 0.72- 41 ng for the typical 5- 120 minute extraction. For the red dot powder, up to 3 ng of ethyl centralite was extracted onto the fibers in 30 min. In the H BL C-(2) powder, large amounts of 2- Ethyl 1-hexanol were extracted. Up to 1.5 ng was extracted in 5 min onto a fiber. Based on these results, the study was extended to the IMS to determine if similar profiles would be obtained by the IMS.

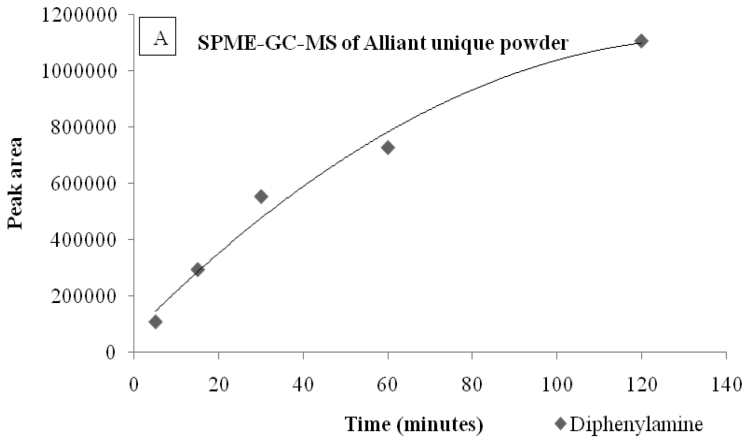
A
SPME-GC-MS of Alliant unique powder
Peak area
1200000
1000000
800000
600000
400000
200000
0
0
20
40
60
80
100
120
140
Time (minutes)
Diphenylamine

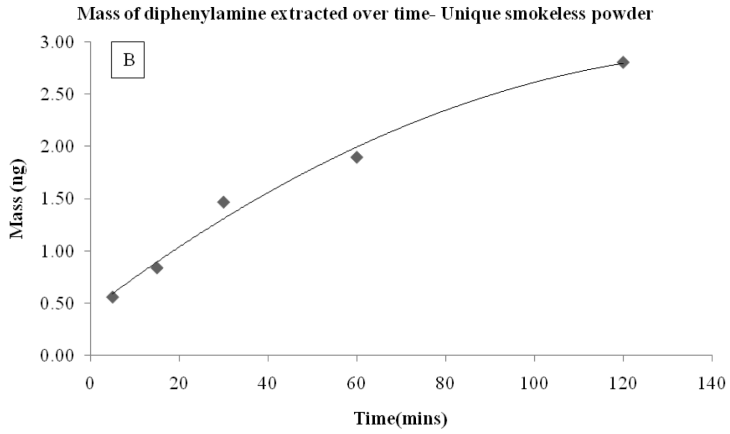
Mass of diphenylamine extracted over time- Unique smokeless powder
B
Mass (ng)
3.00
2.50
2.00
1.50
1.00
0.50
0.00
0
20
40
60
80
100
120
140
Time(mins)

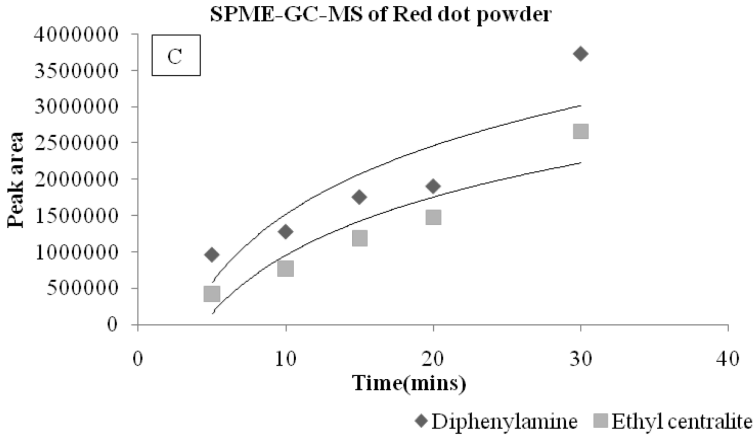
SPME-GC-MS of Red dot powder
C
Peak area
4000000
3500000
3000000
2500000
2000000
1500000
1000000
500000
0
0
10
20
30
40
Time(mins)
Diphenylamine
Ethyl centralite

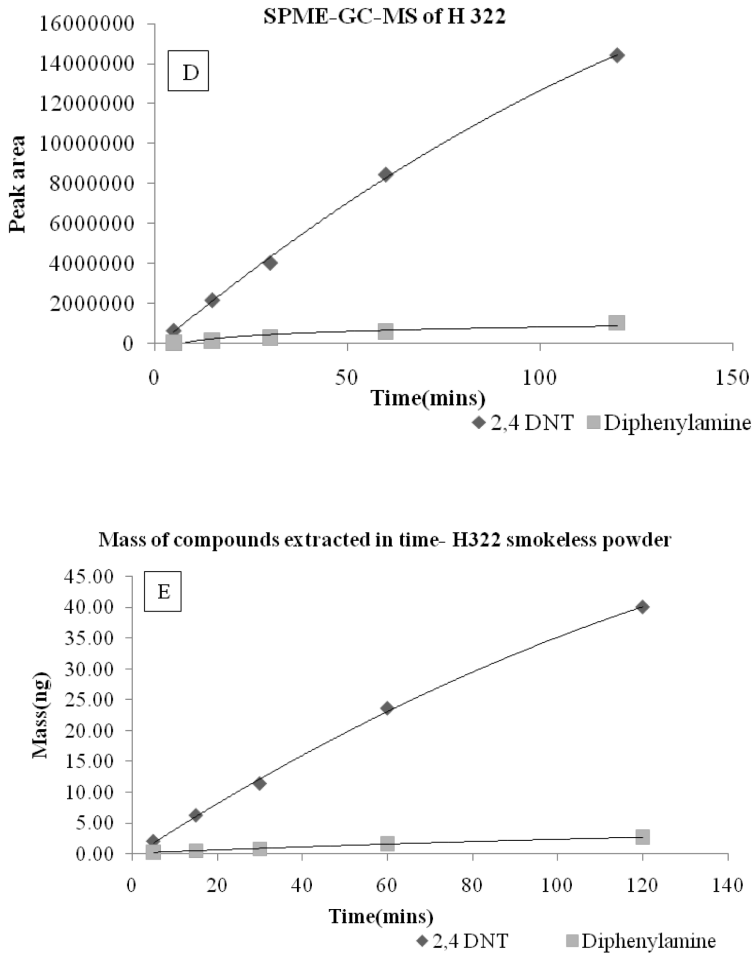

Figure 53: SPME GC-MS results for smokeless powders: A) Alliant Unique extraction profile B) Alliant Unique mass of additives extracted over time C) Alliant Red dot extraction profile D) Hodgdon 322 extraction profile E) H 322 mass extracted over time

4.2. SPME-IMS analysis

Instrumentation and methods:

A General Electric Ion Track Itemiser II IMS instrument shown in Figure 9 A equipped with a detachable SPME-IMS interface as shown in Figure 52 was used for this study. To determine the IMS detection conditions of each analyte, standard solutions containing 50 ng/ μL of the target compounds DPA, EC, 2,4-DNT and 2-ethyl hexanol were used. Each analyte was individually spiked (1 μL) onto an IMS filter and analyzed. The analyte ion peaks were determined by analyzing replicates of the solutions and solvent blanks in both the positive and negative detection modes. The standard solutions were analyzed in two different IMS instruments and the mobility values of the peaks were compared to previously reported values. DPA and EC were detected in the positive mode whereas 2 4-DNT was detected in the negative mode. 2-Ethyl hexanol did not produce any characteristic peaks. It is understood that at ionization and detection settings used, 2-Ethyl hexanol does not produce a product ion that can be detected. The IMS parameters and the mobility values are the same as those listed in Table 3 of chapter II. Once the location of the peaks were identified by solutions of the standards and SPME extraction of the standards, the extractions of known amount of the smokeless powder samples were carried out similarly to the GC studies described above. The SPME fiber containing the extracted analytes was introduced into the IMS interface for analysis. Response curves for each of the smokeless powders were generated by plotting the analyte signal versus the mass extracted.

Calibration graphs necessary to determine the mass of analytes extracted by the fibers during headspace extractions of smokeless powder were generated using the

microdrop printing technique. Solutions of the analytes (10 ng/μL) were prepared in 2-butanol and the jetting parameters were adjusted such that a monodispersed drops was generated with each trigger. The mass response graphs were obtained by delivering different amounts of the analyte onto the IMS substrate by printing increasing number of drops. The lowest mass of the analyte deposited that is equal to three times the standard deviation of the blank signal was determined to be the limit of detection of that analyte on the instrument.

Results and discussion:

The Figures 54 A-C are the plasmagrams for the three analytes DPA, EC and 2,4-DNT. The plasmagrams show that each analyte produces only one ion peak at the concentration tested. It was observed with 2 4 –DNT that at high concentrations a second peak with the same drift time as 2,4,6-TNT was produced. Spangler and Lawless observed this same phenomenon, and demonstrated that the second peak for 2,4-DNT observed at high concentrations and the peak for 2,4,6- TNT were due to the presence of different ions[95]. They also speculated that this peak may be due to the formation of a dinitrobenzyl anion at high concentrations of 2,4-DNT. Addition of a mass spectrometer to the IMS would answer such product ion questions and present more reliable information on the analyte ion identities.

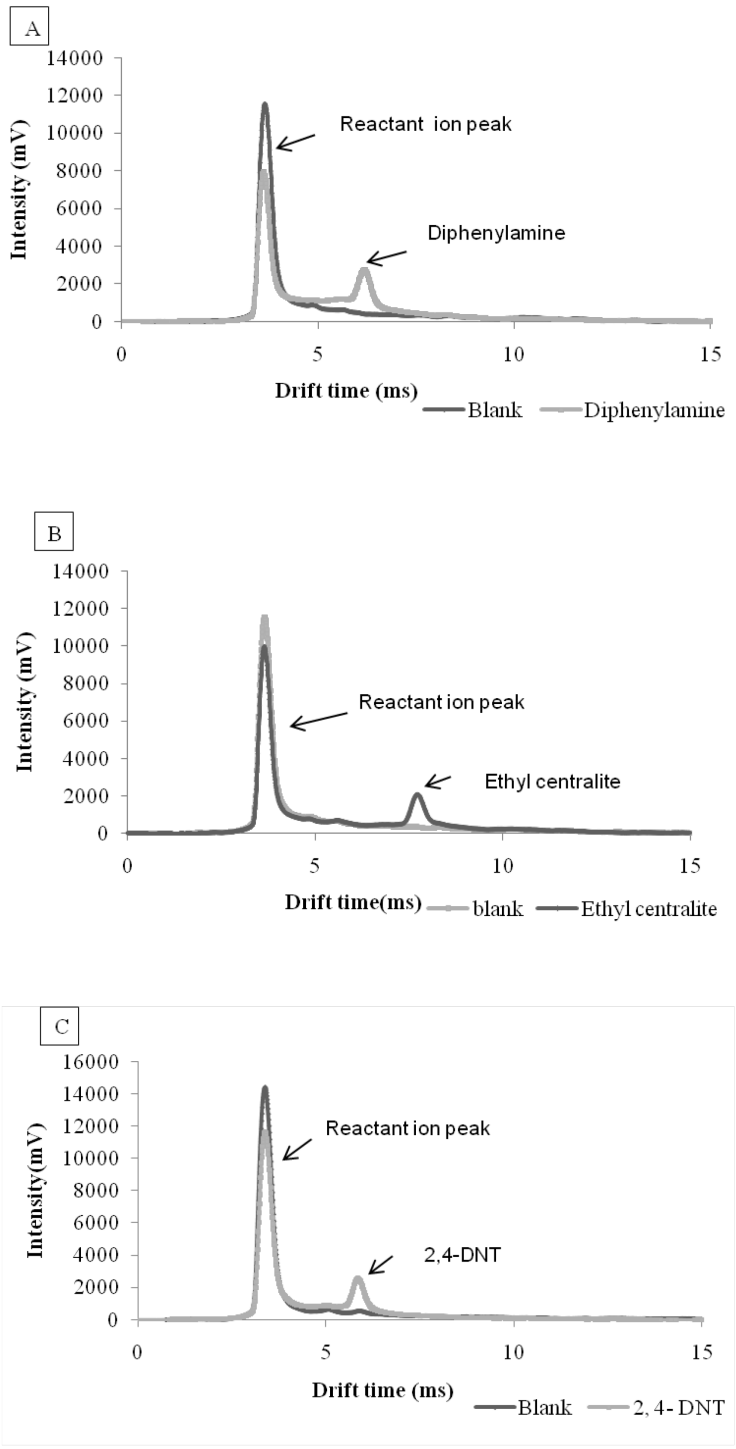

Figure 54: IMS plasmagrams for three analytes of interest- A) Diphenylamine in +ve mode B) Ethyl centralite in +ve mode C) 2,4- dinitrotoluene in -ve mode

On the SPME-IMS analysis of the smokeless powders, results similar to the SPME-GC-MS analyses were obtained. All five powders tested gave distinct peaks for diphenylamine including the Red dot powder that has both DPA and EC. In the Red dot powder, EC was detected lower than the expected intensity. The SPME-GC-MS results demonstrated that both DPA and EC were present in substantial amounts in the headspace with DPA being detected in slightly higher amounts. In order to improve the signal intensities for ethyl centralite, the dopant used in the IMS was changed from ammonia to nicotinamide. In an atmosphere of nicotinamide, slightly higher intensities were observed for EC in the presence of DPA. Shown in Figure 55 is the extraction profile for the Red dot powder using nicotinamide as the dopant. In IMS, there is a preferential ionization when there is more than one analyte present. This is seen the Red dot profile where the DPA which desorbs first is preferentially ionized. Analysis of complex mixtures in the IMS therefore is not straightforward when quantitation is desired. However, the DPA and EC peaks are sufficiently resolved in the positive mode and the detection of two peaks in the headspace of smokeless powders adds significance to the smokeless powder detection alarm. As discussed before 2- Ethyl hexanol did not produce any peaks in the positive or the negative modes of the IMS. Therefore, in the Hodgdon BL C-(2), diphenylamine was the only peak observed. The single-based powders both IMR 4198 and H 322 produced peaks for 2,4 –DNT. The intensities observed for 2,4-DNT was lower than expected and was observed that the analyte desorbs slowly off the fiber and therefore complete desorption was not occurring within the analysis time leading to the lower peak intensities.

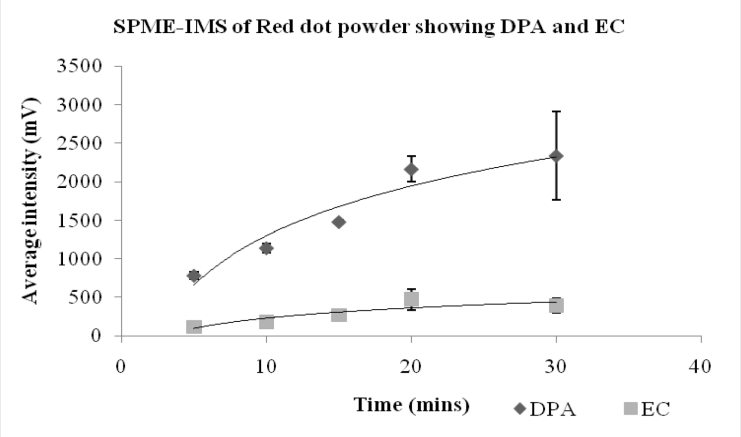

Figure 55: SPME-IMS extraction profile of 100 mg of Alliant Red dot powder

Quantitation of the mass of analytes detected from the headspace of smokeless powders was obtained by the mass response graphs developed by microdrop printing. The mass of EC could not be quantified though the GC-MS results demonstrate that 3 ng of EC was extracted at 30 min. Mass of 2,4-DNT was also not obtained for this study as it was found from the liquid spike studies that 2,4-DNT desorbed very slowly from surfaces leading to incomplete desorptions and inaccurate mass response graphs. The results were compounded by the peak for 2,4-DNT that was observed at low mass loadings and as the mass of 2,4-DNT analyzed increased (above 20 ng), a second peak was observed to be forming with a decrease in the first ion intensity. The 2,4-DNT mass extracted by the fibers as observed from the SPME-GC-MS studies is much higher than 20 ng for both the IMR 4198 and H 322 powders. Diphenylamine was easily quantified in all the powders tested. The mass extracted vs. time graphs for all the powders are illustrated in Figure 56. As can be seen from the graph, the mass of diphenylamine extracted at the shortest time was greater than the detection limits of DPA that were determined to be 0.12 ng from the microdrop printed calibration graph.

The same trend was observed as that of the SPME-GC-MS results with the largest amount of DPA being extracted from the headspace of Alliant Unique double-based powder. All other powders had similar DPA mass in the headspace. The graph also shows that the DPA extraction had not yet reached equilibrium and pre-equilibrium extractions were sufficient to detect DPA even at the lowest extraction times.

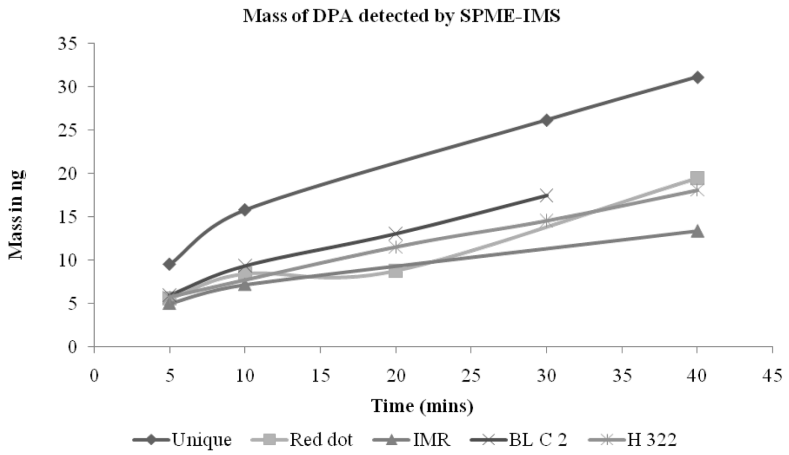

Figure 56: Mass of DPA extracted at different times from the headspace of the five smokeless powders studied by SPME-IMS

Overall Conclusions:

This smokeless powder study helped generate vital information that led to the expansion of the smokeless powders analysis. The hypothesis that the volatile components present in the smokeless powders can be extracted and detected by instrumental techniques was proved right. Though the study was limited to five powders, the results obtained established that there are several compounds present in smokeless powders that can be added to the IMS detection repertoire. In addition, all

the powders studied had DPA in their headspace. This warranted the expansion of the study of smokeless powders to determine differences within manufacturer for different products and within the different lots of the same product. As was observed with the 2-Ethyl hexanol, it is important also to tabulate a list of available compounds detected by chromatographic methods (GC-MS, GC-ECD) and those that can be detected by the current IMS settings without much modification to the manufacturer settings used in those that are already deployed in the field.

5. STUDY OF THE FBI SMOKELESS POWDER SAMPLES

Samples of smokeless powders that are a part of Dr. Ronald Kelly's collection at the FBI were received for analysis at FIU. Apart from the samples, we were also given access to the results of the bulk analysis that were generated at their laboratory. The bulk analysis of all the powder samples received was conducted by extracting the organic additives from 25 mg of powders using methylene chloride for three hours. The extract is injected into a GC-MS equipped with a 30 m DB-5 column. The mass spectrometer used is a mass selective detector (MSD) and therefore gives them the ability to detect nitroglycerin in the same method as the other analytes.

In this collaboration, my role was to develop methods for the extraction and detection of volatile components of the smokeless powder samples that were supplied. Chromatographic and ion mobility spectrometric detection parameters were required to be established to supplement the bulk composition information available with the FBI for the various powders.

Table 6: List of smokeless powders from the FBI sample set

Manufacturer	Number of powders	Double based/ Single based
Alliant	15	100% Double-based
Hodgdon	22	64% Single-based
Accurate	7	43% Single-based
IMR	6	83% Single-based
Vihta Vuori	3	100% Single-based
Winchester	3	100% Double-based
Hercules	2	100% Double-based
Norma	3	33% Single-based
Dupont	3	66% Single-based
Scot Royal Scot	1	Double-based

The two samples sets received contained 65 powders in total with 30 powders in the first set and 35 in the second set. The FBI database or collection of smokeless powder lists over 700 powders collected over 25 years. The samples given to us were chosen carefully to represent various compositions as determined by the bulk analysis of the smokeless powders. Overall, the powder sample set is represented by eight

distributors. The ten brand names listed in Table 6 are due to the fact that some brand names have changed or have been taken over by other distributors over the years. For example, the Hercules brand name powders are now sold under the Alliant brand name and the Dupont powders are sold under the IMR powder name. The Table 6 lists the number of powders per manufacturer that are part of the sample set and the distribution of double and single-based powders. Of the 65 powder samples, 38 powders are double-based while the rest are single-based. Some powders for a manufacturer are duplicates of the same product with different lot numbers. For example, there are four Alliant Red dot powders in the sample set and they are used to study the differences between different lots of a powder.

5.1. SPME-GC-MS analysis

Gas chromatography is a technique of choice when analyzing volatiles. When combined with the appropriate sampling system, it can generate profiles for the volatile components in the headspace above a condensed phase matrix. In this study, a method was developed to generate profiles for a wide range of compounds present in the headspace of smokeless powders. Solid phase microextraction (SPME) is used as a sampling system to trap and concentrate the volatiles onto the extraction phase before desorbing the analytes into the GC-MS inlet.

GC-MS method:

Each of the 65 powders was weighed and 100 mg of each powder was placed in a 15 mL clear glass vial (Supelco (Bellefonte, PA)) and sealed with a phenolic screw

cap with a red rubber/PTFE septum. The powders were allowed to equilibrate for 24 hrs before sampling for 60 min with a 100 μm PDMS fiber. The extractions by the fiber are all pre-equilibrium conditions and a one-hour extraction time was chosen since it would provide opportunity for the more volatile analytes to reach equilibrium on the fiber while extracting detectable amounts of the low volatility compounds. The fiber with the absorbed analytes was desorbed into the GC injection port for 5 min to allow for complete desorption.

A Varian (Palo Alto, CA) CP 3800 gas chromatograph with to a Saturn 2000 ion trap mass spectrometer (GC-MS) as detector was used for this study. A 50 m DB-5 column with 0.25 mm ID and 1 μm film thickness was temperature programmed from 40 ^{o}C to 280 ^{o}C. The program began with a 1 min hold and then increased the temperature to 200 ^{o}C at 15 ^{o}C min^{-1} with a 1 min hold at that temperature. The temperature was then increased to 240 ^{o}C at the rate of 15 ^{o}C min^{-1} and held for 6.50 min at that temperature. From 240 ^{o}C the temperature was increased at a rapid rate of 25 ^{o}C min^{-1} until the column oven temperature was 270 ^{o}C. The final temperature of 280 ^{o}C was reached by ramping the temperature at 5 ^{o}C min^{-1} and holding there at 4 min. The injector temperature was set at 280 ^{o}C in split mode (split ratio 5:1) and using a column flow of 2 mL min^{-1}. The transferline to the ion trap was set to 280 ^{o}C and the ion trap itself was maintained at 180 ^{o}C. The method length was 29.3 min and was optimized to separate and detect most of the volatile components of smokeless powders. The research project described here mainly focussed on the specific additives of smokeless powders and therefore no characterization of the volatiles such

as the residual solvents was included. Nitroglyercine and the nitroso derivatives of diphenylamine, which are compounds of interest, were not detected by the GC method described above. They are known to degrade at the temperatures required for all other analytes. Nitroglycerine therefore was studied in the GC-ECD.

Results and discussion:

1. Overall distribution of volatile additives in smokeless powders:

Headspace profiles were generated for all the sixty-five powders in the sample set by the GC-MS method detailed above and a SPME extraction of one hour. The chromatogram of each powder was carefully studied for peaks of interest and each peak identified using the NIST Mass Spectral library. Due to the multiple peaks observed, the peaks are categorized into the following ten groups to ease data presentation - diphenylamine (DPA), ethyl centralite (EC), 2,4-dinitrotoluene(2,4-DNT), the phthalate group (diethyl phthalate (DEP) and dibutyl phthalate(DBP)) , 2-nitrodiphenylamine (2-NDPA), 4-nitrodiphenylamine (4-NDPA), nitrotoluenes (2,3-DNT, 2,5-DNT, 2,6-DNT, mononitrotolunes and 2,4,6- Trinitrotoluene), methyl centralite (MC), ethylphenylamine (EPA) and miscellaneous analytes (butyl benzoate, diphenyl sulfone, diphenyl formamide and ethyl hexanol). DPA was observed to be the most common additive across the powders with 62 powders having a distinct peak for DPA. Of the three powders in which DPA was not detected, EPA was observed in one powder and could be a degradation product. The diphenylamine derivatives, 2-NDPA and 4-NDPA are sometimes added to powders as stabilizers. As discussed earlier, they are also degradation products of the powder. These products were

generally present in very small amounts in powders with diphenylamine. 2-NDPA was more common than 4-NDPA which was observed only in the presence of 2- NDPA. Of all the powders tested, the Alliant brand of powders had the highest amounts of 2 and 4-NDPA. Of the two centralites, EC was more common. It was usually observed in combination with DPA. 2,4-DNT when present was extracted in large amounts from the headspace of the powders. Forty five percent of the powders showed evidence of 2,4-DNT in the headspace and these powders were equally comprised of both double and single-based powders. In the presence of 2,4-DNT other isomers of 2,4-DNT such as 2,6-DNT, 2,5-DNT and 2,3-DNT were also observed in small amounts with 2,4-DNT being the dominant peak. In some cases, mononitrotoluenes were also observed. 2,4,6, -TNT was detected as very small peaks in the headspace of the Norma powders. The phthalates, DBP and DEP were the two phthalates that were most commonly observed. Compounds classified as miscellaneous compounds include compounds that do not have known specific function in smokeless powders. Ethyl hexanol is present in several powders along with other long chain hexanols. These are expected to be artifacts of the manufacture process along with butyl benzoate and other solvents. No literature sources describing their function in smokeless powder were found. In addition, these compounds are used in several other manufacturing processed and were not considered important for this study.

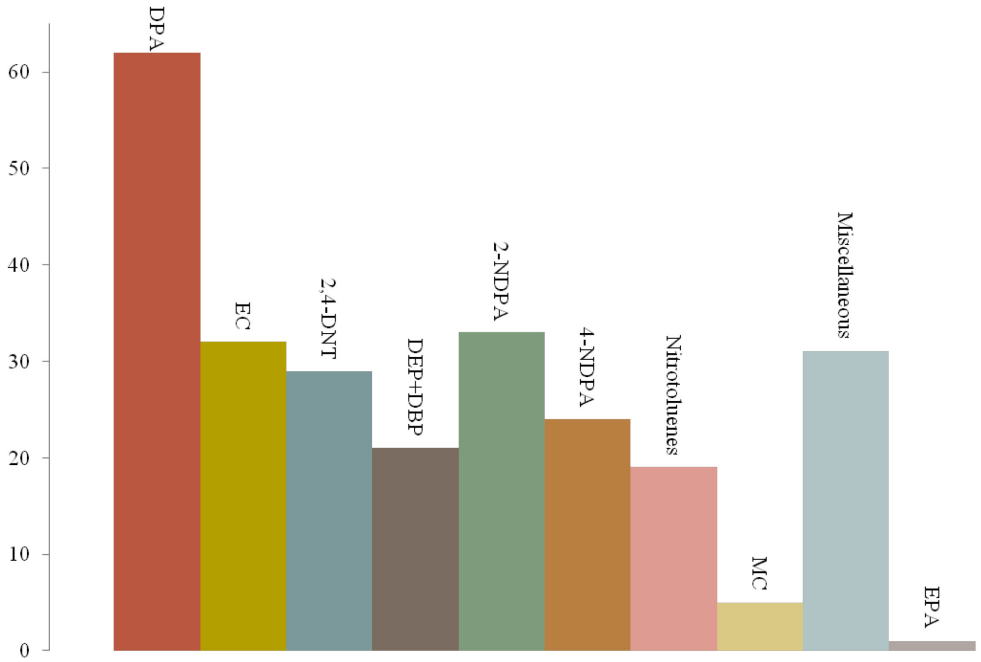

Figure 57: Overall distribution of additives detected by headspace SPME GC-MS analysis of the complete FBI set of 65 smokeless powders

2. Reproducibility studies:

Studies are necessary to determine the reproducibility of the headspace extractions conducted by SPME and the stability of the headspace components of smokeless powders. The information adds confidence to the headspace compositional profile developed for each powder.

a) Reproducibility of SPME extractions:

In this part of the study, the reproducibility of extraction between different fibers was studied. In order to obtain this information, the headspace of two powders was analyzed on the same day with three PDMS fibers to prevent inter-day

variations. Simultaneous extractions were conducted by placing the same amount of the powder in three vials and sampling the headspace with three PDMS fibers. All three fibers used were new such that the condition of the extraction phase on the fibers is the same for all three extractions. The SPME-GC-MS extractions were carried out with the same method described before. Figures 58 A and B demonstrate the variation in the results obtained between the three fibers.

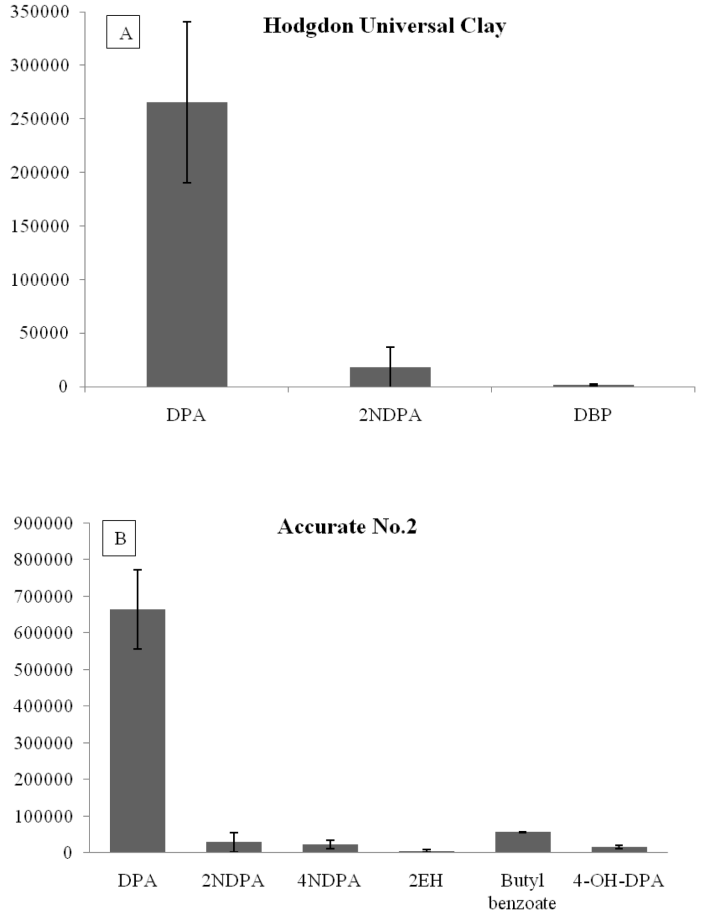

Figure 58: Reproducibility of SPME headspace extractions from smokeless powders A) Hodgdon Universal Clay 60 min extraction B) Accurate No. 2 60 min extraction

Hodgdon Universal Clay powder had three major components in the headspace: DPA, 2-NDPA and DBP. All three analytes were observed in the three extractions. The Accurate No. 2 powder had multiple compounds in its headspace with the major compounds being DPA, 2-NDPA and 4-NDPA. The other compound of interest was 4-hydroxy diphenylamine. This derivative of diphenylamine was not present in any other powder of the seventy powders studied. The other two compounds present in the headspace were 2-Ethyl hexanol and butyl benzoate, which were classified as part of the miscellaneous group of headspace components.

In both the powders, the highest precision was obtained for the diphenylamine extraction. The average percent relative standard deviation (%RSD) was less than 25%. The greatest error was associated with the extraction of the nitrated diphenylamines and was on an average close to 80%. The results of the 2-NDPA in the Hodgdon powder biased the average towards a higher number due to the signal being very close to the limits of detection.

Overall, the study demonstrated that there was consistency in the extractions between different SPME fibers. The compounds in the headspace did not vary in the three samples thus also demonstrating that there was homogeneity in the smokeless powder and the three 100 mg samples of a powder were similar.

b) Reproducibility of the headspace composition of smokeless powders:

Smokeless powders are dynamic materials with several processes occurring at the same time. Degradation of the nitrocellulose and nitroglycerin causes the nitration of the diphenylamine thereby changing the relative ratios of the DPA and nitrated DPA peaks. The evaporation of the volatile compounds could occur over time leading to depletion in the powders. In order to study variation in the headspace of the powders between different days, studies were conducted with five smokeless powders.

The headspace of each of the five powders was sampled five times for 60 min over a period of five days. The extraction and GC-MS detection method used are the same as that used for all GC-MS analysis for this study. The variation of the headspace profile of each of the five powders is shown in Figures 59 A-E. The powders were chosen such that powders with complex headspace profiles and those with simple headspace profiles were included. The graphs represent the variation in all the compounds of interest and the miscellaneous compounds.

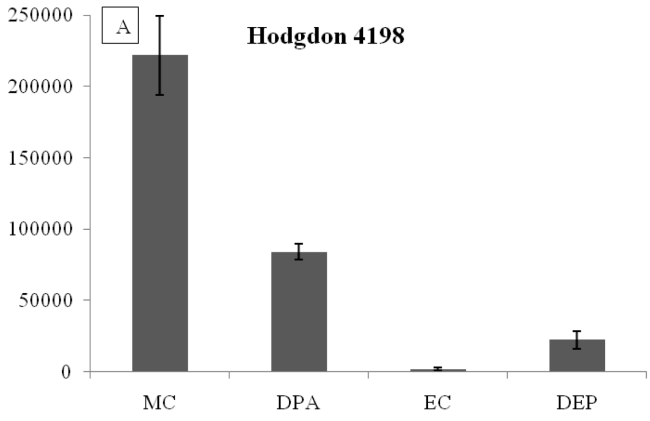

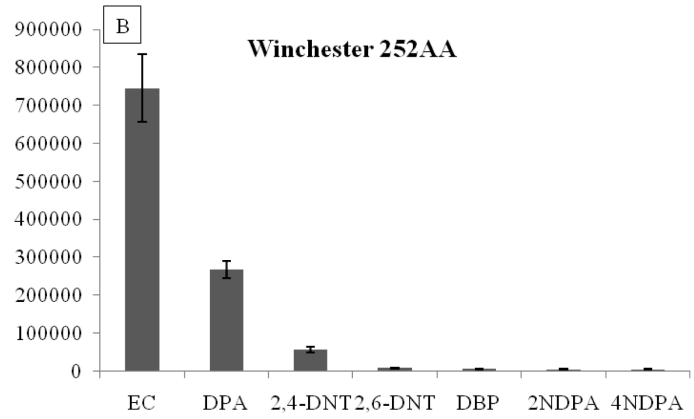
B
Winchester 252AA
900000
800000
700000
600000
500000
400000
300000
200000
100000
0
EC
DPA
2,4-DNT
2,6-DNT
DBP
2NDPA
4NDPA

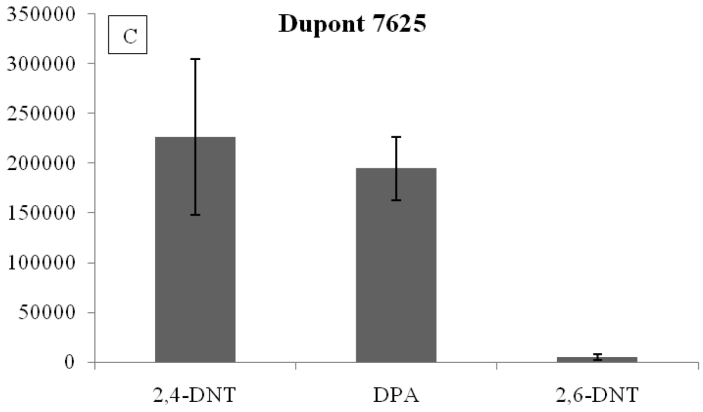
C
Dupont 7625
350000
300000
250000
200000
150000
100000
50000
0
2,4-DNT
DPA
2,6-DNT

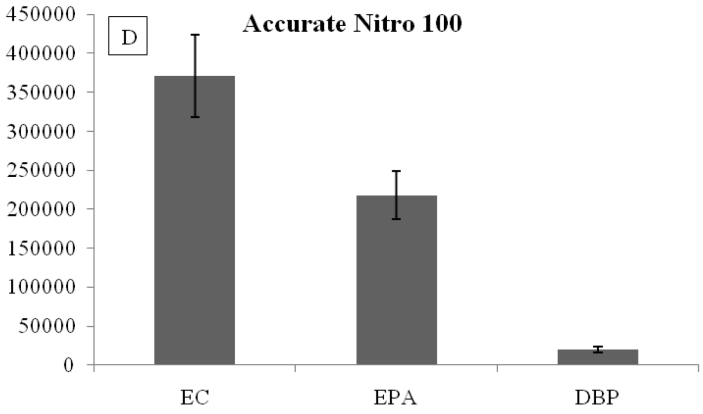
D
Accurate Nitro 100
450000
400000
350000
300000
250000
200000
150000
100000
50000
0
EC
EPA
DBP

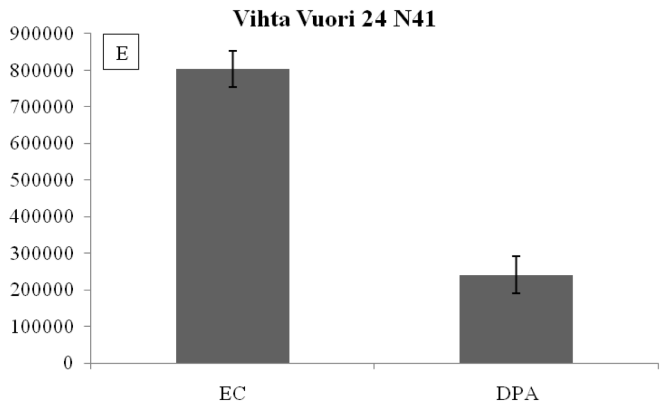

Figure 59: Inter-day variation of headspace extractions A) Hodgdon 4198 B) Winchester 252AA C) Dupont 7625 D) Accurate Nitro E) Vihta Vuori 24 N41

As observed with the earlier reproducibility studies, variation was observed in the extraction of several of the compounds in this study. The precision observed for each powder is summarized in Table 7. Of the powders chosen for this study, DPA was present in four powders and its precision was the highest with the average % RSD being less than 10% for the powders. The nitrated diphenylamines were present only in the Winchester 452 AA powder in low quantities on all days with the variation being at about 60% across the ten days. The variation in the rest of the components in the complex powder was very small with the average being less than 15%. The Dupont 7625 smokeless powder had only three major components with the two biggest headspace contributors being DPA and 2,4-DNT. The isomer 2, 6-DNT was also observed with smaller peaks and had the least precision. Accurate Nitro was one of the three powders in the entire sample set of 70 powders that did not show the presence of DPA in its headspace. In place of DPA, ethylphenylamine (EPA) was observed in the

headspace. This compound was present in substantial amounts and gave good precision over the ten days. The headspace of Vihta Vuori 24 N 41 was dominated by DPA and EC present in substantial amounts and both were reliably extracted with the average % RSD in ten days being 6%.

Overall, the headspace profiles of the five powders tested did not change significantly over the period of ten days. The two nitrated diphenylamines of interest had variations higher than the other compounds though this was to be expected due to the constant inter-conversions between DPA, 2-NDPA and 4-NDPA. The variation of all the compounds detected by GC-MS however fall within the method detection limits. This is useful in generating a composition profile for each powder as detected by GC-MS.

Table 7: Precision associated with SPME- GC-MS headspace analysis of five smokeless powders over ten days

Name of powder	%RSD
Hodgdon 4198	<40%
Winchester 452AA	<15% ,~ 60% for NDPA's
Dupont 7625	<40%
Accurate Nitro 100	<15%
Vihta Vuori 24 N41	6%

3. Compositional profiles:

The headspace profile of each powder varies based on the type and amount of volatile components present. The vapor phase composition of each powder can be obtained by different analysis methods. In this study, composition profiles for the powders based on those volatiles sampled by SPME and detected by GC-MS are generated. These profiles are important visual information about the variety and amounts of the components in the headspace. When targeting volatiles for detection of the powders, these profiles help in determination of those that are most important for unambiguous detection of smokeless powders.

Figure 60 represents the SPME-GC-MS profiles of the Hodgdon brand smokeless powders that are part of the FBI sample set. The graph is plotted such that each of the nine categories of the compounds of interest is plotted by its peak height observed in a 60 min extraction. The detection limits of each of the compounds are listed in the legend of the graph. The graph excludes two other peaks of interest, nitroglycerin and the nitrosodiphenylamine (N-NODPA and 4-NODPA) peaks. The NODPA peaks are highly thermally labile and therefore not seen in the GC methods used. Nitroglycerin will be discussed in the GC-ECD section.

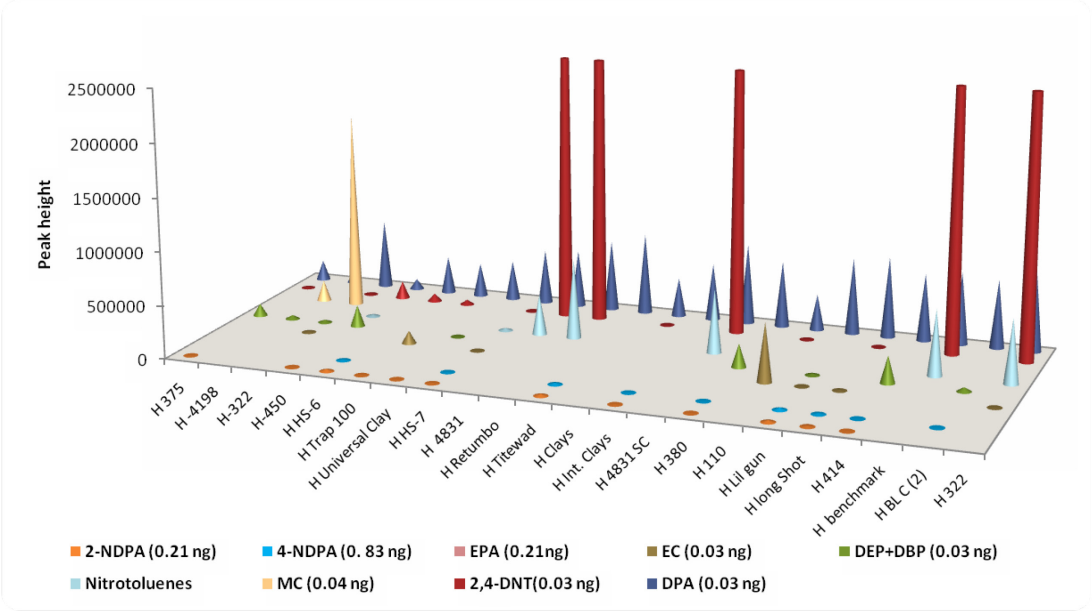

Figure 60: Headspace composition profile of all the Hodgdon powders part of the FBI sample set as obtained by SPME-GC-MS analysis

Based on the graph shown above, it is clear that there is an abundance of information available in the smokeless powders headspace. Each powder has more than one volatile component and therefore a bouquet of compounds can be targeted as volatile signatures of smokeless powders. All the Hodgdon powders have DPA and its headspace concentration varies widely between the powders. The 2,4-DNT was present in 50% of the Hodgdon powders but was present in very high quantities with associated nitrotoluenes in the single-based powders. The smaller constituents of the headspace volatiles were the nitrodiphenylamines with peak heights being close the mass detection limits of the detector.

Overall, the major compounds available reliably for the detection of smokeless powders by SPME sampling and using GC-MS detector were diphenylamine, ethyl and methyl centralite, diethyl and dibutyl phthalate, and 2, 4-dinitrotoluene.

5.2. SPME-GC-ECD analysis

The electron capture detector (ECD) is very sensitive and selective detector for the electronegative compounds. The coupling of the detector to gas chromatography makes the technique an excellent technique for the quantitative analysis of electron capturing compounds. Nitroglycerin is one such compound that gives very high sensitivity in the GC-ECD and has been reported in several literature sources as the choice detection method. GC-ECD coupled with SPME for the extraction and detection of nitroglycerin from post-blast residues has also been reported. . Other studies including the FBI GC-MS bulk studies of smokeless powders have reported the detection of several of the smokeless powder additives including nitroglycerin in the same method. Such methods have used different injector conditions and mass analyzers than those available for this project. In this study, since the GC-MS method being used for the other analytes of interest was not capable of detecting nitroglycerin (NG), an ECD detector was employed to characterize the presence of this compound in double-based smokeless powders

Selection of extraction phase:

The study was carried out in two stages using two separate ECD configurations. In the first stage of the study an Agilent (Santa Clara, CA) 5890 gas chromatograph

equipped with an ECD detector was used to establish nitroglycerin detection from the headspace of smokeless powders. A Restek (Bellefonte, PA) RTX-TNT2 6.0 m column with 1.50 μm i.d. was used with a Restek Uniliner® Siltek 1 mm liner. The GC column oven method was optimized for the highest response of NG. The optimized method had an injection temperature of 220 ^{o}C to ensure complete desorption of the analyte from the PDMS fiber. The detector temperature and the maximum temperature of the oven were both maintained at 300 ^{o}C. Splitless injection mode was used to maximize the sensitivity for NG. The total method run time was 20 min with the column temperature beginning at 80 ^{o}C and increasing to 180 ^{o}C at a rate of 20 ^{o}C/min. Upon reaching that temperature, it was held there for 2 min before increasing to 250 ^{o}C at a rate of 20 ^{o}C/min and held for 3 min at 250 ^{o}C. Finally, the temperature was increased to 300 ^{o}C at a rate of 20 ^{o}C/min and it was held at this temperature for 3 mins.

The 100 μm PDMS fibers were chosen previously as the optimal fibers needed for the complete analysis of smokeless powders due to the large extraction phase volume and its molecular weight compatibility with the analytes of interest. However, for the NG studies, different fibers available were studied to determine the one that was most suitable for extractions from smokeless powders and for the ECD. The three extraction phases studied were Carboxen/polydimethylsiloxane (CAR/PDMS) 85 μm, Polydimethylsiloxane (PDMS) 100 μm and Polydimethylsiloxane/Divinylbenzene (PDMS/DVB) 65 μm film thickness. The Alliant Unique double-based powder sample was weighed and 2.5 mg were placed in sealed quart cans and gallon cans allowing for

1 min equilibrium for the headspace and 5 min extraction. The extraction time was kept short to determine which fiber gave the highest extraction in the shortest time. The graph below illustrates the results obtained for the three fibers.

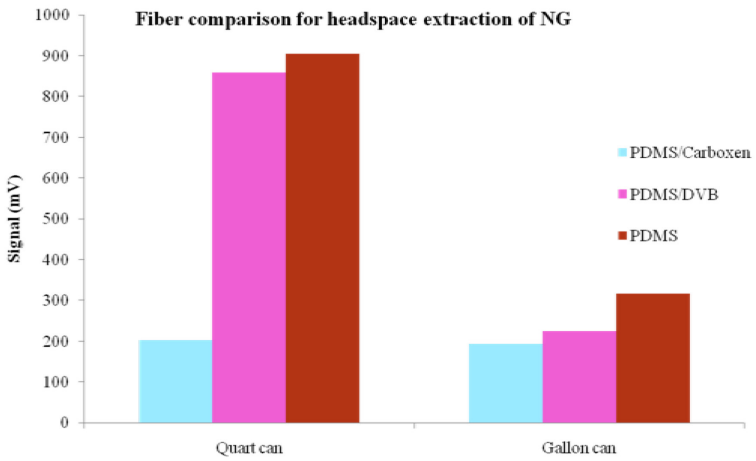

Figure 61: Comparison of GC-ECD intensities from the three SPME fiber chemistries for extraction of NG from a double-based smokeless powder

The graph clearly demonstrates that the CAR/PDMS adsorption fiber was not suitable for the extraction of nitroglycerin from the headspace of smokeless powders. Both the absorption fibers PDMS and PDMS/DVB gave significantly higher responses for the same extraction conditions. Between the two fibers, PDMS gave a slightly higher response. When comparing the two sampling volumes, quart (250 mL) can and gallon (1000 mL) can, the same trend was observed with PDMS fibers giving the highest response. As expected, lower signals were observed for the gallon can sampling but the CAR/PDMS fiber gave similar results with both the gallon and quart

can suggesting that the extraction kinetics for NG on the absorption and adsorption fibers were very different.

The 100 μm PDMS fiber was used for all further studies of extraction of NG and other analytes from the headspace of smokeless powders both for chromatographic and ion mobility spectrometric analysis.

Limits of detection of compounds of interest:

The identity of the different peaks produced in a GC-ECD analysis can only be obtained by analyzing standard solutions of each analyte individually and comparing column retention times. Therefore, when analyzing the complex smokeless powder headspace, standard solutions of each analyte needed to be analyzed to confirm the detection of an analyte. The method was optimized to detect as many compounds as possible while not compromising the response of NG, which is the primary reason to use the GC-ECD. The compounds detected by the ECD were NG, 2,4-DNT, DEP, 2-NDPA, 4- NDPA and 4-NODPA. The two centralites, EC and MC, DPA and N-NODPA were not detected. The ECD was selective only for those with the nitro group present whereas the N-NODPA breaks down into DPA immediately in the injector and cannot be detected.

In order to improve the sensitivity and linear range for NG a micro–ECD cell was used instead of the ECD detector. An Agilent (Santa Clara, CA) 6890N gas chromatograph with the μ-ECD detector was optimized for the detection of NG. The GC method used was very similar to the method used for the ECD detection. The

column, the maximum oven temperature and the detector temperature used were the same as before. The liner was changed to a higher volume, Restek Siltek 4 mm single gooseneck liner with a cup splitter. The method run time was 14.9 min with the column temperature program modified to improve separation of the analytes. The column was held at 80 ^{o}C for 1 min and then increased to 180^{o}C at a rate of 15^{o}C /min. Upon reaching that temperature, it was held there for 3 min. From 180 ^{o}C, the temperature was increased to 240^{o}C at a rate of 15 ^{o}C/min and held for 3 minutes at 240 ^{o}C. The final temperature ramp was to 300 ^{o}C at a rate of 30 ^{o}C /min and held there for the final time of 3 min.

The limits of detection for the compounds of interest were determined for the GC-ECD and the GC- μ ECD by analyzing 1 μL of standard solutions of analytes with different concentrations. The concentration detection limits of NG and 2,4-DNT as obtained by the two detectors are tabulated in Table 8. Significant improvement in detection limits using the μ-ECD is evident for NG from the table. The methods were optimized to accommodate NG and therefore some compounds that can also be detected by both detectors lost sensitivity in the micro-ECD. The two nitrodiphenylamines also showed improvement in detection limits similar to nitroglycerin whereas there was loss in sensitivity for DEP and 4-NODPA.

Table 8: Detection limits of analytes determined by generating response graphs of each additive by liquid injection of standards into the GC-ECD and GC- μ-ECD

Analyte	ECD detection limit (ng/μL)	Micro-ECD detection limit (ng/μL)
NG	1	0.25
2,4-DNT	0.125	0.125

Headspace analysis of smokeless powders:

The smokeless powders analysis was carried out using the same extraction parameters as those used for the GC-MS. A one hour extraction using PDMS fibers of the headspace of 100 mg of smokeless powders was conducted to extract the analytes interest. The SPME fiber was manually desorbed into the injection port of the GC-μ–ECD.

Nitroglycerin was detected from all the double-based powders with a retention time of 5.85 min, while 2,4-DNT was detected with a retention time of 6.83 min. Shown below is a chromatogram for a powders containing both NG and 2,4-DNT in the headspace. The response of NG was very high at 60 min extraction and it was determined that there was a large mass of NG being extracted. Quantitation of the

mass extracted at that time was not possible as the signal was higher than the linear range of the detector for NG. Even at very short extraction times of 1 min the signal was NG was well above the detection limit. This indicated that there was sufficient mass of NG present in the headspace of double-based smokeless powders that can be targeted for smokeless powder detection using IMS.

The GC-μ-ECD results corroborate very well with the FBI bulk analysis data that was provided with the samples. NG and 2,4-DNT were detected in all the powders that the bulk analysis determined also as present. The results also indicate that there is a significant pre-concentration of various analytes onto the SPME fiber. In combination with the GC-MS results, it is understood that for any given extraction at least 3 compounds on an average are extracted.

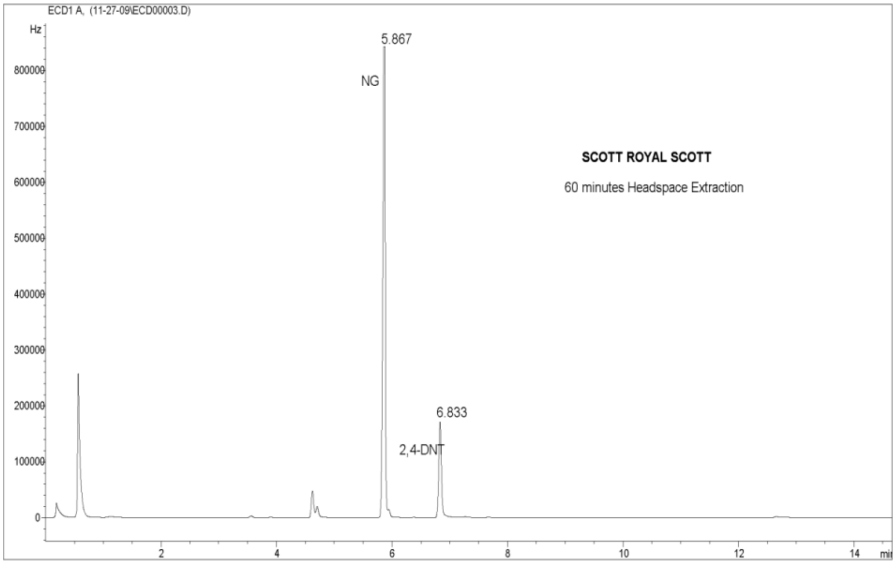

Figure 62: SPME- GC- μ-ECD chromatogram of headspace extraction of a double-based smokeless powder showing the detection of nitroglycerin in the headspace

5.3. SPME-IMS analysis

The analytes specific to smokeless powders that are present in the headspace were determined from the GC-MS and GC- μ-ECD results. These analytes were then studied for ion mobility spectrometry detection. As has already been discussed, SPME-IMS supplies vapor phase analyte sampling and detection to the normally particle sampling instrument. Not all analytes that are detected by spiking onto filter paper can be detected by headspace extractions. This is due to the varying detection limits for each analyte on the IMS and the competition for ionization that is observed when analyzing mixtures in the IMS.

In this portion of the study, each analyte of interest was studied to determine the mode of detection and detection limits. Once the detection limits were established the smokeless powders were studied to determine which of them were detected from the smokeless powder headspace extractions.

1. IMS detection parameters:

An Itemiser II IMS was used for all the studies described in this section. The instrument details are already described in the previous sections and the instrument parameters are listed in Table 3.

Table 9: IMS detection parameters for different smokeless powder additives

Compound name	Detection mode	Drift time (ms)
Nitroglycerin	Negative	3.96 ± 0.030
2,4-DNT	Negative	5.83 ± 0.020
Diphenylamine	Positive	6.20 ± 0.050
Ethyl centralite	Positive	7.66 ± 0.030
Ethyl phenylamine	Positive	5.45 ± 0.030
Dibutyl phthalate	Positive	8.32 ± 0.030, 7.19 ± 0.020
Diethyl phthalate	Positive	7.03 ± 0.020
Methyl centralite	Positive	7.37± 0.030

Each analyte of choice was studied in the positive and the negative mode to determine the mode that produces a well-defined product ion peak that is consistent at various concentrations. Solutions of the analytes were prepared and a 1 μL spike onto a filter was introduced into the IMS. The table above lists the detection mode and the drift times observed for all the compounds in the IMS. Also shown in Figures 63 A-F

are the plasmagrams for the additives of interest. Diphenylamine, ethyl centralite and 2,4-DNT have already been discussed in Chapter III section 4.2.

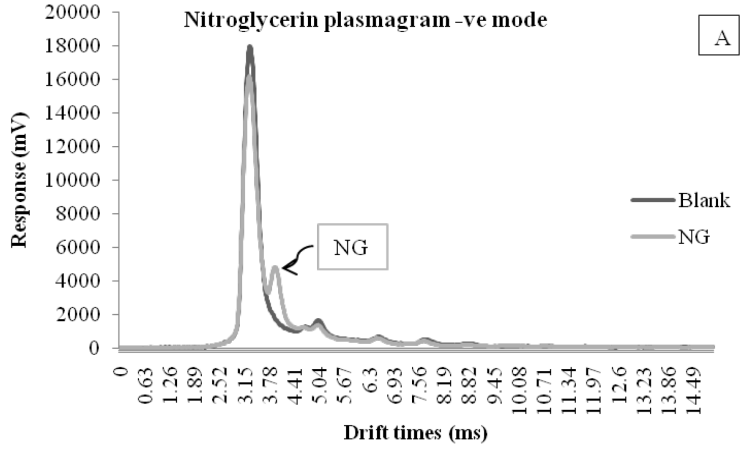

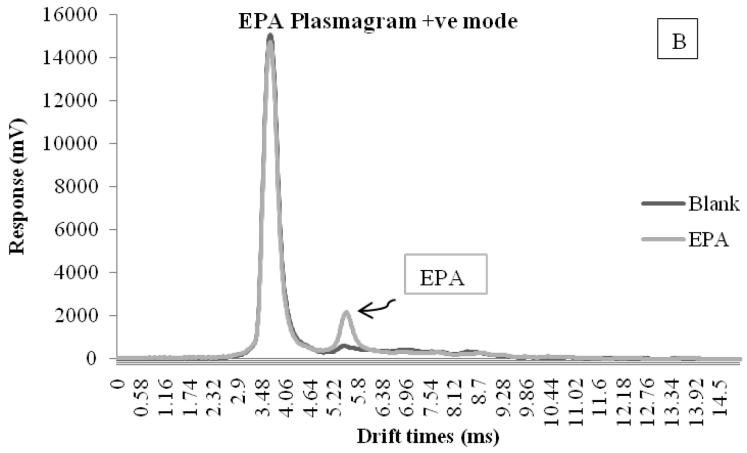

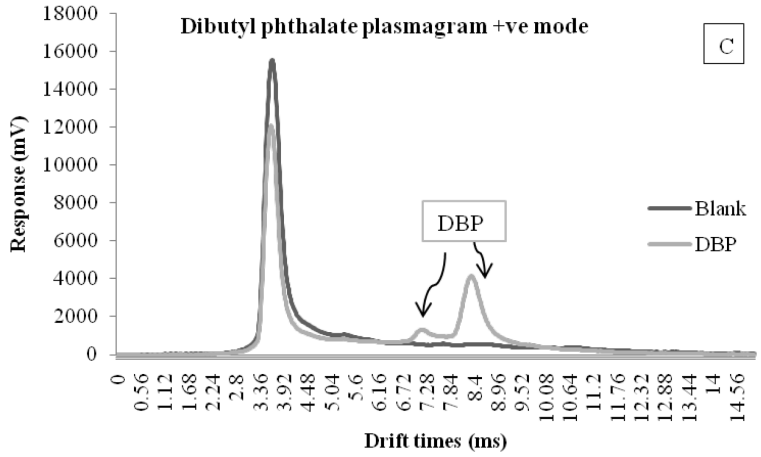
Dibutyl phthalate plasmagram +ve mode
C
Response (mV)
Drift times (ms)
DBP
Blank
DBP

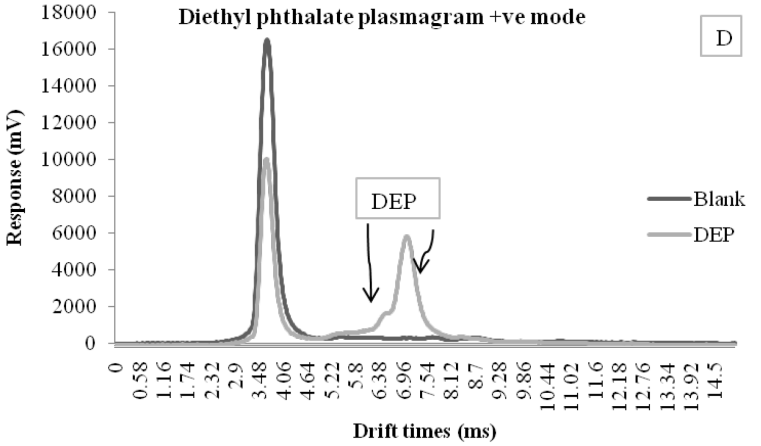
Diethyl phthalate plasmagram +ve mode
D
Response (mV)
Drift times (ms)
DEP
Blank
DEP

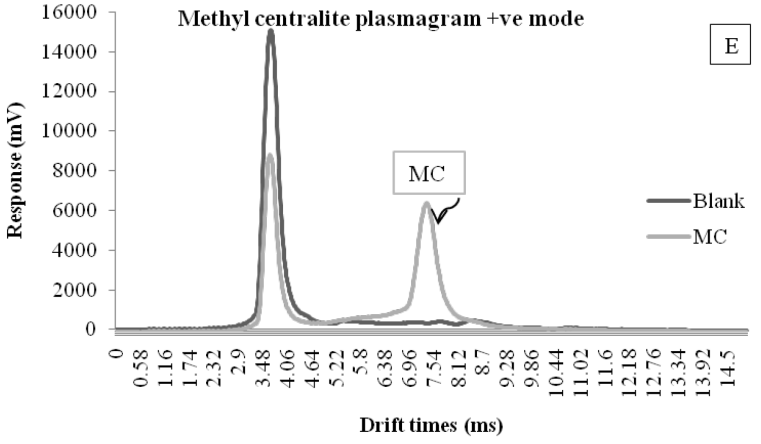
Methyl centralite plasmagram +ve mode
E
Response (mV)
Drift times (ms)
MC
Blank
MC

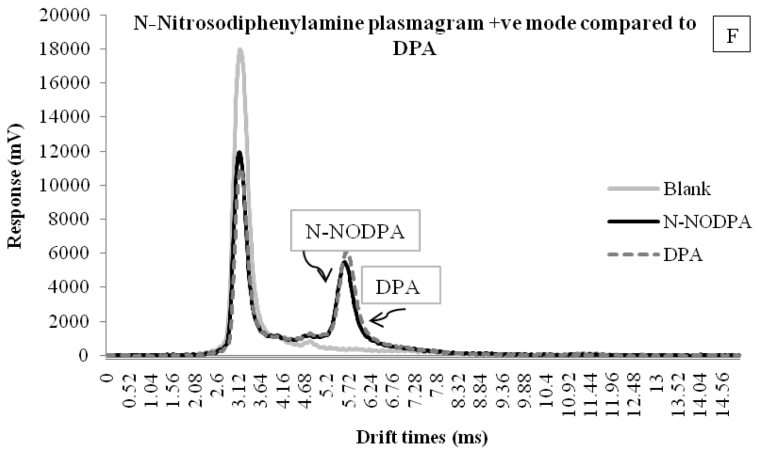

Figure 63: IMS plasmagrams of additives generated by introducing each additive into the IMS by spiking a standard solution onto an IMS substrate A) Nitroglycerin B) Ethylphenylamine C) Dibutyl phthalate D) Diethyl phthalate E) Methyl centralite F) N-nitrosodiphenylamine

Therefore, IMS is capable of detecting two smokeless powder additives in the negative mode and six in the positive mode. Prior to this research, the only alarm that was part of the manufacturer detection menu indicative of smokeless powders was the nitro alarm. With the new peaks, there is a spectrum of compounds that can be used in combination as indicative of smokeless powders. In addition, the drift times of each peak in Table 9 indicate that each peak is sufficiently separated from the other such that there are no overlapping peaks and interfering peaks. However, when simultaneously analyzed all the peaks produced would be so close to each other that they would be affected by each other. However, not all these peaks are anticipated in a single smokeless powder composition. Each smokeless powder may have a combination of one or two of these peaks in the positive mode.

Nitroglycerin produces a single peak of NO_3^- that is very close to the chloride doped reactant ion peak (RIP) in the negative mode. The line is not completely resolved from the RIP and makes quantitation difficult. In the presence of large concentrations of NG a second peak at the same drift time as 2, 4, 6-trinitrotoluene (2, 4, 6-TNT) was observed. This same phenomenon was observed in the analysis of the 2,4-DNT. In the negative mode, 2, 4- DNT produces a single well-defined peak but at high concentrations, the second peak of unknown identity is produced. Since it has the same drift time as 2, 4, 6-TNT, an alarm for the explosive is produced. Thus both NG and 2,4-DNT may produce a second false positive alarm for TNT.

The analytes that produce a single well-defined peak are diphenylamine, ethyl centralite, methyl centralite and ethylphenylamine. They are usually the peaks that are present in large amounts in the headspace as observed from the GC-MS results. Diethyl phthalate and dibutyl phthalate produce more than one peak. Dibutyl phthalate gave one product ion peak at 8.32 ms which was the major peak seen in the plasmagram. A second peak that was seen at 7.19 ms was sufficiently resolved from the other peak, much smaller and appeared to be concentration dependent. Diethyl phthalate had a much more complex plasmagram. A single peak at 7.03 ms was the major product ion peak formed but the front end of the peak baseline was raised and a shoulder peak produced with a shorter drift time. The peak was also affected by concentration but not as much as the peak at 7.03 ms. Several other peaks were also formed at very high mass spikes of the diethyl phthalate.

One of the analytes of interest, N-nitrosodiphenylamine that could not be detected by the gas chromatographic techniques due to it being thermally labile was also analyzed by the IMS. Interestingly, the compound breaks down in the IMS and produces a product ion peak with the loss of the nitroso group. This peak has the same drift time as DPA and as seen in Figure 63 F, the two peaks overlap perfectly. As discussed earlier, N-NODPA is a derivative of DPA that is present in the first stage of the degradation of nitrocellulose and nitroglycerin and the generation of other DPA derivatives. This could indicate that in the headspace extractions of smokeless powders, when DPA is detected in IMS, a small portion of the signal is contributed by the N-NODPA but the contribution cannot be quantified. N-NODPA can be detected by a liquid chromatographic technique and that approach may lead to a better understanding of the amounts present in the bulk. However, the mass of N-NODPA is constantly changing due to the equilibrium between the DPA, production of nitro groups, formation of N-NODPA and its transformation into the secondary derivatives. The nitrated derivates of DPA, 2-nitrodiphenylamine, 4-nitrodiphenylamine which were detected by the GC-MS had very high detection limits in the IMS and many times did not produce a peak. They did not produce characteristic peaks in the negative mode also. However, from the GC-MS results it is evident that the two nitrated species are present in very low amount s in the headspace and the mass extracted as determined GC-MS is very low compared to the detection limits on the IMS. Therefore, in the current extraction and detection conditions, 2-NDPA and 4-NDPA may not be detected in the headspace extractions of smokeless powders by SPME-IMS.

2. Compositional profiles for IMS:

Headspace profiles of smokeless powders similar to those generated by GC-MS were generated for the IMS. The GC-MS profile for the Hodgdon powders is shown in Figure 60. The profiles for the same powders by SPME-IMS analysis is shown below in Figure 64. Though the extraction parameters are the same as the SPME-GC-MS studies, it is important to note that the desorption time for the fiber is in the order of a few seconds for the IMS as compared to the five minute desorption time used for the GC-MS. The analysis also occurs in a few seconds as compared to the 29.33 min method time in the GC-MS. The profiles illustrate the differences between the two analytical techniques for the same extraction parameters of the powders.

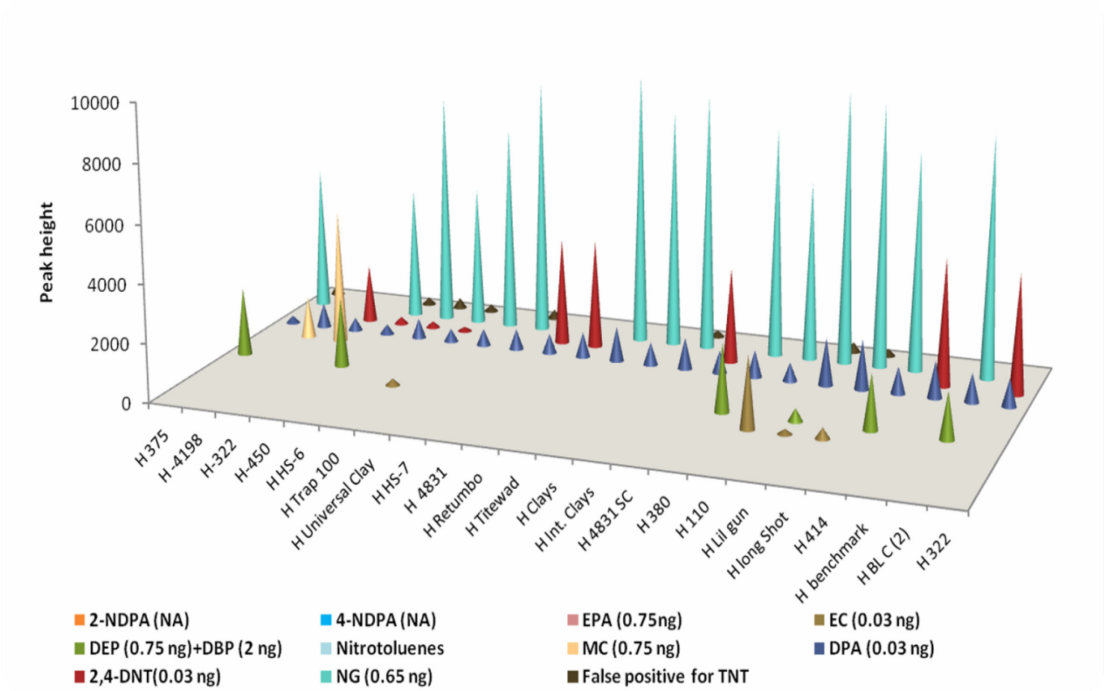

Figure 64: Headspace composition profile of the Hodgdon powders included in the sample set as obtained by SPME-IMS analysis

The profile shown above is significantly different from the GC-MS profile in Figure 60. Earlier it was mentioned that the two nitrated species of DPA, 2-NDPA and 4-NDPA are not detected by the IMS at low mass levels. Therefore, the profile shows complete absence of the peaks at the front end of the graph. In the positive mode, the peaks detected were MC, DEP, DBP, DPA and EC. DPA peak is consistent with the GC-MS results and is detected in all the powders. EC was not detected in all of the powders that showed the presence of EC according to the GC-MS results. In powders, with smaller amounts of EC, the product ion was not formed in sufficient quantity to be detected in the presence of DPA. The MC peak was consistent with the GC-MS results and was detected in both the powders that have MC. The phthalates were detected in most of the powders in which they were present except in those where the amounts observed in GC-MS were very low. This also indicates that the mass extracted was probably smaller than the detection limit of the IMS.

In the negative mode, the major peak observed was the nitro peak indicative that is not specific to nitroglycerin. It was detected in all the double-based powders where nitroglycerin is present in the headspace. The powders where 2,4-DNT is dominant in the headspace do not show evidence of nitroglycerin in the headspace. In cases where there is a large nitro peak, a second peak with the same drift time as 2,4,6-TNT and producing a false alarm is observed. This peak was also added to the profile image shown in Figure 64 to demonstrate that in the negative mode, there are three possible alarms for smokeless powders and that the TNT peak for smokeless powders is

associated with the presence of a large peak for the nitro group. The analysis of the explosive, 2,4,6-TNT does not produce an alarm for NG.

Overall, the IMS profiles demonstrate that inspite of the lack of information regarding the nitrated diphenylamines, there are sufficient peaks to give conclusive detection of smokeless powders from the extraction of headspace volatiles. Most powders show evidence of at least one peak in the positive mode and one in the negative mode. This adds strength to the detection and reduces possible questions of interferences.

5.4. Mass calibration using inkjet printing for SPME

The aim of this research however is not only to demonstrate the detection of the smokeless powder volatiles but also to determine the mass extracted. In order to determine the mass extracted by SPME from the headspace of the smokeless powders in a given time, careful calibration of SPME is required. As has already been discussed, microdrop printing is a technique that can provide accurate mass calibration and will be used in this part of the study for mass determinations of all SPME extractions for GC-MS, GC-ECD and IMS analysis.

Calibration for GC-MS:

The same calibration process as described in section 4 of chapter 1 was utilized for the calibration for the SPME-GC-MS analysis. Each analyte was prepared in a 2-butanol and concentrations ranging from 15,037 ng/μL to 48 ng/μL. Five drops of each solution was printed in triplicate on the extraction phase of the SPME fiber and

desorbed into the injection port of the GC. The mass range tested for every analyte was between 0.032 ng – 10 ng in 665 pL printed. The analytes for which the calibration graphs were developed using this method include methyl centralite, ethylphenylamine, diethyl phthalate, dibutyl phthalate, 2-nitrodiphenylamine and 4-nitrodiphenylamine. To make the printing process simpler, the analytes were grouped in two groups of three analytes each with 4-NDPA, DBP and EPA in one group and 2-NDPA, DEP and MC in the other group. The calibration graphs generated as part of a different study for diphenylamine, ethyl centralite and 2,4-DNT were used for this study also. The method and all experimental parameters were the same for both studies. Shown below in Figures 63 A- I are the calibration graphs generated for all analytes by the microdrop printing method for the GC-MS.

The graphs demonstrate that the response on the GC-MS was linear for all analytes and a linear regression line equation was applied for all the graphs. It is also seen from the graph that not all the analytes have the same mass range and some analytes such as 4-NDPA and EPA have a shorter mass range. They also have higher detection limits. The same two compounds also produced the least correlation in the calibration graph. None of the compounds had any interference in the background at the peak retention time with the baseline being very low and therefore a linear equation with a zero intercept on the y-axis was used. This linear equation was used to correlate the signal obtained by SPME experiments to determine the absolute mass extracted during headspace extractions for GC-MS analysis.

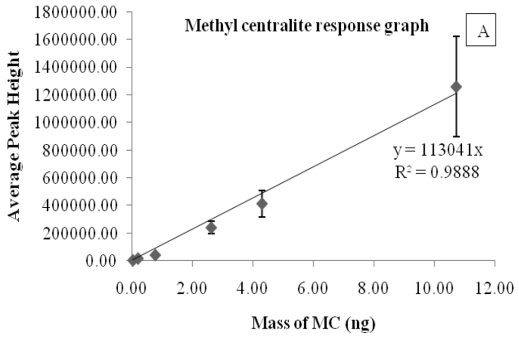
Methyl centralite response graph
A
Average Peak Height
Mass of MC (ng)
y = 113041x
R² = 0.9888

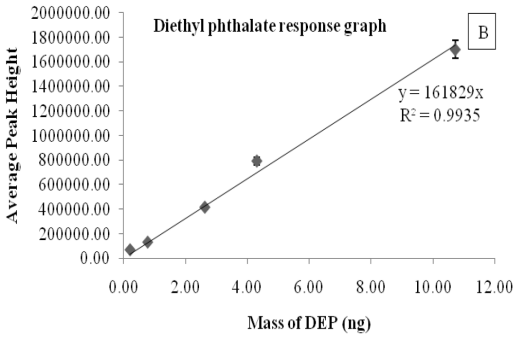
Diethyl phthalate response graph
B
Average Peak Height
Mass of DEP (ng)
y = 161829x
R² = 0.9935

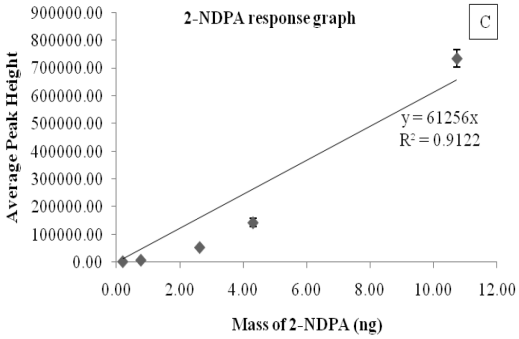
2-NDPA response graph
C
Average Peak Height
Mass of 2-NDPA (ng)
y = 61256x
R² = 0.9122

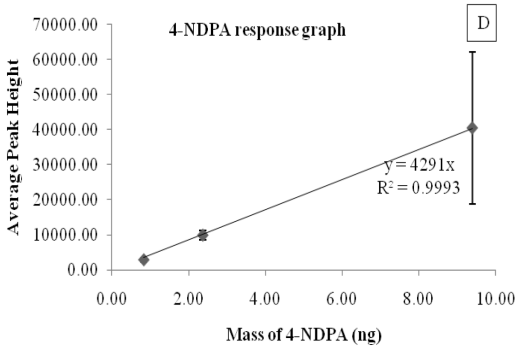
4-NDPA response graph
D
Average Peak Height
Mass of 4-NDPA (ng)
y = 4291x
R² = 0.9993

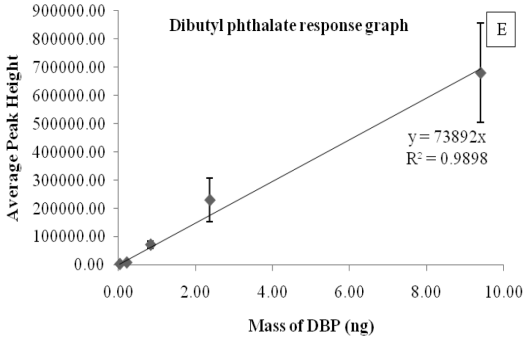
Dibutyl phthalate response graph
E
Average Peak Height
Mass of DBP (ng)
y = 73892x
R² = 0.9898

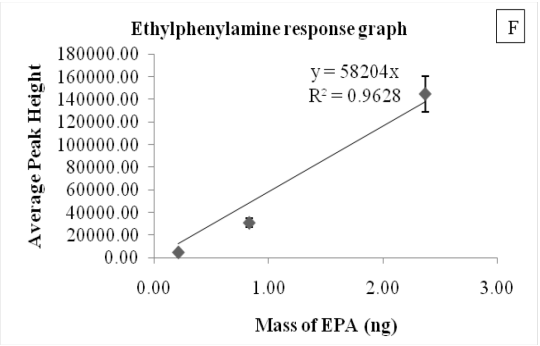
Ethylphenylamine response graph
F
Average Peak Height
Mass of EPA (ng)
y = 58204x
R² = 0.9628

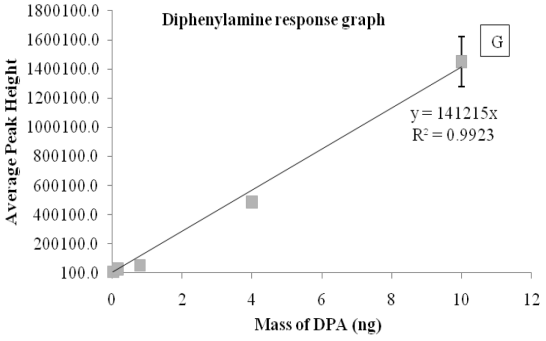
Diphenylamine response graph
G
Average Peak Height
Mass of DPA (ng)
y = 141215x
R² = 0.9923

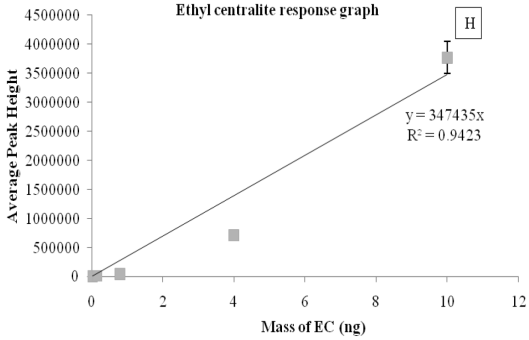
Ethyl centralite response graph
H
Average Peak Height
Mass of EC (ng)
y = 347435x
R² = 0.9423

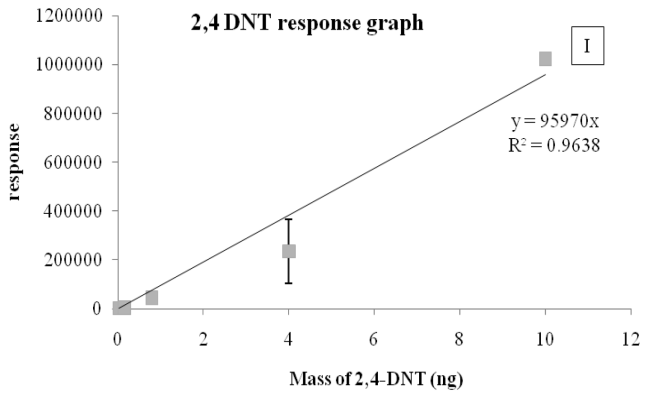

Figure 65: GC-MS graphs generated for SPME calibration by inkjet printing standards onto a SPME fiber A) Methyl centralite B) Diethyl phthalate C) 2-NDPA D) 4-NDPA E) Dibutyl phthalate F) Ethylphenylamine G) Diphenylamine H) Ethyl centralite I) 2,4-DNT

Calibration for IMS

The calibration approach for IMS was also based on microdrop printing. However, the printing was conducted onto an IMS filter instead of a fiber. The results discussed in section 4 of chapter 1 have already demonstrated that for the IMS printing on the fiber or printing on filter yielded similar results. In addition, printing on the filter enables the printing of greater number of drops instead of being limited to 5 drops due to the limited dimensions of the fiber. The volume printed however was still significantly lower than the 1 μL spiked using a pipette/syringe.

The standard for nitroglycerin was obtained from Cerilliant (Round Rock, TX) as an ampule of 1.2 mL of a 1000 ng/ μL solution. The printing solution for nitroglycerin was prepared by diluting the standard with 2-butanol to make a 500 ng/ μL solution

such that each drop printed with the optimized parameters contained 0.067 ng. All the other analytes were diluted from a 1000 ng/ μL standard solution prepared from the analyte standards purchased from Sigma-Aldrich (St. Louis, MO). The printing solution for all analytes was a 400 ng/ μL solution in 2-butanol such that a single drop at optimized parameters contained 0.05 ng. Each analyte has a different mass detection range on the IMS and therefore overall the volume of the solution printed onto a filter varied between 0.4 nL to 266 nL. Shown below are some of the graphs generated by the IMS. The graphs for diphenylamine, ethyl centralite and 2,4-DNT have already been discussed in a previous section.

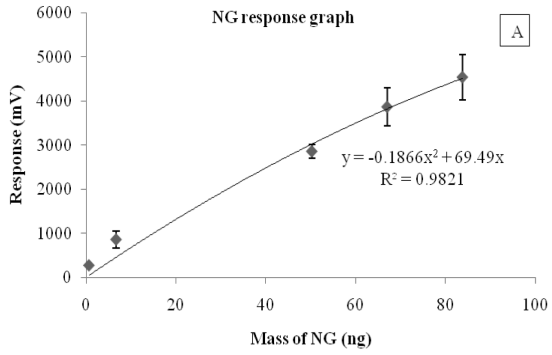

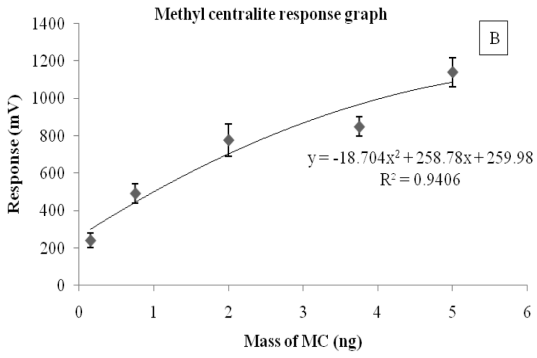

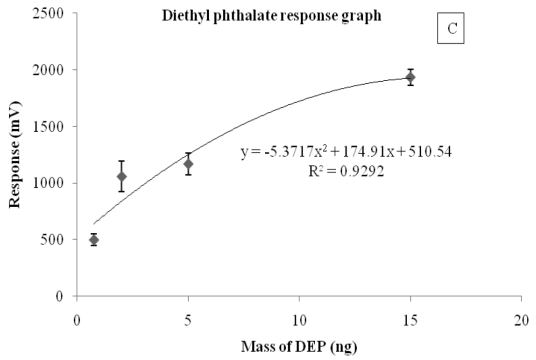

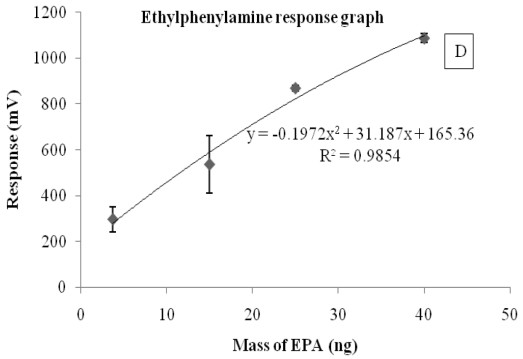

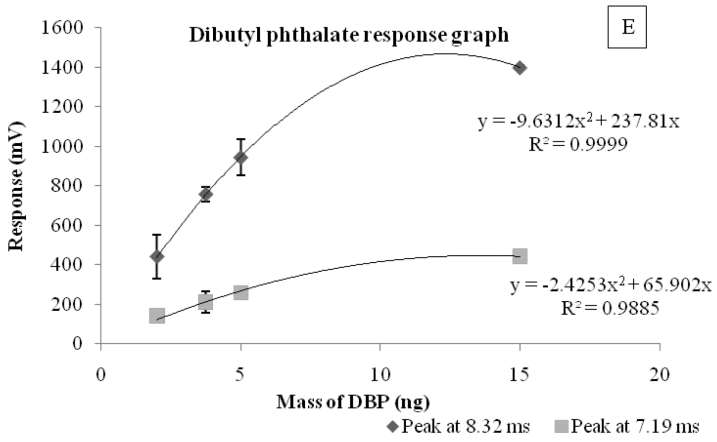

Figure 66: Graphs generated for instrument and SPME calibration using inkjet printing of standards onto an IMS filter A) Nitroglycerin B) Methyl centralite C) Diethyl phthalate D) Ethylphenylamine E) Dibutyl phthalate

The graphs for IMS all depict a second order polynomial best-fit line. The linear range for IMS is usually in the order of one magnitude. The limits of detection for IMS are equated as the smallest absolute mass on the filter that produces a signal for the analyte. The graph 65 E demonstrates the two graphs for both the peaks seen for DBP. The slope of the second smaller peak at 7.19 ms is not the same as the major peak at 8.33 ms indicating that the concentration dependence is not the same. Also, the increase in the peak at 7.19 ms seems to decrease the 8.33 peak and therefore making quantitation difficult for DBP.

Table 10 lists the detection limits for all the analytes of interest as determined for the GC-MS method and the IMS method. While the IMS has the added advantage of the nitroglycercin detection, it is at a disadvantage of not detecting 2-NDPA and 4-NDPA. These two analytes are characteristic of smokeless powders are only seen

when DPA is associated with a source of nitro groups. The GC-MS proved more sensitive for many of these analytes. Similar sensitivities for GC-MS and IMS were obtained for the DPA, EC and 2,4-DNT.

Table 10: Absolute mass limits of detection of analytes on GC-MS and IMS obtained by inkjet printing methods described in section 5.5

Compound	GC-MS (ng)	IMS (ng)
Nitroglycerin (NG)	NA	0.67
2,-dinitrotolunene (2,4-DNT)	0.03	0.03
Diphenylamine (DPA)	0.03	0.03
Ethyl centralite (EC)	0.03	0.03
Methyl centralite (MC)	0.04	0.75
Diethyl phthalate (DEP)	0.03	0.75
Dibutyl phthalate (DBP)	0.03	2
2-nitrodiphenylamine (2-NDPA)	0.21	NA
4-nitrodiphenylamine (4-NDPA)	0.83	NA
Ethylphenylamine (EPA)	0.21	0.75

5.5. Extraction time profiles

As was detailed in the SPME theory section, two equilibriums are to be considered in headspace extractions. The first one is the equilibrium of the analytes in the matrix with the sealed headspace and the second one is the equilibrium of the headspace analytes with the fiber. In all the smokeless powder extraction studies described here, sufficient time was provided for the compounds in the smokeless powders to build equilibrium in the sealed vials. However, when extractions are conducted, sufficient time was not provided for the analytes to develop equilibrium on the fiber. Such extractions are not practical for field applications. Therefore, all studies discussed prior to this section, involved extractions at a 60 min extraction time without consideration of time taken for different analytes to equilibrate onto the fiber. In this section, few powders will be studied to demonstrate the differences in the compounds detected at different extraction times.

Six powders were chosen from each set based on the variation in their composition and their complexity. Each powder was sealed in a vial, allowed to equilibrate and the headspace is sampled with a PDMS fiber for six extraction times: 1, 5, 15, 30, 45 and 60 min. Each powder was analyzed in triplicate for both GC-MS and IMS techniques. For the GC-MS results, the response graphs generated earlier were used to determine the mass of each compound extracted onto the fiber at the different extraction times. For the IMS studies, these calculations were not conducted and the results are represented as time Vs the signal of each compound. In IMS, when analyzing mixtures, quantitation of mass extracted is not accurate as the signal of an

analyte is dependent upon the formation of product ions by the other analytes present in the mixture. As described in Chapter 4, the results of absolute mass present on the fiber for different extractions are independent of the technique used to determine the mass; therefore, the GC-MS calculations are only represented here.

In this section, the graphs for two double-based powders are shown. Hodgdon 450 powder is shown in Figures 67 A and B of which 67 A is the representation of the GC-MS results where the mass extracted in different times in plotted for every analyte and 67 B is the representation of the signal of each analyte of interest present in Hodgdon 450 as detected by IMS at different extraction times. Figures 67 C and D detail the same of Norma Magnum Rifle powder.

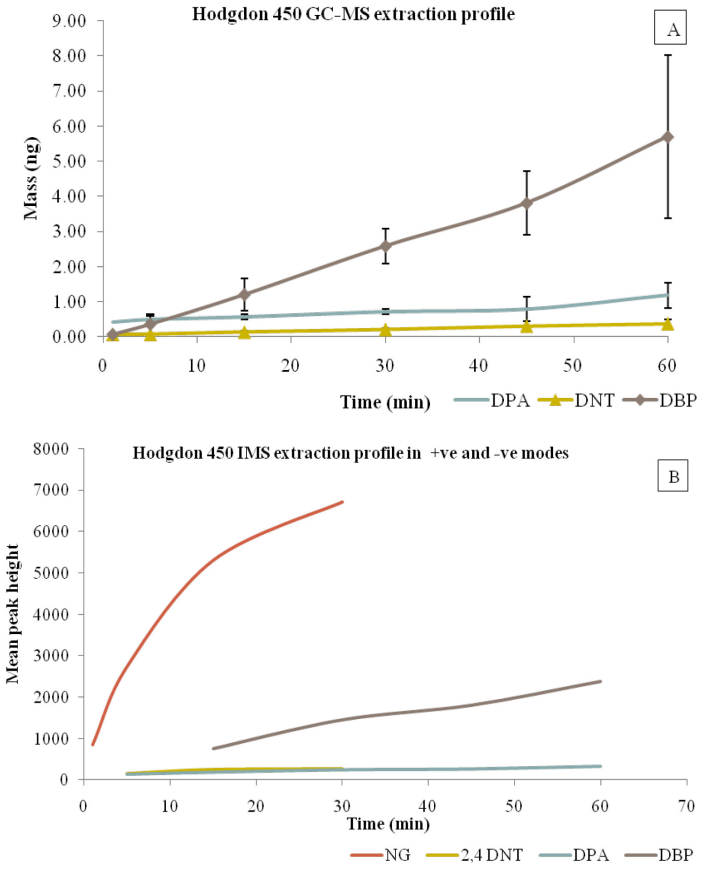

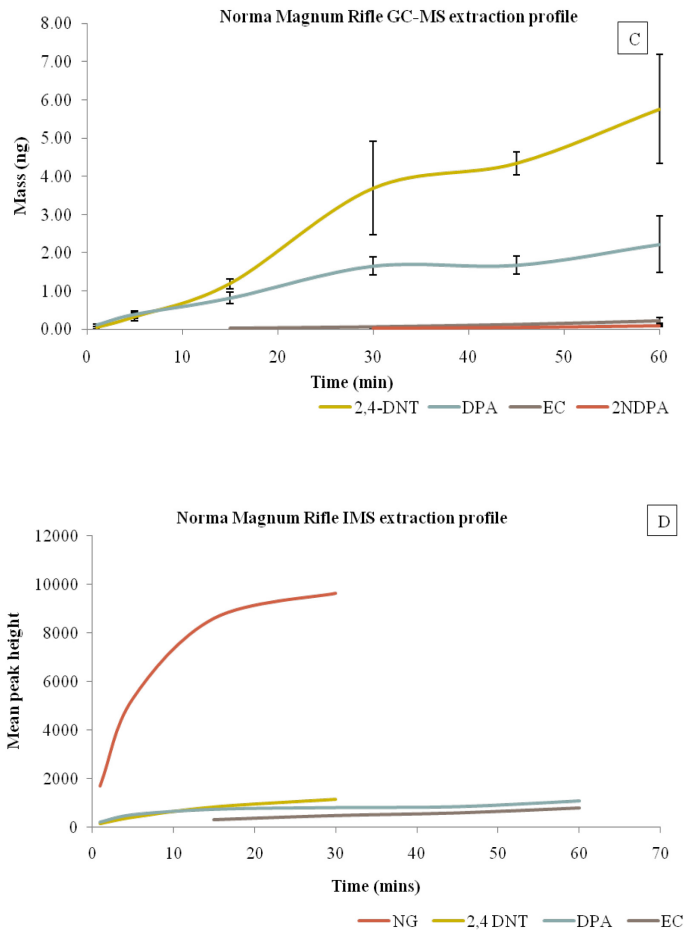

Figure 67: Extraction profiles of smokeless powders A) SPME-GC-MS results of Hodgdon 450 powder with mass of different additives extracted Vs time B) Hodgdon 450 IMS extraction profile in positive and negative IMS modes C) SPME-GC-MS Norma Magnum Rifle mass extracted vs time D) Norma Magnum Rifle powder IMS extraction profile

Hodgdon 450:

For the Hodgdon 450 powder, at the shortest extraction time, all three major analytes, DPA, 2,4-DNT and DBP were detected. However, the mass extracted was

close to the detection limits. DBP was the major contributor to the headspace and the mass extracted varied from 0.07 ng at 1 min to 5.70 ng at a 60 min extraction. For both DPA and 2,4-DNT the mass extracted varied by one order of magnitude between the two times. DPA showed a one order of magnitude increase in mass extracted (0.04 to 0.4 ng) with increase in extraction time from 1 min to 60 min. At the 60 min extraction time DEP and 2-NDPA were also detected but the signal was very close to the detection limit and therefore was not plotted on the graph. Based on these results and the knowledge of the detection limits of these analytes on the IMS one can easily predict the extraction times at which different analytes would be detected in the IMS

The graphs for the IMS are plotted such that both negative and positive mode peaks are represented in the same graph. It is important to note therefore, that the positive and negative mode response scales are not equivalent and therefore the positive mode analyte responses look flat as compared to the negative mode. The negative mode shows presence of two peaks: NG and 2,4-DNT. Both these compounds are highly volatile and generate high signals but the peak for nitroglycerin dominated the negative mode. The extraction times had to be limited to 30 min for the negative mode since the NG peak depleted the reactant ion peak allowing no further detection. In the positive mode, no headspace components were detected at the 1 min mark. At the 5 min extraction time, the DPA peak was present in small amounts. It was also expected from the GC-MS results that DBP would be detected at the 15 min extraction time and this is evident from the graph. However, it has to kept in mind that DBP produces two peaks that contribute to erroneous quantitation. DPA was extracted

well within the detection limits of the IMS and is detected in all extraction times except the 1 min mark.

Norma Magnum Rifle:

Norma Magnum Rifle powder is a double-based powder that has a complex headspace profile with many components. The major compounds detected in the GC-MS were 2,4-DNT, DPA, EC and 2- NDPA with a very small peak for 4-NDPA being detected at 60 min. DPA and 2,4-DNT were the major contributors to the headspace as detected by the GC-MS and were detected at all extraction times. However, shown in the IMS profile is 2,4-DNT only upto 30 min due to the presence of the overwhelming peak of nitroglycerin. The mass of 2,4-DNT and DPA extracted at the 1 min extraction time was higher than the detection limits of the IMS and therefore both were expected to be detected at the 1 min extraction time in the IMS. Based on the GC-MS results the mass of EC extracted at 15 min was above the detection limits of the IMS and therefore, EC was expected to be detected at 15 min. The 2-NDPA peak was not detected in the IMS and the mass extracted even the highest extraction time was very small according to the GC-MS results. The 4-NDPA peak not represented in the graph was only seen at the highest extraction time.

Other powders:

The other powders that were studied similarly include the Dupont 700X, Accurate 4350, Hercules blue dot and Alliant green dot powders. The Dupont 700X has a very simple headspace profile with three components, EPA, EC and NG. The mass

extracted for both EPA and EC at 1 min was not sufficient for IMS detection but was sufficient for detection at the 5 min mark. The Accurate 4350 powder is a single-based powder where no NG was detected in the negative mode of the IMS. The mass of 2,4-DNT extracted was between 0.67 – 50 ng between the lowest and highest extraction times. This mass range was sufficiently high for the IMS and the peak was detected at all extraction times. The Hercules blue dot powder has only NG in the negative mode and in the positive mode DPA was the dominant peak. The mass calculations indicate that EC would be detected only at a 60 min extraction for the IMS and the IMS results prove this. Below this extraction time, a single peak for DPA was seen from the headspace extractions of the powder in the positive mode. Similar observations were made on the Alliant green dot powder whose major components are DPA, EC and NG.

Therefore, using the GC-MS results one is capable of predicting the compounds detected in the IMS at a given extraction time. Based on these results it also becomes easy to choose the right extraction time that would give the most information on the IMS and the GC-MS. These studies provide crucial information about the differences between the detection capabilities of the two techniques. IMS while being a fast and field portable technique is only capable of detecting a few compounds however, it is evident from these results that an extraction time of 5 min is usually sufficient to detect at least one compound in the positive and one in the negative mode.

5.6. Variations within a smokeless powder brand

From the results discussed thus far, it is clear, that there are significant differences in the headspace profiles of the different smokeless powders. It also evident from the

Hodgdon profiles discussed earlier, that a single powder company markets several products and each of these products may have different composition. Also of interest is the variation between different batches of the same product.

Shown below is the comparison of all the Accurate powders included in the study. The graph is a bar graph with the total made to a hundred percent such that the percent contribution of each peak to the headspace can be visualized. From the graph, it is apparent that the products differ widely. Apart from the Accurate Nitro 100 powder, all other powders however, have DPA in them. This powder is also the only powder with EC in its headspace composition. The three powders that have 2,4-DNT have it as an added compound but no major changes to the composition were evident.

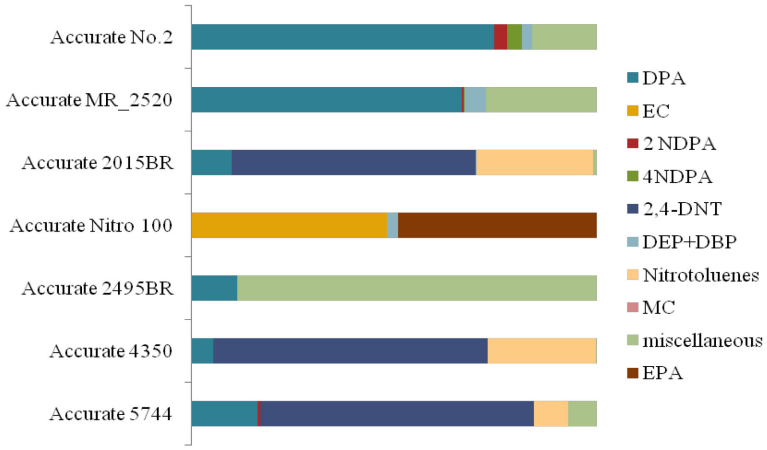

Figure 68: Comparison of the headspace composition of the different Accurate brand powders as obtained by SPME-GC-MS

The entire sample set of seventy smokeless powders discussed in this document had multiple powders of the same product by a manufacturer. For example, there were

five Alliant Red dot powders that were part of the sample set, four of which were given by the FBI whereas the fifth was purchased locally. A few other powders had one or two duplicates. Addressed here are the compositions of the Alliant Red dot and the Hodgdon 322 powders.

Figure 69 A is a representation of the five Alliant powders present in the sample set. Of these powders, the powder with no reference number is the powder that was purchased locally. However, all the Alliant Red dot powder data represented below was obtained within a few days of each other. As is seen from the graph, all the powders have similar compositions. There were no drastic variations in the powders. The four powders obtained from the FBI were very similar in relative peak ratio. The top three powders, R# 758, 757 and 754 were part of the most recent set of the powders and were known to have been purchased by the FBI within 30 days of analysis. The R# 987 was part of the earlier sample set and no information is available on the time of purchase or manufacture of this powder. The Red dot powder with no reference number was purchased locally as part of the FIU sample set more than two years ago. It showed the largest deviation from the other powders that were part of the sample set. The peak ratios were different with the amount of DPA being a lot less than the EC. However, this appears as such due to the presence of the phthalates in the headspace of the powder making the relative ratios of the other peaks appear different. It is well known that phthalates are used in the plastic industry. Several recent studies have indicated that the phthalates leach from the plastic and are released into the container[96,97]. Since, the Red dot powder was purchased and stored in the plastic

container that it came in until 100 mg of it was removed for sampling, it is likely that the phthalate contribution to the headspace of the powders was also due to the container. No information is available on the storage conditions of the FBI powder samples before they were given to FIU and therefore it cannot be said definitively that the phthalates were because of the storage conditions.

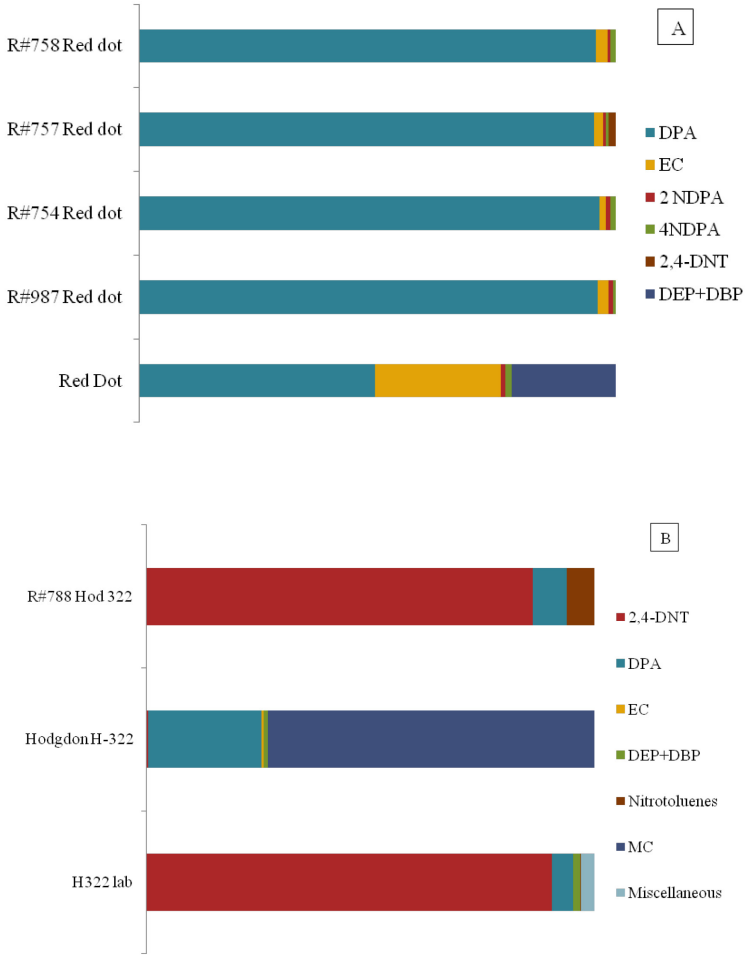

Figure 69: Comparison of headspace composition obtained by SPME-GC-MS of different products of the same brand A) Alliant Red dot powders B) Hodgdon 322 powders

Figure 69 B shown above illustrates the differences between three Hodgdon 322 powders. These three powders are part of three separate sets. The R# 788 was part of the most recently purchased powders by the FBI. The Hodgdon H-322 powder was part of the earlier set of the FBI powders and no purchase date is available for this powder. The complete loss of 2,4-DNT could be explained by its volatility if the powder is old. The presence of methyl centralite unlike the other two powders may indicate that the manufacturer attempted a change in the composition. The H 322 lab powder was purchased locally near FIU and the composition is similar to the R# 788.

Based on these results, it is evident that it is difficult to determine convincingly a powder brand and product based on the headspace profiles. The study described within this document is not intended to determine powder origin. It is only to enable detection of a powder and the peaks detected can indicate the presence or absence of a smokeless powder of unknown origin.

6. OVERALL RESULTS OF SMOKELESS POWDER ANALYSIS

The smokeless powders study was initiated to determine the applicability of solid phase microextraction in combination with GC-MS and IMS for the detection of organic volatiles present in the headspace of smokeless powders. The results described thus far have demonstrated that SPME can be used to extract multiple volatile and semi-volatile compounds from the headspace of the smokeless powder. Several of these compounds can be detected by a combination of detection methods.

Using GC-MS, an array of compounds that are thermally stable and do not degrade in the injector were detected. Combining the results obtained both by the locally purchased powders and those obtained from the FBI, the volatile chemical components of smokeless powder are diphenylamine, ethyl centralite, methyl centralite, diethyl and dibutyl phthalate, 2-nitrodiphenylamine, 4-nitrodiphenylamine, ethylphenylamine, 2, 4-dinitrotoluene and nitroglycerin. Overall, it was found that the most common additive across all powders was diphenylamine. 2,4-DNT was the other additive that was found in several of the powders. It was not exclusive to the single-based powders and was found in double-based powders in combination with other additives. Ethyl centralite was present in many of the powders but was usually extracted in smaller quantities from the headspace as compared to the other analytes. Based on the extraction time profiles for the GC-MS it was also observed that ethyl centralite required more extraction time than other analytes to be absorbed onto the fiber.

On applying the results from the GC-MS and GC-μ-ECD to the IMS, it was learnt that the IMS is also capable of detecting several of these analytes successfully. The only analytes not detected on the IMS that were detected by the chromatography methods were the two nitrated diphenylamines. The mass extracted from the headspace was determined to be to low to be detected by the IMS. Nitroglycerin and 2,4-DNT are detected in the negative mode of the IMS while the rest of the analytes are detected in the positive mode. A combination of the results obtained by the two modes, demonstrated at that extraction times practical for field applications, more than

one volatile component can be detected from the headspace of the powders and can be used for screening and identification of smokeless powders.

7. DISCUSSION AND SIGNIFICANCE

The smokeless powders study resulted in the generation of essential information from both laboratory and field portable analytical techniques that can be used in a variety of ways. This work supplements the available bulk composition data available for smokeless powders and demonstrates that reliable information about smokeless powders can be obtained by using a fast analytical method such as ion mobility spectrometry with less intensive sampling steps. The differences and similarities in the compounds detected between the techniques can be applied to further improve both sampling and detection by IMS.

It is important to note that the study was limited to static closed system sampling. Based on the results observed in this study, it would be beneficial to conduct large volume sampling to mimic real life situations. It is anticipated that better extraction efficiencies would be obtained with a larger more efficient extraction phase. Conducting sampling of fully enclosed explosive devices to determine the amount of volatiles dissipated in such cases would help in improving the SPME sampling method.

Of significance to the sampling and detection of the smokeless powder additives in the field is the presence of interferences. Some of these additives are used in other industries as well and may be present in other commercial products that might produce

false positive alarms. A large-scale study to determine possible interferences for all the analytes and the effects on the reliable detection of smokeless powders is necessary to present a comprehensive picture of the detection of the additives indicative of the presence of smokeless powders.

Studies have been reported for canine studies where volatiles of smokeless powders were studied using GC-MS. However, a large-scale comprehensive study such as this has never been reported. The information generated in this study can also be used for canine studies to determine compounds of canine interest.

The overall aim of this study was to generate a database that can be used by those interested in improving detection and sampling methods. The results obtained from the smokeless powders study indicates that there are variety of target analytes available in the headspace that can be applied to various organic analysis methods. The sample set of seventy smokeless powders studied is representative of the all the smokeless powder compositions manufactured over the years by different manufacturers. The study therefore includes all possible smokeless powder additives of significance but due to the constant changes to composition of the powders by the manufacturers, the profile for a powder may change over the years. Therefore, the profiles and headspace compositions described here are meant only to serve as indicators of volatile components and their variations among the different smokeless powders but not to identify a smokeless powder.

IV. RESEARCH CONCLUSIONS

A detailed account of the research projects undertaken to develop and implement methods for the detection of smokeless powders and the calibration of analytical techniques has been given thus far. The research was derived from the need to calibrate IMS instruments accurately and to help in the determination of the mass available for detection from the headspace of illicit substances. Two salient conclusions can be drawn from the research conducted to address both these needs. Firstly, there are volatile organic compounds available in the headspace of smokeless powder that can be sampled and detected by ion mobility spectrometry and secondly, accurate mass calibration of the detection and sampling techniques used for this purpose can be performed using a microdrop printing method.

At the onset of this dissertation project, two statements were surmised. The drop-on-demand inkjet printing technique was expected to be a reliable mass delivery tool that could be used for the calibration of detectors such as mass spectrometers and ion mobility spectrometers. The research chronicled in Chapter II of this document explored microdrop printing for various detection techniques and gathered ample data to prove this statement to be true and applicable for analytical techniques. The second statement was that there was sufficient information present in the headspace of smokeless powders to allow for their detection by ion mobility spectrometry. Chapter III of this document details the evidence gathered towards evaluating this statement and reveals that smokeless powder additives can be successfully extracted using SPME from the headspace and detected by ion mobility spectrometry. For example, a

closed static system containing 100 mg of Norma Magnum Rifle powder sampled by a SPME fiber for 1 min yielded extracted DPA, 2,4-DNT and NG amounts that were higher than the 0.03 ng detection limits (LOD) for DPA and 2,4-DNT and the 0.67 ng LOD for NG in the IMS. At the same extraction conditions, 15 mins were required to extract a mass of EC that was above the detection limit.

Through the results obtained from the drop-on-demand studies conducted for IMS, it was established that microdrop printing using a drop-on-demand inkjet printer is accurate and precise mass delivery technique. The studies also clearly demonstrate that microdrop printing is a superior method than the traditional methods of introducing absolute mass for IMS detection. Basic studies conducted with various substrates distinctly showed that the response of the IMS to the introduction of the same absolute mass can vary based on the substrate used. This information is very useful for all IMS studies where spiking onto a substrate is used as mass introduction method. The microdrop printing method for IMS also proved that the SPME interface for IMS provided mass transfer into the IMS that was equivalent to the mass transfer from a filter. This is substantial evidence that the absolute mass introduced by a SPME fiber into the IMS can be determined by correlating the signal obtained for the IMS filter. Thus, accurate calibration of SPME experiments for IMS can be obtained. Similar microdrop printing calibration methods for GC-MS showed that the mass transfer between the traditional methods and the printing method was not the same. The results proved that the SPME calibration using microdrop printing gave calibration graphs that were equivalent to the IMS graphs and mass determinations

from both graphs were comparable. Thus, this method can be used for the determination of the mass extracted by SPME headspace extractions.

The calibration methods were developed however to serve a secondary purpose. The primary outcome of this research was the demonstration of the extraction and detection of volatiles and semi-volatiles from the headspace of a variety of smokeless powders. The detection of several of these compounds was demonstrated not only using chromatographic techniques such as GC-MS and GC-ECD but also ion mobility spectrometry. Using the calibration methods developed by microdrop printing, the absolute mass detection limits for each analyte on both detection techniques were determined. The LODs for the different analytes ranged between 0.03- 0.8 ng for the GC-MS and 0.03- 2 ng for the IMS. The calibration method also helped to determine the mass of analytes extracted at different extraction times. This highlighted the differences between the two detection methods and allowed for the prediction of the extraction time necessary for IMS detection of analytes.

The smokeless powder studies were presented as composition profiles that provide a visual representation of the various peaks detected in a single extraction. These composition profiles depict not only the differences in the extracted amounts of analytes within a single powder but also the differences between the relative ratios of peaks among the different powders. Based on the detection limits of the various analytes, the number of peaks detected may vary for different detection techniques. This information is an important supplement to the smokeless powder information

already reported in various literature sources. This is the first reported information about the comprehensive headspace profiles of smokeless powders.

In summary, the smokeless powder study revealed that of the seventy powders studied, 96% of the powders showed the presence of diphenylamine in their headspace that was present in mass sufficient to be extracted and detected by both GC-MS and IMS. About 47% of the powders had ethyl centralite with 2,4-DNT being detected in 44% of the powders. Half the powders had 2-nitrodiphenylamine in their headspace with a lesser percent of 37% having 4-nitrodiphenylamine. In 8% of the powders, methyl centralite was present as the dominant compound in the vapor phase. Apart from these major compounds detected by GC-MS analyses, 57% of the powders were double-based and nitroglycerin is present as the dominant compound in the powders headspace.

This research not only addresses the lack of information regarding the vapor phase composition of smokeless powders but also introduces opportunities for further research. There is scope for improvement of the detection parameters for IMS. Interfacing a mass spectrometer to the IMS can add analyte confirmation capabilities that can help answer questions about the type of product ions formed for several of these analytes. Such information would be vital to understanding IMS parameters that can be changed to improved detection of these analytes. Also important for improving detection of these analytes from the headspace is the improvement of solid phase microextraction phases. An efficient extraction phase with large surface area and one

that selectively absorbs these analytes from the headspace would significantly improve the detection of smokeless powder additives.

The database of the headspace composition of the smokeless powders created will serve as a foundation for further expansion and continuation of this research. The seventy powders studied represent the various smokeless powder compositions currently available on the market. However, the powders available in the market vary over time. Distributors of smokeless powders choose manufacturers of their ingredients necessary for the powder products based on several factors, the most important of which is the economy. The price of the ingredients dictates which manufacturer the distributor chooses and thereby the composition of the products. The brand name by which the distributor chooses to sell the powders may also change over time. The research described in this document therefore should be extended into an on-going effort to develop a comprehensive database to represent the changing compositions of smokeless powders.

REFERENCE LIST

1. Hayes, D. J.; Taylor, D. W. Real time calibration and testing of chemical sensors enabled by precision micro-dispensing technology. Carapezza, E. M., Ed.; SPIE: Orlando, FL, USA, 2005; pp 368-375.

2. Verkouteren M; Windsor E; Fletcher R; Maditz R; Smith W; Gillen G Inkjet metrology and standards for ion mobility spectrometry. *International Journal of Ion Mobility Spectrometry* **2006,** *9* (1), 19-23.

3. Antohe, B. V.; Hayes, D. J.; Ayers, S.; Wallace, D. B.; Grove, M. E.; Christison, M. Portable vapor generator for the calibration and test of explosive detectors. 2009; pp 114-120.

4. Verkouteren M; Gillen G; Taylor, D. W. Piezoelectric Trace Vapor Calibrator. *Rev. Sci. Instrum.* **2006,** *77* (085104), 1-6.

5. Harper, R. J.; Almirall, J. R.; Furton, K. G. Discrimination of smokeless powders by headspace SPME-GC-MS and SPME-GC-ECD, and the potential implications upon training canine detection of explosives. Carapezza, E. M., Ed.; SPIE: Orlando, FL, USA, 2005; pp 638-643.

6. Harper, R. J.; Almirall, J. R.; Furton, K. G. Identification of dominant odor chemicals emanating from explosives for use in developing optimal training aid combinations and mimics for canine detection. *Talanta* **2005,** *67* (2), 313-327.

7. Le, H. P. Progress and Trends in Ink-jet Printing Technology. *The Journal of Imaging Science and Technology* **1998,** *42* (1), 49-62.

8. Lee, E. R. *Microdrop generation;* CRC Press: Boca Raton, 2003.

9. MicroFab Technologies, I. *Drive Waveform effects on Ink-jet Device Performance*;99-03; 99.

10. Calvert, P. Inkjet Printing for Materials and Devices. *Chemistry of Materials* **2001,** *13* (10), 3299-3305.

11. de Gans, B. J.; Duineveld, P. C.; Schubert, U. S. Inkjet Printing of Polymers: State of the Art and Future Developments. *Advanced Materials* **2004,** *16* (3), 203-213.

12. Reis, N.; Ainsley, C.; Derby, B. Ink-jet delivery of particle suspensions by piezoelectric droplet ejectors. *Journal of Applied Physics* **2005,** *97* (9), 094903-094906.

13. MicroFab Technologies, I. *Background on Ink-jet Technology*;99-01; 99 A.D.

14. Fletcher, R. A.; Brazin, J. A.; Staymates, M. E.; Benner, J.; Gillen, J. G. Fabrication of polymer microsphere particle standards containing trace explosives using an oil/water emulsion solvent extraction piezoelectric printing process. *Talanta* **2008,** *76* (4), 949-955.

15. Englmann, M.; Fekete, A.; Gebefugi, I.; Schmitt-Kopplin, P. The dosage of small volumes for chromatographic quantifications using a drop-on-demand dispenser system. *Analytical and Bioanalytical Chemistry* **2007,** *388* (5), 1109-1116.

16. Wu, H. C.; Hwang, W. S.; Lin, H. J. Development of a three-dimensional simulation system for micro-inkjet and its experimental verification. *Materials Science and Engineering A* **2004,** *373* (1-2), 268-278.

17. Dong, H.; Carr, W. W.; Morris, J. F. Visualization of drop-on-demand inkjet: Drop formation and deposition. *Rev. Sci. Instrum.* **2006,** *77* (8), 085101-085108.

18. Verkouteren, R. M.; Verkouteren, J. R. Inkjet Metrology: High-Accuracy Mass Measurements of Microdroplets Produced by a Drop-on-Demand Dispenser. *Analytical Chemistry* **2009,** *81* (20), 8577-8584.

19. Thurow, K.; Kruger, T.; Stoll, N. An Optical Approach for the Determination of Droplet Volumes in Nanodispensing. *Journal of Automated Methods and Management in Chemistry* **2009**.

20. Eiceman, G. A.; Karpas, Z. *Ion Mobility Spectrometry;* 2 ed.; CRC Press: 2005.

21. Creaser, C. S.; Griffiths, J. R.; Bramwell, C. J.; Noreen, S.; Hill, C. A.; Paul T.C.L. Ion mobility spectrometry: a review. Part 1. Structural analysis by mobility measurement. *Analyst* **2004,** *129*, 984-994.

22. Borsdorf, H.; Eiceman, G. Ion Mobility Spectrometry: Principles and Applications. *Applied Spectroscopy Reviews* **2006,** *41*, 323-375.

23. Ewing, R. G.; Atkinson, D. A.; Eiceman, G. A.; Ewing, G. J. A critical review of ion mobility spectrometry for the detection of explosives and explosive related compounds. *Talanta* **2001,** *54* (3), 515-529.

24. Arce, L.; Menθndez, M.; Garrido-Delgado, R.; Valcβrcel, M. Sample-introduction systems coupled to ion-mobility spectrometry equipment for determining compounds present in gaseous, liquid and solid samples. *TrAC Trends in Analytical Chemistry* **2008,** *27* (2), 139-150.

25. Guerra, P.; Lai, H.; Almirall, J. R. Analysis of the volatile chemical markers of explosives using novel solid phase microextraction coupled to ion mobility spectrometry. *Journal of Separation Science* **2008,** *31* (15), 2891-2898.

26. West, C.; Baron, G.; Minet, J. J. Detection of gunpowder stabilizers with ion mobility spectrometry. *Forensic Science International* **2007,** *166* (2-3), 91-101.

27. Cremers, D. A.; Radiemski, L. J. *Handbook of Laser-Induced Breakdown Spectrscopy;* John Wiley & Sons: Hoboken, NJ, 2006.

28. Singh, J. P.; Thakur, S. N. *Laser-induced breakdown spectroscopy;* Elsevier: 2007.

29. Barnett, C.; Cahoon, E.; Almirall, J. R. Wavelength dependence on the elemental analysis of glass by Laser Induced Breakdown Spectroscopy. *Spectrochimica Acta Part B-Atomic Spectroscopy* **2008,** *63* (10), 1016-1023.

30. Rusak, D. A.; Castle, B. C.; Smith, B. W.; Winefordner, J. D. Fundamentals and Applications of Laser-Induced Breakdown Spectroscopy. *Critical Reviews in Analytical Chemistry* **1997,** *27* (4), 257-290.

31. Yaroshchyk, P.; Body, D.; Morrison, R. J. S.; Chadwick, B. L. A semi-quantitative standard-less analysis method for laser-induced breakdown spectroscopy. *Spectrochimica Acta Part B-Atomic Spectroscopy* **2006,** *61* (2), 200-209.

32. Godwal, Y.; Taschuk, M. T.; Lui, S. L.; Tsui, Y. Y.; Fedosejevs, R. Development of laser-induced breakdown spectroscopy for microanalysis applications. *Laser and Particle Beams* **2008,** *26* (01), 95-104.

33. Labutin, T. A.; Popov, A. M.; Lednev, V. N.; Zorov, N. B. Correlation between properties of a solid sample and laser-induced plasma parameters. *Spectrochimica Acta Part B-Atomic Spectroscopy* **2009,** *64* (10), 938-949.

34. Arthur, C. L.; Pawliszyn, J. Solid phase microextraction with thermal desorption using fused silica optical fibers. *Analytical Chemistry* **1990,** *62* (19), 2145-2148.

35. Pawliszyn, J.; Pawliszyn, B.; Pawlizyn, M. Solid Phase Microextraction (SPME). *The chemical educator* **1997,** *2* (4).

36. Pawliszyn, J. Applications of Solid Phase Microextraction. 1999. Cambridge, UK, The Royal Society of Chemistry. RSC Chromatography Monographs. Smith, R. M.

37. Prosen, H.; Zupancic-Kralj, L. Solid-phase microextraction. *TrAC Trends in Analytical Chemistry* **1999,** *18* (4), 272-282.

38. Lord, H.; Pawliszyn, J. Evolution of solid-phase microextraction technology. *Journal of Chromatography A* **2000,** *885* (1-2), 153-193.

39. Bartelt, R. J. Calibration of a Commercial Solid-Phase Microextraction Device for Measuring Headspace Concentrations of Organic Volatiles. *Analytical Chemistry* **1997,** *69* (3), 364-372.

40. Chen, Y. New Calibration Approaches in Solid Phase Microextraction for On-site Analysis. Ph.D University of Waterloo, Ontario, Canada, 2004.

41. Ouyang, G.; Pawliszyn, J. A critical review in calibration methods for solid-phase microextraction. *Analytica Chimica Acta* **2008,** *627* (2), 184-197.

42. Chen, Y.; Pawliszyn, J. Chapter 1 Theory of solid phase microextraction and its application in passive sampling. In *Comprehensive Analytical ChemistryPassive Sampling Techniques in Environmental Monitoring*, Volume 48 ed.; Greenwood, R., Ed.; Elsevier: 2007; pp 3-32.

43. Ouyang, G.; Chen, Y.; Setkova, L.; Pawliszyn, J. Calibration of solid-phase microextraction for quantitative analysis by gas chromatography. *Journal of Chromatography A* **2005,** *1097* (1-2), 9-16.

44. Chen, Y.; O'Reilly, J.; Wang, Y.; Pawliszyn, J. Standards in the Extraction Phase, a New Approach to Calibration of Microextraction Processes. *Analyst* **2004,** *129*, 702-703.

45. Zhou, S. N.; Zhao, W.; Pawliszyn, J. Kinetic Calibration Using Dominant Pre-equilibrium Desorption for On-Site and in Vivo Sampling by Solid-Phase Microextraction. *Analytical Chemistry* **2007,** *80* (2), 481-490.

46. Zhao, W.; Ouyang, G.; Pawliszyn, J. Preparation and application of In-fiber Internal Standardization Solid-Phase Microextraction. *Analyst* **2007,** *132*, 256-261.

47. Ouyang, G.; Pawliszyn, J. Recent developments in SPME for on-site analysis and monitoring. *TrAC Trends in Analytical Chemistry* **2007,** *25* (7), 692-703.

48. Risticevic, S.; Niri, V.; Vuckovic, D.; Pawliszyn, J. Recent developments in solid-phase microextraction. *Analytical and Bioanalytical Chemistry* **2009,** *393* (3), 781-795.

49. Perr, J. M.; Furton, K.; Almirall, J. R. Solid phase microextraction ion mobility spectrometer interface for explosive and taggant detection. *Journal of Separation Science* **2005,** *28* (2), 177-183.

50. Connelly, J. M.; Curby, W. A.; Fox, F. T.; Hallowell, S. F. Detection of Hidden Explosives. In *Forensic Investigation of Explosives*, Beveridge, A., Ed.; CRC Press: Boca Raton, FL, 1998; pp 45-74.

51. Committee on Smokeless and Black Powders *Black and Smokeless powders:Technologies for finding Bombs and the Bomb Makers;* National Academies Press: 1998.

52. Heramb, R. M.; Mccord, B. R. The Manufacture of Smokeless Powders and their Forensic Analysis: A Brief Review. *Forensic Science Communications* **2002,** *4* (2).

53. Hopler, R. B. The History, Development and Characteristics of Explosives and Propellants. In *Forensic Investigation of Explosives*, Beveridge, A., Ed.; CRC Press: 1998; p 1.

54. Moorehead, W. Characterization of Smokeless Powders. In *Forensic Analysis on the Cutting Edge: New Methos for Trace Evidence Analysis*, Blackledge, R. D., Ed.; John Wiley &Sons: 2007; p 241.

55. Hopler, R. B. The History, Development and Characteristics of Explosives and Propellants. In *Forensic Investigation of Explosives*, Beveridge, A., Ed.; CRC Press: Boca Raton, FL, 1998.

56. Yinon, J.; Zitrin, S. *Modern Methods and Applications in Analysis of Explosives;* John Wiley & Sons Inc.: New York, NY, 1993.

57. Bender, E. C. Analysis of low explosives. In *Forensic Investigation of Explosions*, Beveridge, A., Ed.; CRC Press: 1998; p 343.

58. Druet, L.; Asselin, M. A review of stability test methods for gun and mortar propellants, II: Stability testing and surveillance. *Journal of Energetic Materials* **1988,** *6* (3), 215-254.

59. Lussier, L. S.; Gagnon, H.; Bohn, M. A. On the Chemical Reactions of Diphenylamine and its Derivatives with Nitrogen Dioxide at Normal Storage Temperature Conditions. *Propellants, Explosives, Pyrotechnics* **2000,** *25* (3), 117-125.

60. Schroeder, W. A.; Malmberg, E. W.; Fong, L. F.; Trueblood, K. K.; Landerl, J.; Hoerger, D. A. Chromatographic Investigations of Smokeless Powder: Derivatives of Diphenylamine formed in Double-base Powders during Accelarated aging. *Industrial & Engineering Chemistry* **1949,** *41* (12), 2818-2827.

61. Stine, G. Y. An investigation into propellant stability. *Analytical Chemistry* **1991,** *63* (8), 475A-478A.

62. O.Drzyzga; A.Schmidt; K.-H.Blotevogel Reduction of Nitrated Diphenylamine Derivatives under Anaerobic Conditions. *Applied and environmental microbiology* **1995,** *61* (9), 3282-3287.

63. Ritter, H.; Braun, S.; Kaiser, M.; Becher, C. Stabilizer Degradation in Propellants: Identification of Two Isomeric Forms of 2-Nitro-N-nitroso-N-ethylaniline. *Propellants, Explosives, Pyrotechnics* **2008,** *33* (3), 203-208.

64. Tong, Y.; Wei, Z. P.; Yang, C. D.; Yu, J. Y.; Zhang, X. R.; Yang, S. J.; Deng, X. Y.; Xu, Y. C.; Wen, Y. X. Determination of diphenylamine stabilizer and its nitrated derivatives in smokeless gunpowder using a tandem MS method. *Analyst* **2001,** *126* (4), 480-484.

65. Moorehead, W. Smokeless powder characterization-database. Unpublished Work, 2005.

66. Hida, M.; Mitsui, T. Determination of nitrocellulose in smokeless powders using a multivariate analysis for infrared spectra. *Bunseki Kagaku* **1998,** *47* (11), 867-871.

67. Meng, H. H.; Caddy, B. Gunshot residue analysis - A review. *Journal of Forensic Sciences* **1997,** *42* (4), 553-570.

68. Reardon, M. R.; MacCrehan, W. A. Developing a quantitative extraction technique for determining the organic additives in smokeless handgun powder. *Journal of Forensic Sciences* **2001,** *46* (4), 802-807.

69. Andrasko, J. Characterization of Smokeless Powder Flakes from Fired Cartridge Cases and from Discharge Patterns on Clothing. *Journal of Forensic Sciences* **1992,** *37* (4), 1030-1047.

70. Mach, M. H.; Pallos, A.; Jones, P. F. Feasibility of Gunshot Residue Detection via its Organic Constituents . Part I. Analysis of Smokelss Powders by Combined Gas Chromatography-Chemical ionization Mass Spectrometry. *Journal of Forensic Sciences* **1978,** *23* (3), 433-445.

71. Darwin B.Dahl; Peter F.Lott Determination of Black and Smokeless Powder Residues in Firearms and Improvised Explosive Devices. *Microchemical Journal* **1987,** *35* (1), 40-50.

72. David M Northrop; William A.MacCrehan *Smokeless powder residue analysis by capillary electrophoresis*;600-91; National Institute of Justice: Feb, 97.

73. Hopper, K. G.; Mccord, B. R. A comparison of smokeless powders and mixtures by capillary zone electrophoresis. *Journal of Forensic Sciences* **2005,** *50* (2), 307-315.

74. Smith, K. D.; Mccord, B. R.; MacCrehan, W. A.; Mount, K.; Rowe, W. F. Detection of smokeless powder residue on pipe bombs by micellar electrokinetic capillary electrophoresis. *Journal of Forensic Sciences* **1999,** *44* (4), 789-794.

75. Calderara, S.; Gardebas, D.; Martinez, F. Solid phase micro extraction coupled with on-column GC/ECD for the post-blast analysis of organic explosives. *Forensic Science International* **2003,** *137* (1), 6-12.

76. John A Mathis; Bruce R McCord Gradient reversed phase-liquid chromatographic-electrospray ionization mass spectrometric method for the comparison of smokeless powders. *Journal of Chromatography A* **2003,** *988*, 107-116.

77. John A Mathis Development of Chromatography and Mass Spectrometry methods for Explosives Analysis. Ohio University, Mar 2004.

78. John A Mathis; Bruce R McCord Mobile phase influence on electrospray ionization for the analysis of smokeless powders by gradient reversed phase high-performance liquid chromatography-ESIMS. *Forensic Science International* **2005,** *154*, 159-166.

79. Wissinger, C. E.; Mccord, B. R. A gradient reversed phase HPLC procedure for smokeless powder comparison. *Journal of Forensic Sciences* **2002,** *47* (1), 168-174.

80. MacCrehan, W. A.; Patierno, E. R.; Duewer, D. L.; Reardon, M. R. Investigating the effect of changing ammunition on the composition of organic additives in gunshot residue (OGSR). *Journal of Forensic Sciences* **2001,** *46* (1), 57-62.

81. MacCrehan, W. A.; Reardon, M. R. A qualitative comparison of smokeless powder measurements. *Journal of Forensic Sciences* **2002,** *47* (5), 996-1001.

82. MacCrehan, W. A.; Reardon, M. R.; Duewer, D. L. Associating gunpowder and residues from commercial ammunition using compositional analysis. *Journal of Forensic Sciences* **2002,** *47* (2), 260-266.

83. MacCrehan, W. A.; Bedner, M. Development of a smokeless powder reference material for propellant and explosives analysis. *Forensic Science International* **2006,** *163* (1-2), 119-124.

84. Scherperel, G.; Reid, G. E.; Smith, R. W. Characterization of smokeless powders using nanoelectrospray ionization mass spectrometry (nESI-MS). *Analytical and Bioanalytical Chemistry* **2009,** *394* (8), 2019-2028.

85. Mahoney, C. M.; Gillen, G.; Fahey, A. J. Characterization of gunpowder samples using time-of-flight secondary ion mass spectrometry (TOF-SIMS). *Forensic Science International* **2006,** *158* (1), 39-51.

86. Miller, C. J.; Ewing, R. G. Detection of Nitrocellulose and Nitrocellulose Based Explosives Using Ion Mobility Spectrometry. *International Journal for Ion Mobility Spectrometry* **2001,** *4* (2).

87. Colón, Y.; Ramos, C. M.; Rosario, S. V.; Castro, M. E.; Hernández, S. P.; Mina, N. Ion mobility spectrometry determination of smokeless powders on surfaces. *International Journal of Ion Mobility Spectrometry* **2002,** *5* (3), 127-131.

88. Neves, J. L.; Haigh, P. E.; Wu, C.; McGann, W. J. ITMS-MS Analysis of Smokeless Powder. *International Journal of Ion Mobility Spectrometry* **2003,** *6* (2).

89. Oxley, J. C.; Waggoner, L. P. Detection of Explosives by Dogs. In *Aspects of Explosives Detection*, Marshall, M., Oxley, J. C., Eds.; Elsevier: 2009; pp 27-40.

90. Kalkomey, I. Understanding the Black Powder Load. http://www.hunter-ed.com/copyright.htm . 3-30-2009.

91. SMI-LabHut Ltd . HT280T Headspace, Liquid and SPME Autosampler. http://www.labhut.com/products/autosamplers/autosampler_ht280t.php . 2010.

92. Lai, H.; Corbin, I.; Almirall, J. R. Headspace sampling and detection of cocaine, MDMA, and marijuana via volatile markers in the presence of potential interferences by solid phase microextraction-ion mobility spectrometry (SPME-IMS). *Analytical and Bioanalytical Chemistry* **2008,** *392* (1-2), 105-113.

93. Lai, H.; Guerra, P.; Joshi, M.; Almirall, J. R. Analysis of volatile components of drugs and explosives by solid phase microextraction-ion mobility spectrometry. *Journal of Separation Science* **2008,** *31* (2), 402-412.

94. Macias, M. S.; Guerra-Diaz, P.; Almirall, J. R.; Furton, K. G. Detection of piperonal emitted from polymer controlled odor mimic permeation systems

utilizing Canis familiaris and solid phase microextraction-ion mobility spectrometry. *Forensic Science International* **2010,** *195* (1-3), 132-138.

95. Spangler, G. E.; Lawless, P. A. Ionization of Nitrotoluene Compounds in Negative-Ion Plasma Chromatography. *Analytical Chemistry* **1978,** *50* (7), 884-892.

96. Li, X. J.; Zeng, Z. R.; Chen, Y.; Xu, Y. Determination of phthalate acid esters plasticizers in plastic by ultrasonic solvent extraction combined with solid-phase microextraction using calix[4]arene fiber. *Talanta* **2004,** *63* (4), 1013-1019.

97. Wensing, M.; Uhde, E.; Salthammer, T. Plastics additives in the indoor environment - flame retardants and plasticizers. *Science of the Total Environment* **2005,** *339* (1-3), 19-40.

APPENDICES

HEADSPACE COMPOSITION OF SEVENTY SMOKELESS POWDERS BASED ON SOLID PHASE MICROEXTRACTION – GAS CHROMATOGRAPHY MASS SPECTROMETRY (SPME-GC-MS)

Powder name	Ref. No.	Shape and type	Headspace composition								
			NG	DPA	2,4-DNT	EC	MC	DEP + DBP	NT	2-NDPA	4-NDPA
Alliant Red dot, Lot 987	752	Disc/ DB	✔	✔		✔				✔	✔
Alliant Red dot	754	Disc/ DB	✔	✔		✔				✔	✔
Alliant Red dot	757	Disc/ DB	✔	✔	✔	✔				✔	✔
Alliant Red dot	758	Disc/ DB	✔	✔		✔				✔	✔
Alliant Red dot	No Ref	Disc/ DB	✔	✔		✔		✔		✔	✔
Alliant Green dot, Lot 783	753	Disc/ DB	✔	✔		✔		✔		✔	✔
Alliant Green dot	762	Disc/ DB	✔	✔	✔	✔				✔	✔
Alliant Green dot	763	Disc/ DB	✔	✔		✔				✔	✔
Alliant Blue dot	756	Disc/ DB	✔	✔		✔				✔	

Alliant 2400	759	Disc/ DB	✔	✔		✔					
Alliant Herco	760	Disc/ DB	✔	✔		✔				✔	
Alliant Bullseye	755	Disc/ DB	✔	✔		✔					
Alliant Reloader 15	761	Short tube/ DB	✔	✔		✔					
Alliant American Select	765	Disc/ DB	✔	✔							
Alliant Power Pistol	766	Disc/ DB				✔					
Alliant Unique	764	Disc/ DB	✔	✔		✔				✔	
Alliant Unique	No Ref.	Disc/ DB	✔	✔		✔				✔	✔
Accurate 5744	164	Short tube/ DB	✔	✔	✔				✔	✔	
Accurate 4350	275	Long tube/ SB		✔	✔				✔		
Accurate 2495BR	277	Long tube/ SB		✔							
Accurate Nitro 100	282	Disc/ DB	✔			✔		✔			

Accurate 2015BR	351	Short tube/ SB		✔	✔			✔	✔		
Accurate MR 2520	750	Ball/ DB	✔	✔				✔		✔	✔
Accurate No.2	751	Flat Ball/ DB	✔	✔				✔		✔	✔
DuPont 700X	132	Disc/ DB	✔	✔	✔					✔	✔
Dupont PB	134	Disc/ SB		✔			✔				
DuPont SR-7625	241	Disc/ SB		✔	✔				✔		
IMR 4198	No Ref.	Long tube/ SB		✔	✔						
IMR 4198	775	Long tube/ SB		✔	✔				✔		
IMR 4007 SSC	769	Short tube/ SB				✔	✔				
IMR 3031	771	Long tube/ SB		✔	✔				✔		
IMR 7625	774	Disc/ SB		✔				✔			
IMR 4320	770	Short tube/		✔	✔				✔		

		SB									
IMR HI Skor	772	Disc/ DB	✔	✔		✔					
Hercules Blue dot	290	Disc/ DB	✔	✔		✔		✔		✔	✔
Hercules Herco	211	Disc/ DB	✔	✔						✔	✔
Hodgdon BL C (2)	No Ref.	Flat ball/ SB		✔				✔			
Hodgdon BL C (2)	768	Flat ball/ SB		✔				✔		✔	
Hodgdon H-322	No Ref.	Short tube/ SB		✔	✔			✔	✔		
Hodgdon H-322	101	Short tube/ SB		✔	✔	✔	✔	✔			
Hodgdon 322	788	Short tube/ SB		✔	✔	✔			✔		
Hodgdon H-450	108	Ball/ DB	✔	✔	✔			✔	✔	✔	
Hodgdon H-375	40	Flat ball/ DB	✔	✔	✔			✔		✔	
Hodgdon H-4198	100	Long tube/ SB		✔			✔	✔			

Hodgdon HS-6	113	Flat ball/ SB		✔	✔					✔	✔
Hodgdon Trap 100	124	Flat ball/ DB	✔	✔	✔	✔				✔	
Hodgdon Universal Clay	286	Disc/ DB	✔	✔				✔		✔	
Hodgdon HS-7	365	Flat ball/ DB	✔	✔	✔	✔			✔	✔	✔
Hodgdon 4831	777	Long tube/ SB		✔	✔				✔		
Hodgdon Retumbo	779	Short tube/ SB		✔	✔				✔		
Hodgdon Titewad	780	Flat ball/ SB		✔						✔	✔
Hodgdon Clays	782	Disc/ DB	✔	✔	✔						
Hodgdon Int. Clays	783	Disc/ DB	✔	✔						✔	✔
Hodgdon 4831 SC	784	Short tube/ DB	✔	✔	✔				✔		
Hodgdon 380	785	Ball/ SB		✔				✔		✔	✔
Hodgdon	786	Flat		✔	✔	✔					

110		ball/ SB									
Hodgdon Lil gun	787	Flat ball/ SB		✔		✔		✔		✔	✔
Hodgdon long Shot	773	Flat ball/ DB	✔	✔	✔	✔			✔	✔	✔
Hodgdon 414	776	Flat ball/ SB		✔				✔		✔	✔
Hodgdon benchmark	781	Short tube/ SB		✔	✔				✔		
Norma R-1	70	Short tube/ SB		✔		✔		✔			
Norma N-201	81	Short tube/ DB	✔	✔	✔				✔		
Norma Magnum Rifle	482	Short tube/ DB	✔	✔	✔	✔		✔	✔	✔	✔
Scot Royal Scot	255	Disc/ DB	✔	✔	✔	✔	✔	✔	✔		
Vihta Vuori 20N29	656	Long tube/ SB		✔		✔					
Vihta Vuori 24N41	657	Long tube/ SB		✔		✔					

Vihta Vuori N 133	767	Short tube/ SB		✔		✔					
Wincheste r 571	128	Flat ball/ DB	✔	✔	✔					✔	✔
Wincheste r 748	778	Flat ball/ DB	✔	✔				✔		✔	✔
Wincheste r 452AA	227	Flat ball/ DB	✔	✔	✔	✔		✔	✔	✔	✔

Legend:

SB: Single-based powder

DB: Double-based powder

NG: Nitroglycerin

DPA: Diphenylamine

2,4-DNT: 2,4-dinitrotoluene

EC: Ethyl centralite

MC: Methyl centralite

DEP+DBP: Phthalates (Diethyl phthalate and Dibutyl phthalate)

NT: Nitrotolunes

2-NDPA: 2-nitrodiphenylamine

4-NDPA: 4-nitrodiphenylamine

VITA

MONICA JOSHI-KUMAR

May 3, 1982	Born, Andhra Pradesh, India
2003	B.S. Chemistry, Biochemistry and Microbiology
	St. Francis Degree College for Women, India
2003	General Proficiency Award
	St. Francis Degree College for Women, India
2005	M.S. Forensic Sciences (Forensic Chemistry and Toxicology)
	Osmania University, India
2006 – 2009	Teaching Assistant and Research Assistant
	Florida International University, Miami
2008	Scholarly Forum: Best Presenter
	Florida International University, Miami
2009	Gordon Research Conference: Best Poster Award
	Les Diablerets, Switzerland
2010	Dissertation Evidence Acquisition award
	Florida International University, Miami

PUBLICATIONS AND PRESENTATIONS

Gura S, **Joshi M**, Almirall J. SPME calibration using inkjet microdrop printing, **Submitted** to Analytical BioAnalytical Chemistry journal.

Joshi M, Gura S, Almirall J. Detection of odor signatures of smokeless powders using solid phase microextraction coupled to an ion mobility spectrometer. Part II. To be submitted to Forensic Science International.

Joshi M, Delgado Y, Guerra P, Lai H, Almirall J. Detection of odor signatures of smokeless powders using solid phase microextraction coupled to an ion mobility spectrometer. For. Sci. Int. 2009, Volume 188, 1, 112-118

Joshi M. Oral and poster presentation, GRC - Detecting Illicit Substances: Explosives and Drugs , Les Diablerets, Switzerland – June 2009

Joshi M. Oral presentation, FAME 2009- ACS, Orlando, Florida – May 2009

Joshi M. Oral presentation, GSA – Scholarly Forum, Florida International University, Miami – March 2008

Joshi M. Oral presentation, AAFS, Washington, D.C. – February 2008

Joshi M. Poster presentation, GRC - Detecting Illicit Substances: Explosives and Drugs, Big Sky, Montana - September 2007

Joshi M. Poster presentation, Nanoelectronic Devices for Defense & Security (NANO-DDS) Conference, Arlington, VA – June 2007

Joshi M. Oral presentation, AAFS, San Antonio, TX - February 2007

Joshi M. Oral presentation, FACSS, Orlando, FL – September 2006

Joshi M. Poster presentation,Ion mobility spectrometry Conference, Honolulu, Hawaii - July 2006

Joshi M. Poster presentation, TSWG Explosives Detection Conference, Miami, FL - June 2006

Lai H, Guerra P, **Joshi M**, Almirall J, Analysis of volatile components of drugs and explosives by solid phase microextraction-ion mobility spectrometry. J. Sep. Sci. 2008, 31,402-412.